UNIVERSITY OF ZAGREB
FACULTY OF GRAPHIC ARTS

Gorazd Golob

ELASTOMER SURFACE ENERGY MODIFICATION APPLYING OXYGEN AND NITROGEN PLASMA TREATMENT WITH LASER DEACTIVATION OF THE SURFACE

DOCTORAL THESIS

Supervisors: Dr. Sc. Mladen Lovreček, Professor
Dr. Sc. Miran Mozetič, Professor

Zagreb, 2011

SVEUČILIŠTE U ZAGREBU
GRAFIČKI FAKULTET

Gorazd Golob

PROMJENA POVRŠINSKE ENERGIJE ELASTOMERA PRIMJENOM KISIKOVE I DUŠIKOVE PLAZME UZ LASERSKU DEAKTIVACIJU POVRŠINE

DOKTORSKI RAD

Mentori: Prof. dr. sc. Mladen Lovreček
Prof. dr. sc. Miran Mozetič

Zagreb, 2011

University of Zagreb
Faculty of Graphic Arts
Doctoral study “Graphic Engineering and Graphic Design”

Doctoral thesis

UDK: 533+544+760=111
Scientific Area: **Technical Sciences**
Scientific Field: **Graphic Technology**

Elastomer surface energy modification applying oxygen and nitrogen plasma treatment with laser deactivation of the surface

Gorazd Golob

Thesis performed at:
University of Zagreb, Faculty of Graphic Arts
“Jožef Stefan” Institute, Department of Surface Engineering and Optoelectronic, Ljubljana
University of Ljubljana, Faculty of Pharmacy
Faculty of Natural Sciences and Engineering
National Institute of Chemistry, Ljubljana
University of Pardubice, Faculty of Chemical Technology
Savatech, d.o.o., Kranj
LPKF Laser & Elektronika d.o.o., Naklo

Supervisors: Dr. Mladen Lovreček, Professor
Dr. Miran Mozetič, Professor

Short abstract:
The aim of the thesis was to investigate the surface energy, roughness and other properties of NBR and EPDM “rubber blankets“, to modify the surface properties with an oxygen and nitrogen plasma treatment, and to defunctionalize the surface by applying UV and IR lasers. The characterization of the surface energy with contact angle measurements, SEM, XPS, FTIR-ATR and roughness analysis of the investigated elastomers and their components provided a description of the surface free energy, polarity, chemistry and other surface characteristics of the mentioned materials.

Number of pages: 205
Number of figures: 74
Number of tables: 14
Number of references: 148
Original in: English

Key words: elastomer, rubber blanket, plasma, surface energy, laser

Date of the thesis defense:

Reviewers: Dr. Sc. Stanislav Bolanča, Professor, head
Dr. Sc. Mladen Lovreček, Professor, supervisor
Dr. Sc. Miran Mozetič, Professor, supervisor
Dr. Sc. Marta Klanjšek Gunde, Assistant professor, external member
Dr. Sc. Vesna Džimbeg-Malčić, Assistant professor, member

Thesis deposited in:

Sveučilište u Zagrebu
Grafički fakultet
Doktorski studij "Grafičko inženjerstvo i oblikovanje grafičkih proizvoda"

Doktorski rad

UDK: 533+544+760=111
Znanstveno područje: **Tehničke znanosti**
Znanstveno polje: **Grafička tehnologija**

Promjena površinske energije elastomera primjenom kisikove i dušikove plazme uz lasersku deaktivaciju površine

Gorazd Golob

Rad je izrađen:
Sveučilište u Zagrebu, Grafički fakultet
Inštitut "Jožef Stefan", Odsek za tehnologijo površin in optoelektroniko
Univerza v Ljubljani, Fakulteta za farmacijo
Naravoslovnotehniška fakulteta
Kemijski inštitut, Ljubljana
Univerzita Pardubice, Fakulta chemicko-technologická
Savatech, d.o.o., Kranj
LPKF Laser & Elektronika d.o.o., Naklo

Mentori: prof. dr. sc. Mladen Lovreček
prof. dr. sc. Miran Mozetič

Kratki sažetak:
Cilj doktorske teze je istraživanje površinske energije, hrapavosti i drugih karakteristika NBR i EPDM gumenih navlaka, modifikacija površinskih svojstva obradom pomoću kisikove i dušikove plazme te defunkcionalizacija površine primjenom UV i IR lasera. Karakterizacija površinske energije mjerenjem kontaktnog kuta, SEM, XPS, FTIR-ATR i analiza hrapavosti ispitivanih elastomera i njihovih komponenti, daje opis površinske energije, polarnosti i drugih površinskih svojstava spomenutih materijala.

Broj stranica: 205
Broj slika: 74
Broj tablica: 14
Broj referencija: 148
Jezik izvornika: engleski

Ključne riječi: elastomer, gumena navlaka, plazma, površinska energija, laser

Datum obrane:

Reviewers: prof. dr. sc. Stanislav Bolanča, predsjednik
prof. dr. sc. Mladen Lovreček, mentor
prof. dr. sc. Miran Mozetič, mentor
doc. dr. sc. Marta Klanjšek Gunde, vanjska članica
doc. dr. sc. Vesna Džimbeg-Malčić, članica

Rad je pohranjen:

If you interact with things in your life, everything is constantly changing.

And if nothing changes, you're an idiot.

Umberto Eco (Spiegel Online, 2009)

Acknowledgements

After more than three years of study and two years of hard work, my doctoral thesis is finished. It is time now to present the results to the colleagues investigating in the same field and to a wider scientific community, to surrender to their criticism and common search for the ways to continue the work begun here. Despite being undersigned with my name, the thesis was prepared with a friendly support of many people who believed in my work and me; therefore, I would like to take this opportunity to express my gratitude.

Main thanks go to the supervisors, Dr. Sc. Mladen Lovreček and Dr. Sc. Miran Mozetič, for their effort, advice, patience, kindness and time devoted to me. Without their support, this thesis would never exist.

Special thanks to Dr. Sc. Darko Agić, who encouraged me to begin the doctoral study and indicated the path to the goal; Dr. Sc. Marie Kaplanová for the introduction into the world of surface energy and help with the measurements, Dr. Sc. Marta Klanjšek Gunde for great ideas, tips, extensive discussions and help with opening all the necessary doors; Ljubica Kraljević Trobec for the support from the company Savatech in submitting the samples and providing the knowledge on rubber technology, which she forwarded to me.

I highly appreciate the support by Dr. Sc. Vili Bukošek, Drago Kovačič, Dr. Sc. Odon Planinšek, Dr. Sc. Stane Srčič and Dr. Sc. Alenka Vesel, who acquainted me with the hi-tech research equipment and methods, and helped me to attain significant results in the investigation with their contribution and advice.

For the help in conducting measurements, access to laboratory equipment, advice and support I would like to thank Kristina Eleršič, Biljana Govedarica, Dr. Sc. Diana Gregor Svetec, Dr. Sc. Nina Hauptman, Dr. Sc. Jiři Hejduk, Janez Japelj, Dr. Sc. Dejana Javoršek, Ita Junkar, Dr. Sc. Tomaž Kos, Petra Lotrič, Jana Rozman, Dr. Sc. Barbara Simončič, Dr. Sc. Zoran Šušterič, Janez Trtnik and Dr. Sc. Raša Urbas. I met most of them for the first time during the research, some I have known for some time now; nevertheless, they all friendly helped me to overcome the problems, and they significantly contributed to the results and comments in the work in front of you.

Moreover, many thanks go to the institutions and enterprises, where the research was conducted, i.e. University of Zagreb, Faculty of Graphic Arts; "Jožef Stefan" Institute, Department of Surface Engineering and Optoelectronics; University of Ljubljana, Faculty of Pharmacy, and Faculty of Natural Sciences and Engineering; National Institute of Chemistry, Ljubljana; University of Pardubice, Faculty of Chemical Technology, Savatech d. o. o., Kranj and LPKF Laser & Elektronika d. o. o., Naklo.

I would like to thank Barbara Luštek Preskar for editing the English text.

Thanks to the Public Fund of the Republic of Slovenia for Human Resources Development and Scholarships for the financial support.

Thanks to Lea, Gašper, Miha, Aleš and Dominika for their patience, support and help.

Gorazd

Zahvala

Nakon više od tri godine studija i dvije godine napornog rada doktorska disertacija je napisana. Došlo je vrijeme da rezultate prezentiram kolegama, koji istražuju na istom području, i široj znanstvenoj javnosti te da se prepustim njihovoj kritici i zajedničkom traženju puteva za nastavak ovdje započetog rada. Disertacija potpisana je mojim imenom, ali nastala je uz prijateljsku podršku mnogih ljudi, koji su vjerovali u mene i moj rad, zato želim iskoristiti priliku da se svima zahvalim.

Glavna zahvala ide mentorima, dr. sc. Mladenu Lovrečeku i dr. sc. Miranu Mozetiču, za njihove napore, savjete, strpljivost, ljubaznost i vrijeme posvećeno meni. Bez njihove podrške ovaj rad ne bi nastao.

Posebice zahvaljujem dr. sc. Darku Agiću, koji me ohrabrio da započnem doktorski studij i naznačio put prema cilju; dr. sc. Marie Kaplanovi za uvođenje u svijet površinskih energija i pomoć kod mjerenja, dr. sc. Marti Klanjšek Gunde za odlične ideje, savjete, opsežne razgovore i pomoć kod otvaranja svih vrata; Ljubici Kraljević Trobec za podršku u poduzeću Savatech, kod dobivanja uzoraka i znanja o gumarstvu, koja mi je proslijedila.

Visoko cijenim podršku dr. sc. Vilija Bukoška, Draga Kovačiča, dr. sc. Odona Planinška, dr. sc. Staneta Srčiča i dr. sc. Alenke Vesel, koji su me upoznali vrhunskom opremom i metodama za istraživanje, te svojim radom i savjetima pomogli do bitnih rezultata istraživanja, za koje se zahvaljujem.

Za pomoć kod provođenja mjerenja, pristupa laboratorijskoj opremi, savjete i podršku zahvaljujem se Kristini Eleršič, Biljani Govedarici, dr. sc. Diani Gregor Svetec, dr. sc. Nini Hauptman, dr. sc. Jiřiju Hejduku, Janezu Japlju, dr. sc. Dejani Javoršek, Iti Junkar, dr. sc. Tomažu Kosu, Petri Lotrič, Jani Rozman, dr. sc. Barbari Simončič, dr. sc. Zoranu Šušteriču, Janezu Trtniku in dr. sc. Raši Urbas. Večinu spomenutih upoznao sam tokom istraživanja, sa nekima poznajem se već dugo, ali svi su mi prijateljski pomogli prevladavanju problema i znatno pridonijeli rezultatima i komentarima u radu, koji je pred vama.

Isto tako zahvala ide institucijama i poduzećima, u kojima se provodilo istraživanje: Sveučilište u Zagrebu, Grafički fakultet; Institut "Jožef Stefan", Odsjek za tehnologiju površina i optoelektroniku; Sveučilište u Ljubljani, Fakultet za farmaciju i Prirodoslovno-tehnološki fakultet; Kemijski institut u Ljubljani; Sveučilište u Pardubicama, Kemijsko-tehnološki fakultet; Savatech d. o. o., Kranj i LPKF Laser & Elektronika d. o. o., Naklo.

Za lektoriranje teksta na engleskom jeziku zahvaljujem se Barbari Luštek Preskar.

Zahvaljujem se Javnom fondu Republike Slovenije za razvoj kadrova i stipendije za financijsku podršku.

Hvala Lei, Gašperu, Mihi, Alešu i Dominiki za strpljivost, podršku i pomoć.

Gorazd

Zahvala

Po več kot treh letih študija in dveh letih trdega raziskovalnega dela je doktorska disertacija napisana. Prišel je čas da z rezultati seznanim kolege, ki raziskujejo na istem področju, in širšo znanstveno javnost ter se izpostavim njihovi kritiki in skupnemu iskanju poti za nadaljevanje tukaj začetega dela. Pod disertacijo sem sicer podpisan sam, vendar je nastala s prijazno podporo in pomočjo mnogih ljudi, ki so verjeli vame in v moje delo, za kar bi se jim ob tej priložnosti rad zahvalil.

Glavna zahvala gre obema mentorjema, dr. Mladenu Lovrečku in dr. Miranu Mozetiču, za njun trud, nasvete, potrpežljivost, prijaznost in čas, ki sta mi ga namenila. Brez njune podpore tega dela ne bi bilo.

Posebej se zahvaljujem dr. Darku Agiću, ki me je spodbudil k doktorskemu študiju in mi nakazal pot do cilja; dr. Marie Kaplanovi za uvajanje v svet površinskih energij in pomoč pri meritvah; dr. Marti Klanjšek Gunde za odlične ideje, nasvete, izčrpne pogovore in za vsa vrata, ki mi jih je pomagala odpreti; Ljubici Kraljević Trobec za pridobljeno podporo v podjetju Savatech, pri pridobivanju vzorcev in znanja o gumarstvu, ki mi jih je posredovala.

Visoko cenim podporo dr. Vilija Bukoška, Draga Kovačiča, dr. Odona Planinška, dr. Staneta Srčiča, in dr. Alenke Vesel, ki so me seznanili z vrhunsko raziskovalno opremo in metodami, ter mi s svojim delom in nasveti pomagali do ključnih rezultatov raziskave, za kar se jim zahvaljujem.

Za pomoč pri izvedbi meritev, dostop do laboratorijske opreme, nasvete in podporo se zahvaljujem tudi Kristini Eleršič, Biljani Govedarici, dr. Diani Gregor Svetec, dr. Nini Hauptman, dr. Jiřiju Hejduku, Janezu Japlju, dr. Dejani Javoršek, Iti Junkar, dr. Tomažu Kosu, Petri Lotrič, Jani Rozman, dr. Barbari Simončič, dr. Zoranu Šušteriču, Janezu Trtniku in dr. Raši Urbas. Večino navedenih sem spoznal šele med tem raziskovalnim delom, nekatere poznam že dolgo, vsi pa so mi prijateljsko pomagali pri premagovanju težav in pomembno doprinesli k rezultatom in komentarjem v delu, ki je pred vami.

Zahvala gre tudi ustanovam in podjetjem, kjer je potekalo raziskovalno delo: Univerza v Zagrebu, Grafična fakulteta; Inštitut "Jožef Stefan", Odsek za tehnologijo površin in optoelektroniko; Univerza v Ljubljani, Fakulteta za farmacijo in Naravoslovnotehniška fakulteta; Kemijski inštitut v Ljubljani; Univerza v Pardubicah, Kemijsko-tehnološka fakulteta; Savatech d. o. o., Kranj in LPKF Laser & Elektronika d. o. o., Naklo.

Za lektoriranje angleškega teksta se zahvaljujem Barbari Luštek Preskar.

Zahvaljujem se Javnemu skladu Republike Slovenije za razvoj kadrov in štipendije za finančno podporo.

Hvala Lei, Gašperju, Mihu, Alešu in Dominiki za potrpežljivost, podporo in pomoč.

Gorazd

Abstract

The aim of the thesis was to investigate the surface free energy, roughness and other surface properties of NBR and EPDM lithographic offset “rubber blankets“, to functionalize the surface properties with an oxygen and nitrogen plasma treatment, and to defunctionalize the surface by applying IR and UV lasers. The characterization of the surface free energy with contact angle measurements using test liquids with different surface tension and polarity, SEM (scanning electron microscopy), XPS (X-ray photoelectron spectroscopy), and roughness analysis of the investigated elastomers and their components provided a description of specific surface functional groups that are in correlation with the surface free energy, polarity and other surface characteristics of elastomers. Therefore, their adsorption potential changes and their hydrophilic/ oleophilic or hydrophobic/oleophobic properties can indirectly be evaluated.

The chemical analysis of the surface of elastomer (“rubber blanket“) after the plasma and laser treatment, compared to the untreated samples, showed significant changes only in sulphur used as the curing agent. Other, less significant changes in the chemical composition occurred due to the chemical reactions of plasma species with the silica filler or additives, rather than with the basic macromolecular structure of the elastomer. With the uncured crude rubbers, there were no apparent chemical changes after the oxygen plasma or UV laser treatment, while there were simultaneously significant changes in the surface free energy and polarity. With crude rubber, the changes took place due to the changes in the macromolecular structure of the surface.

“Rubber blanket“ is a well-known ink transfer media in lithographic offset and other conventional or digital printing techniques, where it is used as the secondary printing forme. The rendering of the “rubber blanket“ surface by using a plasma and laser treatment for a selective defunctionalization is opening new possibilities in using the “rubber blanket“ as an image carrier in the printing process and thus offers a new challenge for future research.

Keywords: elastomer, offset rubber blanket, plasma, surface free energy, laser

Sažetak

Cilj doktorske teze je istraživanje površinske slobodne energije, hrapavosti i drugih svojstva površine NBR i EPDM ofsetnih "gumenih navlaka", funkcionalizacija površinskih svojstva obradom pomoću kisikove i dušikove plazme te defunkcionalizacija površine primjenom IR i UV lasera. Karakterizacija površinske slobodne energije mjerenjem kontaktnog kuta primjenom testnih tekućina sa različitom površinskom napetošću i polarnošću, SEM (skenirna elektronska mikroskopija), XPS (spektroskopija rendgenskim zrakama) i analiza hrapavosti ispitivanih elastomera i njihovih komponenti, daje kvantitativni opis za plazmu specifičnih površinskih funkcionalnih grupa, koje su u korelaciji s površinskom energijom, polarnošću i drugim površinskim svojstvima spomenutih materijala, tako da se mogu procijeniti promjene adsorpcijskog potencijala, odnosno njegova hidrofilna/oleofobna ili hidrofobna/ oleofilna svojstva.

Kemijska analiza površine elastomera ("gumene navlake") nakon obrade plazmom i laserom, u usporedbi sa neobrađenim uzorcima, pokazuje velike promjene samo kod sumpora, koji je korišten za vulkanizaciju. Druge, manje vidljive promjene u kemijskoj strukturi nastale su zbog kemijskih reakcija čestica plazme sa silika punilom ili sa dodacima, radije nego sa osnovnom makromolekularnom strukturom elastomera. Kod nevulkanizirane sirove gume nema vidljivih kemijskih promjena nakon obrade kisikovom plazmom ili UV laserom, uz istovremene značajne promjene površinske slobodne energije i polarnosti. Kod sirove gume promjene su uzrokovane promjenom makromolekularne strukture površine.

"Gumena navlaka" dobro je poznati medij za prijenos tiskarske boje u ofsetnom i drugim konvencionalnim i digitalnim tiskarskim tehnikama, gdje djeluje kao sekundarna tiskovna forma. Zapisivanje na površinu "gumene navlake" pomoču obrade plazmom i laserom za selektivnu defunkcionalizaciju, otvara nove mogučnosti u njezinoj upotrebi o ulogi nosioca slike u tiskovnom procesu i time novi izazov za buduča istraživanja.

Ključne riječi: elastomer, ofsetna gumena navlaka, plazma, površinska slobodna energija, laser

Proširenи sažetak

Gorazd Golob

Promjena površinske energije elastomera primjenom kisikove i dušikove plazme uz lasersku deaktivaciju površine

1 Uvod

U uvodnom poglavlju disertacije definirani su osnovni pojmovi i mehanizmi plošnog tiska, u engleskom jeziku poznatog pod imenom "lithography". Ista riječ koristi se i na području proizvodnje mikročipova, gdje se ponekad, uz konvencionalne, koriste i tiskarske tehnike za postizanje prikladne funkcionalnosti čipa od silicija, koje nisu bile predmet ove studije. Postavljen je glavni cilj istraživanja površinskih svojstava elastomera: redukcija broja elemenata u ofsetnom plošnom tisku, objedinjavanjem funkcionalnosti tiskovne forme i gumene navlake, čime se otvara prilika za razvoj u području konvencionalnih i digitalnih tehnika tiska. Modifikacija slobodne površinske energije elastomera, kemijske promjene površine i promjene u hrapavosti kod funkcionalizacije uz primjenu plazme i diskretna defunkcionalizacija primjenom lasera, za dobivanje površina sa različitim svojstvima postavljeni su kao glavni predmeti istraživanja.

2 Osnove

Prikazane su osnove terminologije, materijala, procesa i fenomena u procesima grafičke reprodukcije, koje značajno utječu na postizanje ciljeva, metoda i rezultate istraživanja. Pregled literature i preliminarni testovi stvaraju osnovu za oblikovanje hipoteze istraživanja.

2.1 Tiskovne forme

Tiskovne forme za konvencionalni plošni tisak sa oleofilnim/ hidrofobnim tiskovnim elementima i hidrofilnim/oleofobnim netiskovnim površinama omogućuju tiskanje u plošnom tisku, korištenjem prikladne otopine za vlaženje i odgovarajuće tiskarske boje, koja sadrži nepolarne molekule viših masnih kiselina. Kod bezvodnog (suhog) plošnog tiska selektivno obojenje oleofilnih tiskovnih elemenata omogućeno je prekrivanjem netiskovnih površina tankom oleofobnom silikonskom prevlakom.

Poznatih je mnogo patentiranih rješenja izrade tiskovnih formi od tvrdog feromagnetnog materijala, keramike, poluvodiča, silicija, cirkonija ili aluminija, koji se mogu obraditi plazmom, laserom, električnim nabijanjem, magnetiziranjem ili korištenjem drugih tehnika za reverzibilno podešavanje njihovih površinskih svojstava. Samo jedan od tih patenta bazira na elastomernoj površini, laminiranoj na temeljnoj ploči.

Slobodna površinska energija tiskovnih i netiskovnih površina tiskovne forme u plošnom tisku prikazana je na osnovu literature (MacPhee; Lovreček, Gojo, Dragčević) i na osnovu izračuna iz izmjerenih kontaktnih kutova sa testnim tekućinama. Na konvencionalnoj tiskovnoj formi zadovoljava približno 30 mJ/m^2 razlike u slobodnoj površinskoj energiji između tiskovnih i netiskovnih površina. Na tiskovnoj formi za bezvodni plošni tisak dovoljna je razlika od 20 mJ/m^2 ukupne slobodne površinske energije uz 13 mJ/m^2 razlike u disperznoj komponenti između netiskovnih i tiskovnih površina. Razlike u kemijskom sastavu tiskovnih i netiskovnih elemenata određene su metodom FTIR-ATR, dok je razlika u hrapavosti izmjerena aparatom Mahr M1.

2.2 Elastomeri

Prikazane su definicije i osnovna svojstva elastomera te objašnjene razlike između gume ili sirove gume (nevulkanizirane) i elastomera (križno povezane makromole-kule, vulkanizacija). Opisan je kemijski sastav sintetskih guma tipa NBR, EPDM i T (prema nomenklaturi ASTM), koje su korištene za izradu elastomera u gornjem, završnom sloju ispitivanih ”gumenih navlaka”.

2.3 Gumene navlake

Višeslojni, kompozitni materijal, poznat pod nazivom ”gumena navlaka”, s gornjim, završnim slojem od prikladnog elastomera, mora imati dobra mehanička i kemijska svojstva uz zadanu ukupnu debljinu. Na tiskarskom stroju namješta se na valjak, koji se nalazi između plošnog cilindra sa tiskovnom formom i tiskovnog cilindra, koji nosi tiskovnu podlogu (najčešće papir). Na kvalitetu otiska ima značajan utjecaj podešavanje odgovarajućeg tiskovnog tlaka i mehanička obrada površine ”gumene navlake” (najčešće brušenjem).

2.4 Slobodna površinska energija

Slobodna površinska energija može biti definirana kao razlika u privlačnim silama između molekula na površini i molekula unutar materijala, odnosno kao višak energije na površini materijala. Metode za određivanje slobodne površinske energije baziraju na mjerenju kontaktnih kutova kod kapi testnih tekućina na ravnoj, homogenoj površini materijala. Osnovnu matematičku jednadžbu za izračunavanje slobodne površinske energije tvrdog materijala na osnovu izmjerenog kontaktnog kuta i poznate slobodne površinske energije testne tekućine postavio je Young. Nadopunjene metode Fowkesa, Owensa i Wendta, Wuja te van Ossa, Chaudhurya i Gooda, omogućuju određivanje ukupne slobodne površinske energije uz disperznu i polarnu komponentu, odnosno komponenata, koje zbrojene daju ukupnu slobodnu površinsku energiju. Rezultat izračunavanja ukupne slobodne površinske energije i njenih komponenta ovisi o korištenoj metodi. Za izračunavanje slobodne površinske energije hrapave površine koriste se metode Wenzela u slučaju dobrog kontakta kapi tekućine s površinom ili Cassie i Baxter metoda u slučaju tekućine koja nije u kontaktu sa površinom.

2.5 Modifikacija svojstava površine elastomera

Slobodna površinska energija, odnosno adhezija elastomera prema tekućinama i drugim materijalima može se podesiti na sličan načina kao kod drugih polimera, gdje se koriste različite metode: pranje vodom, čišćenje otapalima, mehaničko čišćenje, kemijsko jetkanje, kemijsko premazivanje, taloženje akrilatnim premazima, mokra kemijska obrada, fluorinacija, obrada plamenom, koronom, plazmom, jetkanje uz bombardiranje ionima, obrada mlazom elektrona, intenzivno UV zračenje, obrada laserom, elektrostatičko pražnjenje.

Kao posebno zanimljive detaljnije su obrađene metode funkcionalizacije na osnovu mehaničke promjene hrapavosti, promjene makromolekularne strukture, obrade plazmom i laserom. Mehaničkom obradom odnosno brušenjem mogu se postići ekstremne razlike u svojstvima površine, od super-hidrofilnosti do super-hidrofobnosti, ovisno o intenzitetu obrade i o svojstvima polimera. Oksidacija elastomera (na bazi prirodne gume) kemijskim tretiranjem daje hidrofilnu površinu, koja nakon zagrijavanja u vodi ponovno prelazi u hidrofobno stanje, ovisno o preoblikovanju makromolekularne strukture površine.

Obrada površine plazmom uzrokuje kemijske promjene, oduzimanje ili depoziciju materijala. Ovi procesi mogu se događati istovremeno, a od karakteristika plazme ovisi koji će učinak biti dominantan. Aktivacija polimera plazmom je zamjena kemijskih grupa ili njihovih komponenti na osnovnom lancu polimera. Dubina takve funkcionalizacije je vrlo mala, do nekoliko molekula. Za funkcionalizaciju koristi se plazma na osnovu različitih plinova npr. O_2, N_2, He, Ar, NH_3, N_2O, CO_2 i zrak ili njihove kombinacije. Kratki sažetci objava različitih autora pokazuju da se prikladnim izborom vrste i uvjeta primjene plazme mogu postići veoma različita svojstva površine polimera odnosno elastomera.

Laserskom obradom površine mogu se postići različite promjene, koje se temelje na lasersko induciranoj plazmi, fotokemijskim ili fototermalnim pojavama, kao što su uklanjanje materijala (ablacija), kemijska degradacija, preklapanje cis-trans izomerizacije ili njihovim kombinacijama.

Iz pregleda objavljenih radova može se zaključiti, da se izvode vrlo različita istraživanja djelovanja plazme ili lasera na polimere pod različitim uvjetima, a koja daju međusobno slabo usporedive rezultate. Medjutim, ti rezultati ukazuju na jasno vidljive i mjerljive promjene svojstava površine, koja može nakon obrade imati veću ili manju hidrofilnost, odnosno slobodnu površinsku energiju.

2.6 Znanstveni izazov i hipoteze

Smanjena potrošnja materijala, energije i skraćivanje vremena proizvodnje kod visoke kvalitete, uz niske troškove i okolišu prijateljska proizvodnja glavni je stručni izazov. U suvremenom tiskarskom stroju ofsetni valjak s ”gumenom navlakom” ima samo jednu funkcionalnost, to je prenošenje tiskarske boje s tiskovne forme na tiskovnu podlogu. Stvaranjem tiskovnih i netiskovnih površina na ”gumenoj navlaci”, konvencionalna tiskovna forma postaje suvišna. Godišnja potrošnja u svijetu je 50 milijardi m^2, pa bi već djelomična zamjena tiskovnih formi s ”gumenim navlakama”, koje bi sadržavale tiskovne elemente i netiskovne površine, značila veliki doprinos u pogledu troškova i okoliša.

Značajan podsticaj u tom smjeru je patentirana (Mozetič i suautori) funkcionalizacija materijala s diskretnom defunkcionalizacijom korištenjem mlaza elektrona. Na osnovu

preliminarnih ispitivanja s komercijalno dostupnim uzorcima ”gumene navlake” pokazala se mogućnost prikladne funkcionalizacije primjenom kisikove plazme. Time se otvaraju i nova moguća područja primjene u tisku i u produkciji elektroničkih komponenti.

Znanstveni pristup zahtijeva dobru pripremu uzoraka, kontrolirane uvjete kod njihove obrade i prikladne mjerne metode za stvaranje čvrstih znanstvenih zaključaka i doprinosa. ”Gumena navlaka” tehnički je materijal sa nepoznatim (neobjavljenim) karakteristikama. Za svaki tip gumene navlake koristi se smjesa različitih sirovih guma iz različitih izvora, s različitim sredstvima za križno povezivanje makromolekula i dodacima. Proizvodni uvjeti npr. temperatura ili vrijeme za svaku proizvodnu operaciju tretiraju se kao industrijska tajna. Poznata i kontrolirana su samo svojstva gotovog proizvoda.

Početni znanstveni izazov uključuje proučavanje fizikalnih i kemijskih svojstava funkcionalizirane ”gumene navlake”, obrađene kisikovom ili dušikovom plazmom. Tipične metode za određivanje funkcionalizacije odnosno slobodne površinske energije, temelje se na mjerenju kontaktnih kutova, dok se za određivanje promjena u kemijskoj strukturi površine u literaturi najčešće spominju XPS, FTIR-ATR i AFM.

Površinska svojstva sirovina za proizvodnju ”gumene navlake” određena su samo za najčešće korištene sirove gume i silika punila.

Za diskretnu defunkcionalizaciju površine ispitana je metoda zagrijavanja laserom, čime bi se provela redukcija i/ili resetirala makromolekularna struktura elastomera. Prema literaturi očekivalo se vraćanje funkcionalizirane površine u početno stanje uz manje kemijske ili strukturne razlike, koje bi na kraju eksperimenta mogli identificirati i interpretirati.

Time su postavljene slijedeće hipoteze istraživanja:

Površinska energija navlake može se značajno povećati obradom pomoću plinske plazme kod niskog tlaka.

Površinska energija se povećava nastankom površinskih funkcionalnih grupa.

Površinska energija se povećava zbog porasta doze O ili OH radikala do zasićenja koje nastaje kod određene doze.

Povećanjem površinske energije povećava se adsorpscijski kapacitet tretirane površine.

Lokalno zagrijavanje prikladnim laserom omogućuje selektivnu defunkcionalizaciju površine.

3 Uzorci materijala

Uzorci ”gumenih navlaka”, sirovih guma i punila dobiveni su od Savatech d.o.o., Kranj, proizvođača ”gumenih navlaka”. Sve tekućine, korištene u pripremi uzoraka ili kod mjerenja, bile su p.a. čistoće.

3.1 Gumene navlake

Korištene su ”gumene navlake”, prikazane u tablici S1.

Tablica S1: Uzorci ”gumenih navlaka”, korišteni za ispitivanje.

Trgovačko ime navlake	Oznaka	Sirova guma	Polarnost	Punilo	Sredstvo za križno povezivanje
Advantage UV Red	RED	EPDM	Nepolarna	Silika	Sumpor
Advantage UV Black	BLACK	EPDM	Nepolarna	Carbon black	Sumpor
Advantage Plus	LIGHT BLUE	NBR/TM 90/10	Polarna (NBR)	Silika	Sumpor
Advantage DUAL	BLUE	NBR/TM 90/10	Polarna (NBR)	Silika	Sumpor, jače križno povezivanje
Advantage Expression	CYAN	NBR/TM 90/10	Polarna (NBR)	Silika	Sumpor
Advantage 8848	8848	BR/XNBR 90/10	Nepolarna (BR) Polarna (XNBR)	Silika	Sumpor

Svaki tip ”gumene navlake” prikladan je samo za određene uvjete tiska. Navlake na bazi EPDM gume koriste se za tisak sa UV polarnim tiskarskim bojama, dok se navlake na bazi NBR sirove gume koriste za tisak sa konvencionalnim nepolarnim uljanim tiskarskim bojama.

Svi uzorci bili su izrezani na komade prikladne veličine približno 10 × 50 mm, očišćeni papirom natopljenim etanolom i osušeni najmanje 15 minuta prije tretiranja ili mjerenja.

3.2 Sirova guma

Korištena su tri uzorka NBR i jedan uzorak EPDM sirove gume, prikazani u tablici S2.

Tablica S2: Uzorci sirove gume (specifikacija prema proizvođaču/dobavljaču)

Trgovačko ime	Oznaka	Savatech koda	Specifikacija
Europrene 19.45 GRN	Glass 2	1047	NBR, Polimeri Europa, Italy 19 % akrilonitrila, Mooney viskoznost 45 MU (internal)
Krynac 33.30 F	Glass 1	2215	NBR, Bayer Elastoméres, France 33 % akrilonitrila, Mooney viskoznost 30 MU (ISO 289)
Europrene 45.60 N	Glass 3	7167	NBR, Polimeri Europa, Italy 45 % akrilonitrila, Mooney viskoznost 60 MU (internal)
Keltan 8340 A	Glass 4	7394	EPDM, DSM Elastomers 55 % etilena, 5.5 % ENB (etiliden-norbonen) termonomera Mooney viskoznost 80 MU (ISO 289)

Za obradu plazmom i laserom te za većinu mjerenja uzorci bili su razrezani na male komade, rastopljeni u toluenu i naneseni u tankom sloju na laboratorijsko staklo, gdje je nakon sušenja dobiven suhi sloj debljine ~ 0,1 mm. Na uzorcima Glass 1 i Glass 4 dobivena je relativno glatka i ravna površina, kod Glass 1 površina ostala je ljepljiva nakon sušenja. Površina Glass 2 i Glass 3 nakon sušenja postala je hrapava i neravna. Zbog nepravilnosti na površini moguć je utjecaj na rezultate mjerenja, neka mjerenja se nisu izvodila na tim uzorcima.

3.3 Silika punilo

Za mjerenja korištene su dvije vrste silike, Ultrasil 7000 GR u granulama s oznakom A i modificirana silika VP Coupsil 6508 u obliku bijelog praška sa oznakom B. Prema literaturi silika, čije su čestice promjera nekoliko nm, bitno utječe na svojstva elastomera. Zbog jake adhezije između čestica čiste silike, stvaraju se djelići, agregati i aglomerati veličine od 10 nm do 1000 nm.

4 Znanstvene metode i oprema

Za pripremu i obradu uzoraka korišteni su laboratoriji na Prirodoslovno-tehnološkom fakultetu, Sveučilišta u Ljubljani, Inštituta "Jožef Stefan" u Ljubljani i tvrtke LPKF Laser & Elektronika d.o.o. u Naklom. Za izvođenje mjerenja, uz opremu na navedenim lokacijama, koristila se oprema u laboratorijima Fakulteta za farmaciju, Sveučilišta u Ljubljani, Kemijskog instituta iz Ljubljane, poduzeća Savatech d.o.o. iz Kranja te Sveučilišta u Pardubicama, Češka Republika.

Određena oprema bila je na raspolaganju samo kratko vrijeme. Mjerenja plazmom ili laserom obrađenih uzoraka, zbog mogućeg kratkotrajnog učinka obrade, po pravilu bila su provedena tijekom jednog dana. Neka od mjerenja bila su iz tih razloga izvedena samo u ograničenom obimu, ali zadovoljavajućem za realizaciju istraživanja i donošenje osnovnih zaključaka.

4.1 Obrada plazmom

Obrada kisikovom ili dušikovom plazmom prema literaturi povećava hidrofilnost polimernih uzoraka.

Korišten je laboratorijski plazma reaktor u obliku staklene cijevi, spojene sa vakuumskom pumpom i priključkom za dovod plina, indukcijski spojene sa RF generatorom. Svi uzorci bili su izloženi kisikovoj plazmi s gustoćom neutralnih atoma $5 \times 10^{21}\ m^{-3}$ ($4 \times 10^{21}\ m^{-3}$), gustoćom elektrona $8 \times 10^{15}\ m^{-3}$ i elektronskom temperaturom 45000 K za 0, 3, 9, 27, 81, 243 i 729 s. Uzorci bili su tretirani kod potencijala –15 V. Tlak kod niskog vakuuma bio je 75 Pa. Nakon tretiranja plazmom izmjereni su kontaktni kutovi s vodom, a sva mjerenja su ponovljena nakon 3 i 24 h.

Pokazalo se da je maksimalni efekt obrade postignut kod vremena od 27 s, bez vidljivih oštećenja površine. U nastavku ispitivanja svi uzorci bili su obrađeni pod istim uvjetima kod 27 s. Za obradu dušikovom plazmom isto tako korišteno je vrijeme obrade od 27 s.

4.2 Laserska obrada

Nakon bezuspješnih pokušaja obrade laserima niske snage, korišteni su profesionalni IR i UV laseri, koji se koriste za ablaciju i markiranje u proizvodnji elektroničkih

komponenti i na drugim područjima. Snaga pulsa lasera bila je podešena za postizanje jedva vidljive promjene na površini uzorka.

Nd:YAG IR laser (1064 nm) prosječne snage 16 W podešen je promjenom struje napajanja LED svjetla, promjenom rastera (širine laserske zrake) i fokusa na realnu snagu pulsa 621 W kod frekvencije 200 kHz uz trajanje pulsa 85 ns. Tako podešenim laserom obrađeni su uzorci RED, LIGHT BLUE i BLUE, dok podešavanje za uzorak BLACK, zbog prevelike snage pulsa, nije bilo uspješno, jer je i kod najmanje podešene snage dolazilo do jake ablacije površine.

Nd:YAG UV laser (355 nm) prosječne snage 5 W podešen je promjenom frekvencije, rastera odnosno širine zrake i promjenom fokusa za RED, LIGHT BLUE i BLUE uzorak na prosječnu snagu od 0,17 W sa realnom snagom pulsa od 140 W. Manje dodatne promjene za pojedine uzorke postignute su pomakom uzorka izvan fokusa. Za BLACK uzorak izvedeno je podešavanje na 4,95 mm izvan fokusa.

4.3 Određivanje slobodne površinske energije

Za mjerenje kontaktnih kutova korišten je aparat Krüss DSA 100 uz programsku opremu DSA1 v. 1.9 sa standardnim tekućinama: voda, dijodometan, formamid i etilen glikol. Mjerenje bilo je izvedeno približno 20 s nakon aplikacije kapi tekućine, kada je postignuta mirna i stabilna slika kapi, koja se može snimiti i koristiti za izračunavanje kontaktnog kuta pomoću programske opreme.

Za izračunavanje slobodne površinske energije korištene su metode prema Owensu, Wendtu, Rabelu i Kaelble-u; Wu-ju i prema van Ossu & Goodu. Djelomično korištena je i metoda EOS (equation of state).

4.4 Skenirna elektronska mikroskopija – SEM

Korištena su dva SEM uređaja, JEOL JSM-6060LV za dobivanje slika površine uzoraka i Carl Zeiss FE-SEM SUPRA 35 VP opremljen sa EDS Oxford Instruments Inca 400 jedinicom za kemijsku analizu površine. Svi uzorci bili su prije snimanja ili analize vakuumsko napareni tankim slojem Au/Pd za povišenje električne vodljivosti. Kod kemijske analize tu presvlaku treba oduzeti od rezultata.

SEM-EDS radi na principu mjerenja karakterističnih rendgenskih zraka, uzbuđenih primarnim mlazom elektrona, koji sadržavaju informaciju o sastavu materijala do dubine približno 1 μm. Tehnika je prikladna za određivanje udjela elemenata s visokom atomskom masom npr. za punila i dodatke; podaci o sastavu organskih polimera manje su pouzdani.

4.5 Fourierova transformirana infracrvena spektroskopija - smanjenje totalne refleksije – FTIR-ATR

Na aparatu Perkin Elmer Spectrum GX1 pomoću ATR uređaja snimljeni su IR spektri u srednjem području 500–4000 cm^{-1}. Analiza snimljenih spektara izvedena je pomoću modula AnalyseItIR KnowItAll programske opreme tvrtke Bio-Rad Laboratories.

FTIR-ATR tehnika daje uvid u kemijske grupe i vezove na površini uzoraka. U ovom slučaju korišten je kristal dijamanta s relativno visokim refrakcijskim ideksom (n = 2,4), koji daje podatke do dubine uzorka približno 1,176 μm, uz najjači signal s površine uzorka.

4.6 Fotoelektronska spektroskopija rendgenskim zrakama – XPS

Korišten je aparat Physical Electronics Inc., model TFA, koji u visokom vakuumu djeluje na uzorak rendgenskim zrakama, koje uzrokuju emitiranje fotoelektrona različitih energija vezanja, karakterističnih za pojedine elemente iz kojih proizlaze. Ovom metodom može se odrediti kemijski sastav uzoraka do dubine približno 5 nm. Od svih korištenih metoda ova je najprikladnija za dobivanje informacija o kemijskom sastavu površine uzorka.

4.7 Druge mjerne metode

Korišteni su različiti optički mikroskopi. Za mikroskopske slike uzoraka korišten je mikroskop Leica sa maksimalnim povećanjem 35 ×, opremljen digitalnom kamerom.

Mjerenje hrapavosti izvedeno je perthometrom Mahr M1, hrapavost je izračunana iz profila površine i prikazana pomoću parametara hrapavosti R_a, R_z i R_{max}.

Dinamička mehanička analiza – DMA guma i elastomera izvedena je uređajem TA Instruments model Q 800. Uzorak, pričvršćen u mehanizam u zatvorenoj komori, tretira

se kod različitih mehaničkih opterećenja, u širokom rasponu temperatura. Na osnovu analize ponašanja uzorka izračunavaju se različiti značajni parametri npr. temperatura staklastog prijelaza Tg i tan δ, koji predstavlja omjer modula gubitaka prema modulu skladištenja.

UV-VIS spektroskopija u širokom spektralnom području valnih duljina 200–2000 nm omogućuje izračunavanje spektralne absorpcije pretvaranjem vrijednosti refleksijskih spektralnih vrijednosti u absorpcijske pomoću Beer-Lambertovog zakona. Korišten je spektrofotometar Perkin Elmer Lambda 950.

Inverzna plinska kromatografija – IGC na aparatu Agilent Technologies 6890N korištena je za određivanje površinskih svojstava silika punila, kod kojega metoda mjerenja kontaktnih kutova nije prikladna. Kod te metode mjeri se vrijeme ili koncentracija para otapala, koje prolaze kroz cijev, napunjenom praškastim uzorkom.

Mjerenje veličine i distribucije čestica silika punila izvedeno je na aparatu Malvern Instruments Master Sizer 2000, koji radi na principu difrakcije laserskih zraka. Za razbijanje aglomerata korištena je ultrazvučna obrada uzoraka u kupki od acetona, ali bez značajnog uspjeha.

Mikroskopija na atomsku silu – AFM korištena je za karakterizaciju površine uzorka kod ekstremno velikog povećanja. Rezultat mjerenja je profil površine, na kojeg utječu mehaničke kontaktne sile, van der Waalsove sile, kapilarne sile, kemijske veze, magnetne i druge sile, ovisno o uvjetima mjerenja. Ova metoda korištena je samo za dva uzorka.

Hvatanje boje izvedeno je prema Kangovoj modificiranoj metodi, kod koje se mjeri udio kapi tiskarske boje, prenesene s površine uzorka na standardni papir. Korištena je fleksografska tiskarska boja na vodenoj osnovi na odgovarajućem laboratorijskom uređaju.

5 Rezultati studije

Prikazani su samo najznačajniji rezultati. Drugi rezultati istraživanja prikazani su u prilogu, u objavljenim radovima sa međunarodnih konferencija.

5.1 Kontaktni kutovi i slobodna površinska energija

Iz grafičkog prikaza postignutih kontaktnih kutova sa vodom za korištene uzorke vidi se utjecaj vremena tretiranja plazmom na funkcionalizaciju površine i stabilnost promjene unutar 24 h. Grafički prikaz (slika S1, S2) izračunate slobodne površinske energije za uzorke ”gumenih navlaka” i sirovih guma pokazuje velike razlike u slobodnoj površinskoj energiji između netretiranih i plazmom i/ili laserom tretiranih površina uzoraka.

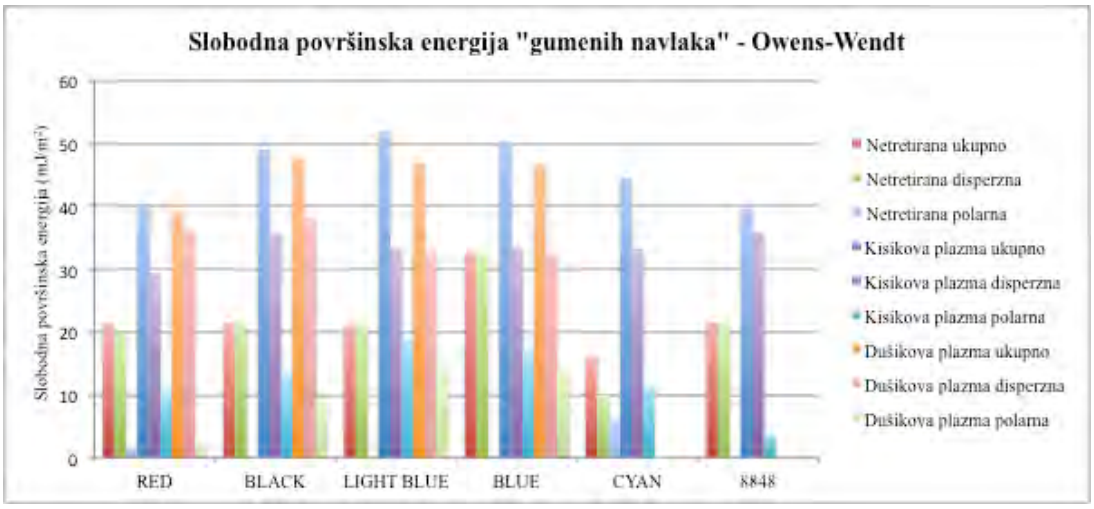

Slika S1: Površinska slobodna energija uzoraka ”gumenih navlaka”.

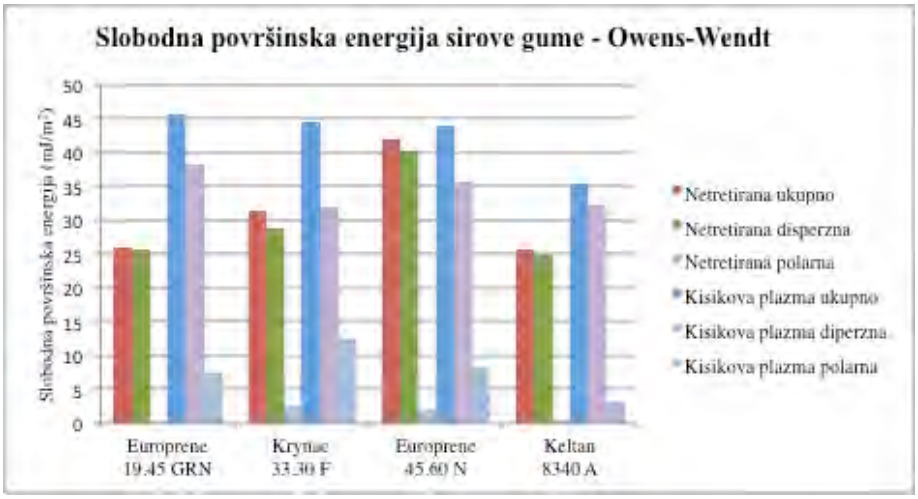

Slika S2: Površinska slobodna energija sirovih guma.

5.2 SEM slike

Na slikama dobro je vidljiva razlika između netretiranih i plazmom i/ili laserom tretiranih površina uzoraka.

SEM-EDS analiza BLUE uzorka pokazuje relativno male promjene udjela C, O, Al, Si, S, Ti, i Zn kod tretiranja plazmom i/ili laserom.

5.3 FTIR-ATR spektri i interpretacija rezultata

Razlike između netretiranih i tretiranih uzoraka prisutne su samo na nekoliko uskih područja spektra, iz kojih se vidi povećanje ili smanjenje udjela karakterističnih grupa ili vezova kod različitih tretiranja površine uzorka. Prikazani su samo rezultati za RED i BLUE uzorke gumenih navlaka. Spektri netretirane NBR i EPDM sirove gume (slika S3) skoro su identični nakon tretiranja plazmom i/ili laserom.

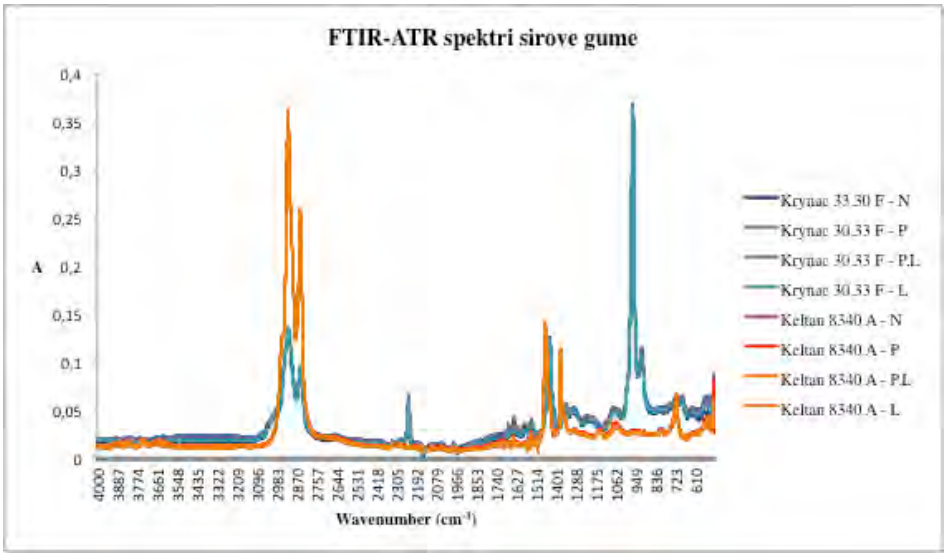

Slika S3: FTIR-ATR spektar sirovih guma (N – tretirano, P – tretirano kisikovom plazmom, L – tretirano UV laserom).

5.4 Rezultati XPS analize

Iz tabličnog prikaza rezultata analize RED i BLUE uzoraka vidljive su značajne razlike kod S2p (sumpor) i manje razlike kod drugih elemenata: C1s, N1s, O1s, Si2p i Zn2p3. Grafički prikaz promjena kemijske strukture nakon tretiranja plazmom nadopunjuje prikaz u tablici.

5.5 Slike snimljene optičkim mikroskopom i kamerom

Prikazane su ekstremne razlike u površini uzoraka nakon tretiranja.

5.6 Rezultati mjerenja hrapavosti

Iz izmjerenih hrapavosti RED i BLUE uzoraka prije i nakon tretiranja plazmom vidljive su samo manje razlike u hrapavosti.

5.7 Rezultati DMA analize

Iz kompleksnog grafičkog prikaza rezultata analize elastomera i sirove gume izdvojene su samo vrijednosti T_g i tan δ, koje su značajne za ovo istraživanje, ostale vrijednosti koriste se samo kao mjerilo mehaničkih svojstava materijala.

5.8 UV-VIS absorpcijski spektri

Iz absorpcijskih spektara vidljive su velike razlike u absorpciji između BLACK u usporedbi sa RED, LIGHT BLUE i BLUE uzoraka u IR području, dok su te razlike vrlo male u UV području. Pored absorpcijskih spektara na grafu su prikazane i valne duljine u istraživanju korištenih UV i IR lasera.

5.9 Rezultati inverzne plinske kromatografije – IGC

Prikazana je razlika u retencijskom vremenu za pare acetona između nemodificiranog i modificiranog silika punila.

5.10 Veličine čestica silika punila

Grafički prikaz i numerički podaci daju uvid u veličine i distribuciju čestica nemodificiranog i modificiranog silika punila.

5.11 Rezultati analize mikroskopom na atomsku silu - AFM

Grafički prikaz RED i BLUE netretiranih uzoraka daje uvid u strukturu površine i tipični profil površine gumenih navlaka.

5.12 Rezultati mjerenja hvatanja tiskarske boje

Tablični prikaz razlika u hvatanju boja na starim i novim uzorcima pokazuje razlike između različitih uzoraka bez značajne korelacije s preostalim rezultatima mjerenja.

6 Komentari i zaključak

Rezultati istraživanja potvrđuju očekivanja izdvojena na početku rada. Glavni ciljevi su postignuti, tako da se mogu prvi zaključci predstaviti znanstvenoj javnosti. Uvodni komentari prikazani su uz rezultate istraživanja, u ovom poglavlju prikazani su komentari, zapažanja i interpretacije značajnih rezultata.

6.1 Diskusija rezultata

Uzorci i metode istraživanja, veoma su osjetljivi na promjene uvjeta tokom pripreme i obrade uzoraka npr. vremena, temperature, relativne vlažnosti zraka u laboratoriju i na druge utjecaje. Sami uzorci bili su nehomogeni, hrapavi, ponekad neravni, uzorci sirove gume bili su ljepljivi. Ljudski faktor je vrlo značajan i skoro sve korištene metode ovise o znanju, iskustvu i ispravnim odlukama pri radu. U svim slučajevima, zaključci se temelje samo na rezultatima, kod kojih su razlike u izmjerenim vrijednostima potpuno jasno vidljive.

Određivanje prikladnog vremena tretiranja kisikovom plazmom pokazuje postizanje najmanjeg kontaktnog kuta s vodom kod 27 s za različite ”gumene navlake”. Manja odstupanja posljedica su samog procesa, greške kod mjerenja, nepravilne pripreme uzoraka ili nekih drugih razloga. Stabilnost promjene nakon 3 i 24 h omogućila je tretiranje laserom i različita mjerenja unutar 24 h.

Tretiranje dušikovom plazmom omogućuje funkcionalizaciju površine u manjoj mjeri nego primjenom kisikove plazme, zbog toga veći dio istraživanja proveden je tretiranjem uzoraka kisikovom plazmom.

Elastomeri na osnovu NBR sirove gume u literaturi često se nazivaju “polarni”. Netretirani NBR elastomeri imaju vrlo loše izraženu polarnu komponentu, koja značajno poraste nakon tretiranja, ali ostaje puno manja s obzirom na disperznu komponentu slobodne površinske energije.

Tokom ispitivanja pokazalo se, da tretiranje kisikovom plazmom NBR ili EPDM ”gumenoj navlaci” može značajno povisiti slobodnu površinsku energiju. Postignuta razlika između netretirane i plazmom tretirane ”gumene navlake” otvara mogućnost zapisivanja tiskovnih i netiskovnih površina na navlaci. Trajnost tako napravljene

“gumene tiskovne forme”, u kontaktu sa tiskovnim materijalom, valjcima za nanošenje otopine za vlaženje i valjcima za nanošenje tiskarske boje ostaje za sada nepoznata i predstavlja predmet daljnjih istraživanja. Za specifično ograničeno područje slobodne površinske energije i polarnosti gumene navlake potrebno je razviti i prilagoditi tekućine (otopina za vlaženje, tiskarska boja) s prilagođenim svojstvima (ukupna slobodna površinska energija uz prikladnu disperznu i polarnu komponentu), za nastavak istraživanja u tom smjeru.

Korištenje dušikove plazme daje manje promjene u postignutoj slobodnoj površinskoj energiji. Prema literaturi (Vesel i suautori) na površini teflona stvaraju se nove kemijske grupe kod tretiranja dušikovom plazmom, što nije slučaj kod tretiranja kisikovom plazmom. Taj fenomen trebalo bi istražiti kod NBR i EPDM elastomera.

Tretiranje sirove NBR gume kisikovom plazmom pokazuje značajnu ovisnost postignute promjene o udjelu akrilonitrilnih grupa. Kod malog udjela akrilonitrila promjena je značajna, dok je kod velikog udjela akrilonitrila promjena slobodne površinske energije vrlo mala. Za netretirane uzorke izmjerena razlika u slobodnoj površinskoj energiji u jakoj korelaciji je s udjelom akrilonitrila.

Defunkcionalizacija ”gumenih navlaka” upotrebom IR i UV lasera bila je samo djelomično uspješna u vraćanju svojstava površine na početne vrijednosti prije tretiranja plazmom. Očito korištenje samo UV lasera za tretiranje površine daje značajno manju slobodnu površinsku energiju kod EPDM tipa gumene navlake, dok je ta vrijednost malo viša kod NBR tipa gumene navlake, ako se usporede s netretiranim uzorcima. Promjene prouzrokovane UV laserom puno su manje u usporedbi s promjenama nakon tretiranja kisikovom plazmom.

Tretiranje uzoraka IR i UV laserom daje obećavajuće rezultate. Defunkcionalizacija nakon tretiranja plazmom samo je djelomično postignuta, pa time nije upotrebljiva za dobro zapisivanje na funkcionaliziranu površinu. To bi trebalo poboljšati promjenom kemijskog sastava uzoraka, korištenjem sredstva za križno povezivanje ili dodataka, koji bi se bolje odazivali na različite metode tretiranja plazmom ili laserom. Fino podešavanje procesa funkcionalizacije i defunkcionalizacije nije bilo moguće u dosadašnjim istraživanjima i trebalo bi se realizirati u budućnosti.

Na SEM slikama potvrđene su promjene u strukturi površine nakon tretiranja plazmom ili laserom.

Rezultati kemijske analize samo jednog BLUE uzorka pomoću SEM-EDS metode ne daju pouzdanu informaciju o kemijskim promjenama nakon tretiranja različitim metodama. Razlike u sadržaju kisika i ugljika pokazuju više vrijednosti nakon tretiranja kisikovom plazmom, manje vrijednosti nakon tretiranja UV laserom prethodno plazmom tretiranih uzoraka i još manje vrijednosti nakon tretiranja samo UV laserom.

Promjene u udjelu kisika i ugljika mogu se objasniti oksidacijom površine nakon tretiranja plazmom i stvaranjem CO i CO_2 plinova, koji se uparavaju na površini tokom tretiranja UV laserom. Prisutnost silicija i cinka u korelaciji je sa ugljikom i kisikom. Vodik nije detektiran, zbog toga ova metoda nije prikladna za analizu ugljikovodika. Trebali bi proširiti istraživanje i usporediti rezultate dobivene SEM-EDS metodom sa rezultatima, dobivenim drugim metodama.

FTIR-ATR kemijska analiza površine RED uzorka nakon tretiranja pokazuje promjene na dva vrha spektra, iz kojih se vidi smanjenje udjela SO_2 i CNH vezova te smanjenje udjela CH, CH_2 i CH_3 grupa. Za BLUE uzorak povećana absorpcija može biti rezultat oduzimanja polimernog materijala tokom tretiranja, nakon tretiranja na površini ostaje veći udio silika punila. Kemijske promjene preostalog elastomera nisu detektirane.

FTIR-ATR spektar EPDM i NBR sirove gume prije i poslije tretiranja ostaje nepromijenjen što upućuje na nepromijenjenu kemijsku strukturu površine do dubine ~ 1 μm. Ta tvrdnja nije u korelaciji sa razlikom u površinskoj slobodnoj energiji, određenoj prema metodi Owens-Wendt. Očigledno promjene proizlaze iz promjene strukture ili topologije površine, a ne formiranjem novih grupa ili drugih kemijskih promjena na površini uzorka. Osim toga promjene tokom tretiranja uzoraka UV laserom mogu se objasniti prekidom vezova makromolekularne strukture, kod koje svi elementi i većina vezova, pa time i kemijska struktura, ostaju nepromijenjeni, dok se mobilnost kraćih polimernih lanaca povećava. Rezultate može se također objasniti relativno velikom dubinom penetracije tokom FTIR-ATR mjerenja. Promijenjena kemijska struktura tankog gornjeg sloja površine možda ne može dovoljno pridonijeti promjeni izmjerenog FTIR-ATR spektra.

Rezultati XPS analize RED i BLUE uzoraka pokazuju značajne promjene u kemijskoj strukturi površine između netretiranih i kisikovom plazmom tretiranih uzoraka samo kod kisika vezanog na sumpor, gdje dolazi do formiranja SO_3 grupa, dok druge značajne kemijske promjene površine nisu vidljive. Vrijednosti za kisik, silicij i sumpor bile su više nakon tretiranja kisikovom plazmom, dok su vrijednosti za ugljik (i dušik kod BLUE uzorka) bile niže kod obadva elastomera.

Na osnovu analize samo dvoje uzoraka zaključci ne mogu biti pouzdani, zato bi ispitivanja trebalo ponoviti sa preostalim uzorcima i korištenjem drugih metoda, uzimajući u obzir dubinu penetracije kod FTIR-ATR i dubinu uzbuđenja za SEM-EDS i XPS metode mjerenja.

Rezultati mjerenja hrapavosti pokazuju na neznačajne razlike između netretiranih i kisikovom plazmom tretiranih elastomera. Izmjerene vrijednosti hrapavosti prezentirane su u preciznosti od 1 nm. Za mekani, elastični materijal takva preciznost nije realna. Pouzdanije rezultate trebali bi dobiti upotrebom prikladne visoko precizne bezkontaktne metode.

Temperatura staklastog prijelaza T_g, izmjerena upotrebom DMA metode je u korelaciji sa udjelom akrilonitrilnih grupa kod NBR sirove gume. Promjene u površinskoj slobodnoj energiji bez prateće kemijske promjene površine sirove gume sa niskom T_g (ispod 23 ºC) može se objasniti velikom amorfnom komponentom materijala vrlo male kristaliničnosti, koja dozvoljava visoku mobilnost makromolekularne strukture polimera. Priroda mobilnosti i restrukturiranja nije sasvim jasna, međutim može se objasniti rotacijom dijelova makromolekula, reorientacijom oblika makromolekule, mobilnošću stranskih grana, koje stvaraju "nano travu" kod obrade plazmom, ili drugim vrstama mobilnosti prouzrokovanih jednom od metoda obrade.

Mobilnost makromolekula elastomera može se kombinirati promjenama u kemijskom sastavu površine, koja je nastala kao rezultat kemijske reakcije komponenata plazme, najviše sa sredstvom za križno povezivanje, punilom ili dodacima, jer su ti djelići slabo vezani na osnovnu makromolekularnu strukturu i rijetko na sam polimer.

SEM slike promijenjene makromolekularne strukture u nm rezoluciji uzoraka pretežno amorfne sirove gume teško je napraviti zbog visoke energije kod vakuumskog naparavanja Au/Pd i mlaza elektrona kod snimanja. AFM metoda trebala bi dati bolje rezultate.

UV-VIS absorpcijski spektri elastomera pokazuju razlike s obzirom na IR i UV laserske emisijske spektre. Podešavanje laserskih uređaja na taj način moglo se unaprijed predvidjeti. Konačne vrijednosti za dobivanje jedva vidljivih razlika dobivene su nakon prikladnog postupka finog podešavanja.

Rezultati inverzne plinske kromatografije i mjerenja veličine čestica manje su značajni za ovu studiju. Dokazano je, da je silika punilo materijal sa vrlo aktivnom površinom. Veličina čestica i njihova distribucija pokazuju tipičnu tendenciju stvaranja aglomerata punila.

Metodom AFM snimljena topografija površine uzoraka kod visoke rezolucije potvrđuje prikladnost same metode za analizu promjena na površini, koja će se ubuduće koristiti za analizu topografskih promjena nakon tretiranja uzoraka.

Rezultati mjerenja hvatanja boje samo su informativni. Sama metoda je zanimljiva ali ne daje pouzdane rezultate. Objašnjenje rezultata za RED uzorak, koji se bitno razlikuju od rezultata za druge uzorke, treba potražiti primjenom drugih metoda.

6.2 Zaključak

Elastomeri i sirove gume sa amorfnim osobinama prikladni su materijali za funkcionalizaciju tretiranjem pomoću plazme i za defunkcionalizaciju upotrebom lasera. U budućnosti obadva procesa trebalo bi unaprijediti.

Promjene slobodne površinske energije elastomera navodno nastaju zbog promjena u strukturi površine, slijedeći Wenzelov model. U tom slučaju teško je kontrolirati i predvidjeti promjene u slobodnoj površinskoj energiji nakon procesa funkcionalizacije i defunkcionalizacije upotrebom tretiranja plazmom ili laserom.

Hipoteze bile su djelomično potvrđene:

Nakon tretiranja kisikovom i dušikovom plazmom kod niskog tlaka slobodna površinska energija ofsetne ”gumene navlake” povećava se za 20 mJ/m^2 do više od 30 mJ/m^2. Razlike u slobodnoj površinskoj energiji između funkcionalizirane i defunkcionalizirane ”gumene navlake” u dobroj su korelaciji sa tiskovnim i netiskovnim površinama komercijalno dostupnih konvencionalnih i bezvodnih tiskovnih formi.

Povećanje slobodne površinske energije ofsetnih ”gumenih navlaka” djelomično je posljedica formiranja površinskih funkcionalnih grupa, koje su rezultat kemijske reakcije komponenata plazme sa sumporom (sredstvo za križno povezivanje), punilom i pojedinim dodacima, i djelomično promjenom strukture površine. Obrada sirove gume plazmom ne uzrokuje nikakve kemijske promjene na površini.

Slobodna površinska energija povećava se nakon obrade plazmom do neke vrijednosti, približno 20-30 mJ/m^2. Superhidrofilnost uz kontaktni kut sa vodom blizu 0º nije postignuta. Povećana prisutnost O i OH radikala nije bila postignuta, tako da je efekt najviše ovisan od sredstava za križno povezivanje, punila i dodatka.

Povećanjem slobodne površinske energije povećava se absorpcijski kapacitet obrađene površine. To je potvrđeno smanjenim kontaktnim kutom sa vodom na površinama, koje su tretirane plazmom.

7 Bibliografija

Ovo poglavlje sadrži popis slika, tablica, neuobičajenih skraćenica, kojima slijedi popis web stranica, patenata i objavljenih radova, knjiga, prezentacija, predavanja i disertacija. Preostali objavljeni radovi, koji su opće poznati na tom području istraživanja, i neposredna komunikacija sa kolegama, koji su pomogli kod mjerenja, komentarom metoda, rezultata i zaključaka, bez odgovarajućih referencija, nisu uključeni u popis, iako su doprinijeli konačnim rezultatima.

8 Prilog

Prikazani su radovi, objavljeni u zbornicima međunarodnih konferencija.

Table of Content

1 INTRODUCTION

Traditional graphic communication is based on many conventional and digital printing techniques. Conventional printing techniques are classified and named upon the functionality and shape of printing and non-printing elements on image carrier. In relief printing technology, printing elements are raised over non-printing areas, in gravure printing they are recessed, in screen printing they are in form of openings at the mesh. In lithography printing and non-printing elements are at the same planographic level. They are distinguished by their surface properties. During printing process hydrophilic non-printing areas are protected by dampening solution based on water. After that, greasy printing ink is applied on printing elements. There are other possibilities for use of planographic printing process like waterless lithography or inverse lithography based on water based inks. Image carrier based on aluminium printing plate for conventional printing process is typically made once and is capable to give us many identical prints, in some cases over one million.

The word "lithography" (from Greek *λίθος – lithos*, "stone" + *γράφω – grapho*, "to write"), naming today's most important printing technique, was allocated to the technique by its inventor Alois (Aloys) Senefelder, who used limestone from Solnhofen to make the first planographic prints in 1796. The image is drawn on the surface of a polished stone with a fat or oil based hydrophobic medium. Afterwards, an aqueous solution of gum arabic weakly acidified with HNO_3 is applied onto the stone. The function of this solution is to create a hydrophilic layer of $Ca(NO_3)_2$ and gum arabic on all non-image surfaces. The limestone based lithography is obsolete and interesting only as a fine-art technique. [URL1, URL2]

Every printing process may be performed directly from the printing plate or indirectly as an offset printing technique using an intermediate blanket cylinder covered with a "rubber blanket". The latter is used to achieve a better print quality, especially on rough print substrates; however, an additional element on the press means additional costs and an additional source of problems. The first offset printing press for printing on metal, patented by Robert Barclay in 1875, used specially prepared cards as an intermediate medium. It was later replaced by a more suitable "rubber blanket". The first offset lithographic press for the printing on a paper substrate was invented and

build in 1903 by Ira Washingtion Rubel, while the patent was simultaneously and independently also given to Caspar Hermann. [URL1]

Many digital printing techniques are similar to the conventional ones. With electrophotography, electrography, magnetography and some other techniques, the printing and non-printing elements are at the same planographic level and they are distinguished by their ink accepting or ink repelling character, achieved with a discrete electric charge or magnetic field on the surface of the image carrier. Typically, the image carrier for digital printing techniques enables only one print and has to be reimaged afterwards using the same or a newly rendered image. At digital printing, another distinction between the direct and offset printing principle is present.

The word “lithography” is often used to describe the process of fabrication of microchips and other microelectronic components. Microlithography and nanolithography refer specifically to lithographic patterning methods capable of structuring the material on a fine scale. Among them, photolithography, electron beam lithography, interference lithography, X-ray lithography, extreme ultraviolet lithography, magnetolithography, scanning probe lithography and surface-charge lithography are well-known. One of the modern lithographic techniques is micro and nanoimprint lithography, where the micro or nanoscale relief printing technique is used instead of direct rendering with the UV light or some other electromagnetic radiation. At the beginning of the process, the nanoscale features are written into a master, typically photoresist, Si, or some other hard material, using a slow, high-resolution technology, e.g. e-beam lithography. The relief master can then be used as a stamp or to make a mould from which features are rapidly and repeatedly stamped into a softer resist film, or by applying a proper “functional ink” on the surface. [1]

The starting point of the research work was the studies of the surface properties of the materials used in conventional lithography as one of the printing techniques, a possible reduction in the number of elements used in the printing press by merging the functionality of the printing plate and “rubber blanket”, and opening new possibilities in the development of conventional and digital printing technology.

This professional background was upgraded by involving proper research methods for the study of the surface free energy and other surface characteristics of “rubber

blankets", and the methods for changing their properties in an irreversible or reversible way by using different types of plasma and lasers. The aim of the proposed thesis was the modification of the surface free energy of the "rubber blanket" for offset lithographic printing, combined with a discrete defunctionalization to get two areas with different surface properties. The main subject of the study was the changes in the chemical composition and roughness of the surface layer of a "rubber blanket" after the treatment.

2 BACKGROUND

A short overview of the printing technology should provide a description of basic terms, materials, processes and phenomena of significant importance for understanding the aim, methods and results of this investigation.

A summary of literature overview, the first experience obtained during the preliminary tests and confirmation of the basic idea thus became the starting point for the creation of research hypotheses.

2.1 Lithographic printing plates

The printing plate for conventional lithographic printing is the image carrier with oleophilic/hydrophobic image elements and hydrophilic/oleophobic non-printing areas. It works well with a proper dampening solution and greasy printing ink. Waterless lithography (known also as driography), introduced by 3M Company in the late 1960s, is based on only one liquid, i.e. the printing ink. The image elements are oleophilic, while the non-printing areas are covered with an oleophobic silicone layer. The difference in the oleophilicity of the printing and non-printing areas provides the possibility of selective inking of the printing plate. Some successful experiments using water based inks are also known using the same principle, however, with hydrophilic printing elements and hydrophobic non-printing areas. This technique is known as inverse lithography. [URL3, Pat.1, 2]

2.1.1 Short overview

Limestone was in regular use until the middle of the 20th century. Senefelder, the inventor of lithography, recognized that limestone is not practical, since the heavy stones with thickness of over 50 mm are not suitable for transportation, manipulation and use in a printing press; therefore, he proposed and used the plates made of Zn and even special paper. Today, the basic material for the carrier is aluminium; nevertheless, in some cases, other metals, polyester or paper are used.

The hydrophilic non-printing areas of conventional metal Al plates are made of the Al_2O_3 layer on an electrochemically grained surface. For the making of the printing areas, several methods have been used. The first patent for the photo imaging layer based on bichromated gelatin was given to Fox Talbot in 1852. Newer methods for rendering of the printing plates, based on light sensitized colloids and contact exposure using positive or negative film, remained in everyday use until the end of the 20th century. All modern printing plates are pre-sensitized and ready for a conventional contact exposure or adapted to one of CtP (computer to plate, computer to press etc) methods. The first imaging layer for the production of pre-sensitized plates was based on the novolak-diazonaphtoquinone resists, developed by the company Kalle in 1940. The first plates on the market were the Kalle Ozatek plates, which were made available around 1950. The conventional plates for contact exposure with the imaging layer based

on improved novolak-diazonaphtoquinone or photopolymer are still used. The same material, used for the imaging layer, was later introduced as photoresist and is still in use for the microelectronic component production.

The first CtP installations based on a spark discharge technology were made by the companies Presstek in 1988 and Heidelberg, which introduced the GTO-DI printing press in 1991. The first thermal CtP system was Krause LaserStar in 1989. Modern CtP systems are based on thermal technology using melting, fusing, polymerization, decomposition or ablation with an IR laser (800–1100 nm), photochemical reaction (photo-polymerization) with a violet laser (405 nm) or Ag-salt diffusion during the developing process after the laser exposure of silver halides.

There are some patented technologies [Pat.2, Pat.3, Pat.4, Pat.5, Pat.6, Pat.7, Pat.8, Pat.9, Pat.10, Pat.11, Pat.12, Pat.13, Pat.14, Pat.15, Pat.16, Pat.17, Pat.18, Pat.19, Pat.20] using different rendering principles of the printing and non-printing areas which include the plasma and laser treatment of elastomer with reversible rendering to get a reusable plate. Typically, the patented plates are based on a hard surface material, e.g. ferromagnetic, ceramic, semiconductor, silicon, zirconium or aluminium. The imaging is achieved by using plasma, laser, electric charge, magnetic field and other techniques, which are not all suitable for the use on an elastomer. Only one patent [Pat.7] was given to the process using an elastic surface layer, laminated on the supporting plate. None of the solutions known from the presented patents has been accepted by professionals for everyday use in the printing proces.

2.1.2 Functionality of lithographic printing plate

There are many properties expected from the printing and non-printing areas of the printing plate, e.g. durability (number of impressions), resolution (typically acceptable reproduction quality obtained by rendering the positive and negative 6 μm thin microlines on control wedge), dimensional stability, equal thickness and good hydrophobicity or hydrophilicity of different areas. The plate should be adapted to at least one well-known conventional or CtP imaging technology, it should be environment-friendly and reasonably priced.

To get the reference values for further investigations, a basic analysis of one conventional pre-sensitized aluminium-based plate with a positive imaging layer (PO7

plate from the company Cinkarna Celje, exposed and developed according to the producer's instructions) and one polyester-based plate for waterless printing (Presstek PEARLdry plate, sample taken from Omni Adast press, where such plates are usually applied) were made. All the printing and non-printing areas were made from different materials. In consequence, quite different values were expected.

The surface free energy of the two analysed commercially available plates, calculated with the Owens Wendt method using the contact angle measurements with water, diiodomethane and formamide, are presented in Figure 1.

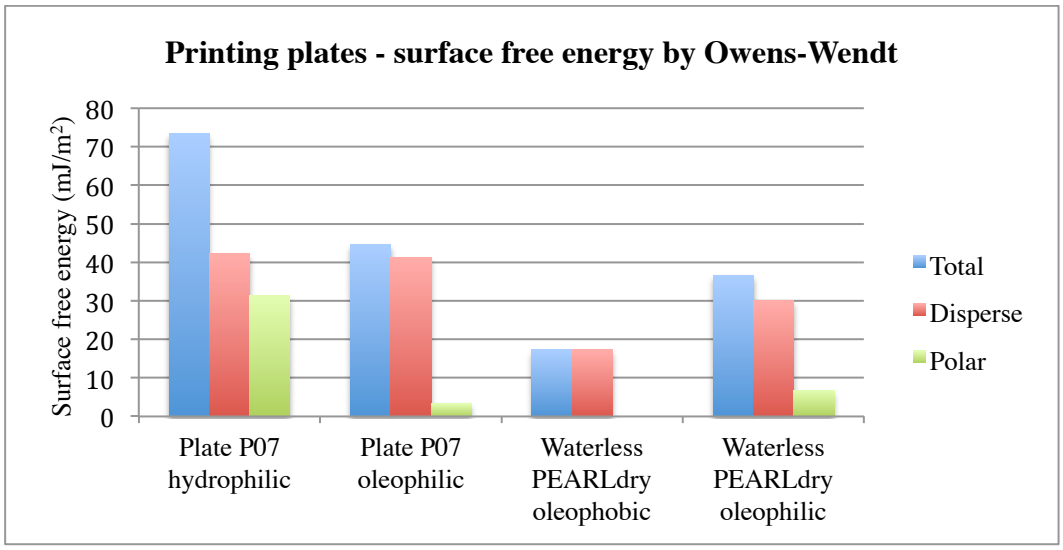

Figure 1: *Total, disperse and polar part of typical non-printing (hydrophilic/oleophobic) and printing (oleophylic) areas of conventional PO7 and waterless PEARLdry printing plates.*

The difference in the surface free energy for the non-printing (hydrophilic) areas in the total and polar component being approx. 30 mJ/m^2 with a practically unchanged disperse component, presented in Figure 1, suffices to get a proper distinction between the non-printing (hydrophilic) and printing (oleophilic) areas on a conventional PO7 printing plate for wet offset lithographic printing. For a waterless printing plate, the values for the printing (oleophilic) areas are higher if compared to the non-printing (oleophobic) areas by approx. 20 mJ/m^2 for the total and 13 mJ/m^2 for the disperse component of the surface free energy, and there is no polar component of the surface free energy on the non-printing (oleophobic) areas. The oleophilic areas for the conventional compared to the waterless printing plate have the

values which are by approx. 8 mJ/m^2 higher for the total and 9 mJ/m^2 for the disperse component, but by 3 mJ/m^2 lower for the polar component of the surface free energy.

According to the literature, the hydrophilic state is defined with the contact angle with water on a solid surface < 90º, while at contact angles > 90º, the surface is hydrophobic. In professional references, a distinction between the printing (hydrophobic/oleophilic) and non-printing (hydrophilic/oleophobic) areas under normal conditions for conventional offset lithographic printing should be defined and adjusted at lower contact angles; however, there is no general agreement. For the printing plates, the hydrophobic state is characterized with the contact angle with water > 50º, and the hydrophilic state with the contact angle with water < 10º [Pat.20]. The contact angle with the dampening solution (water with 5% vol. water-soluble organic compound) on the print areas give 52.72º and 16.13º on the non-printing oleophilic areas [3]. A general overview and summary of the surface tensions (surface free energies) for typical offset lithographic materials according to MacPhee can be seen in Table 1.

Table 1: *Calculated interfacial tensions for typical lithographic materials*. [4]

Material	Surface free energy with respect to vapour (mJ/m^2)			Interfacial tension with other materials (mJ/m^2)	
	Dispersion bond component α^2	Polar bond component β^2	Total γ	Ink	Dampening solution
Plate image area	36.5	2.9	39.4	0.2	9.3
Plate non image area	24.8	44.6	69.4	27.9	9.7
Rubber blanket	26.9	4.8	31.7	0.8	4.4
Ink	32.5	2.1	34.6	–	9.0
Dampening solution	14.7	14.4	29.1	9.0	–

γ - interfacial surface tension (surface free energy)
α - square root of that part of γ due to dispersion type (London) bonding forces
β - square root of that part of γ due to polar type (Keesom) bonding forces

The contact angle with water for the hydrophilic areas of the PO7 plate is 4.6º and for the oleophilic areas 71.2º, measured by using the sessile drop technique. The

oleophobic area of a waterless plate has 114.0º and oleophilic areas 76.5º contact angle with water. Both plates are well accepted by printers and give good results in the printing process if a proper dampening solution combined with a conventional printing ink for a conventional process, or a special printing ink for waterless lithographic printing is used.

Pure aluminium used as the basic material for the PO7 plate has a hydrophobic character. To make its surface hydrophilic, an electrochemical graining and anodic oxidation process using an electrochemical treatment in an acid bath is used. Complex salts and other chemical compounds on the surface, and a treatment with a gum arabic solution and other chemicals contribute to the final surface properties. [5]

For the imaging (printing) layer of a conventional aluminium based plate and both (oleophilic and oleophobic) layers of a waterless plate, organic compounds are used. The hydrophilicity/hydrophobicity of layers depends mostly on their polarity, i.e. degree to which charges are separated. The greater the electronegativity difference between the atoms in a bond, the more polar the bond. Higher polarity means higher hydrophilicity of the material surface. There are several classifications of functional groups according to their surface properties.

Table 2: *Functional groups ranked by boiling points and polarity.* [URL4]

Group name	Boiling point (ºC)	Polarity	Sample name
Amide	222	1	ethanamide
Acid	118	2	acetic acid
Alcohol	117	3	propanol
Ketone	56	4, 5	acetone
Aldehyde	49	4, 5	propanal
Amine	49	6	propylamine
Ester	32	7	methyl metanoate
Ether	11	8	methyl ethyl ether
Alkane	- 42	9	propane

The functional groups ranked by their boiling points and polarities are presented in Table 2. The correlation between the boiling point and polarity is evident; the higher

the boiling point, the lower the polarity. Typical hydrophilic and lipophilic (oleophilic) groups of non-ionic surfactants are presented in Table 3.

Table 3: *Groups with HLB (hydrophilic – lipophilic balance) assigned empirical numbers to HLB scale.* [6]

Hydrophilic group	HLB	Lipophilic group	HLB
-SO_4Na	38.7	-CH-	– 0.475
-COOK	21.1	-CH_2 -	– 0.475
-COONa	19.1	-CH_3 -	– 0.475
Sulfonate	~ 11.0	-CH=	– 0.475
-N (tertiary amine)	9.4	-(CH_2-CH_2-CH_2-O-)	– 0.150
Ester (sorbitan ring)	6.8		
Ester (free)	2.4		
-COOH	2.1		
-OH (free)	1.9		
-O-	1.3		
-OH (sorbitan ring)	0.5		

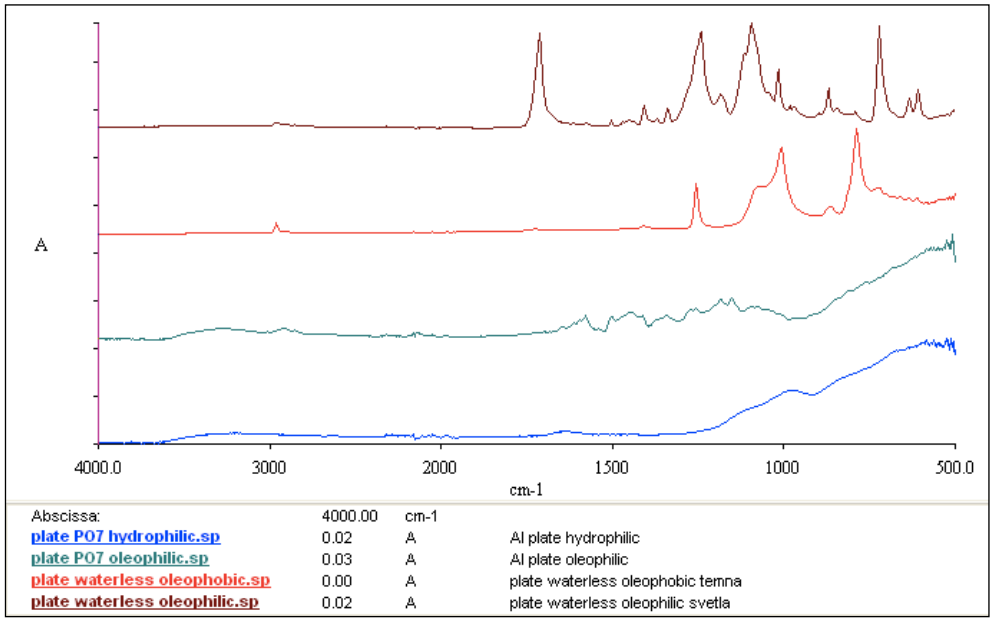

Figure 2: *FTIR-ATR spectra of typical non-printing and printing areas of conventional PO7 and waterless printing plates measured with Perkin-Elmer Spectrum GX1 apparatus.*

The FTIR-ATR (Fourier transform infrared – attenuated total reflectance) spectra for typical printing and non-printing surface areas are presented in Figure 2. An overview of possible chemical bonds and chemical groups on the surface was performed with the analysis of IR spectra peaks using the KnowItAll – AnalyzeIt IR software.

The hydrophilic areas of the conventional PO7 printing plate are made of aluminium covered with an Al_2O_3 layer with residual traces of ketones, amides, ethers, nitrogen and phosphor compounds at 1637 and 977 cm^{-1} peaks with many C=O, C=N and some CN, C-O-C, P-O-R and P-O groups.

The oleophilic layer of a conventional PO7 printing plate consists of ketones, nitrogen compounds, carbo acid and salt: sulphur compounds at 1579 cm^{-1} peak with C=O, NO_2 and NH groups; other nitrogen compounds at 1452 cm^{-1} peak with C=N and N=N groups; amines, carbo acid and sulphur compounds at 1344 cm^{-1} peak with C-N, C=O and SO_2 groups; halogens and sulphur compounds at 1188 cm^{-1} peak with C-F and SO_2 groups; alkanes and sulphur compounds at 1154 cm^{-1} peak with C-C, N=S=O and SO_2 groups; and ethers at 1056 cm^{-1} peak with C-O-C groups.

The oleophobic area of a waterless PEARLdry plate consists of halogen and silicon containing compounds at 1275, 1009, 790 and 723 cm^{-1} peaks with C-F, CH_3, Si-O-Si, Si-C and C-Cl groups.

The oleophilic area of waterless PEARLdry plates consists of carbo acid and ketones at 1713 cm^{-1} peak with C=O groups; carbo acid and phosphor compound at 1409 cm^{-1} peak with OH and P-CH_2 groups; amines at 1341 cm^{-1} peak with C-N groups; carbo acid and halogens at 1243 cm^{-1} peak with C-O and C-F groups; ethers at 1096 cm^{-1} peak with C-O-C groups; Si-O at 1018 cm^{-1} peak with Si-O-Si groups; 3 ring ether and silicon compounds at 872 cm^{-1} peak with C-O-C and Si-F groups; and halogens at 724 cm^{-1} peak with C-F and C-Cl groups.

A typical chemical composition of hydrophilic and oleophilic surfaces was partly confirmed with an IR spectra analysis. For the final confirmation, an additional chemical analysis of the surface areas should be performed.

R_a (roughness average), R_z (mean roughness depth) and R_{max} (maximum roughness depth) were measured in four directions (left to right and opposite, top to down and

opposite) for at least three times, and the mean values and σ (standard deviation) were calculated from the original data by using MS Excel (Table 4).

Table 4: *Roughness of typical non-printing and printing areas of conventional PO7 and waterless PEARLdry printing plates measured with Mahr M1 stylus apparatus.*

Roughness parameter	Plate PO7 hydrophilic		Plate PO7 oleophilic		Waterless PEARLdry oleophobic		Waterless PEARLdry oleophilic	
	Value	σ	Value	σ	Value	σ	Value	σ
R_a (µm)	0.464	0.031	0.422	0.087	0.074	0.011	0.070	0.008
R_z (µm)	3.302	0.236	2.866	0.471	0.635	0.135	0.583	0.092
R_{max} (µm)	3.870	0.347	3.922	1.412	0.941	0.305	0.996	0.399

The roughness values for a conventional PO7 printing plate are similar for the printing and non-printing areas, and relatively high compared to a waterless printing plate. The values for the printing and non-printing areas on a waterless PEARLdry printing plate are similar as well. Obviously, the surface roughness is not the most important and sufficient surface property to achieve a proper hydrophilic/oleophilic or oleophobic/oleophilic distinction of the surfaces in a lithographic printing process.

The focus of further investigations should be oriented more to the surface free energy and polarity of possible printing and non-printing areas, rather than to the surface roughness of the printing plate. An advantage of the rough surface of hydrophilic non-printing areas on a conventional printing plate displays in better coating adhesion of the oleophilic imaging layer and during printing, in greater water-carrying capacity. [4]

2.2 Elastomers

Plastics or polymers (from Greek *πολυ – poli*, "many" + *μερος – meros*, "part") are ubiquitous. The two major classifications are thermosetting (set, cured or hardened in permanent shape) and thermoplastic (not set or cured under heat, but softened to a mobile, flowable state, upon cooling they hold their shape) materials.

Thermoplastics can be classified into amorphous or semicrystalline plastics. Most polymers are either completely amorphous or have an amorphous component even if they are highly crystalline. Amorphous polymers are hard, rigid glasses below the T_g (glass transition temperature), while above T_g, they become soft and flexible and can be shaped. Crystalline polymers have the melting point above their T_g. Crystalline polymers are less rigid above their T_g, but will not flow until the temperature is above the crystalline melting point. At ambient temperature, the crystalline/semicrystalline plastics have greater rigidity, hardness, density, lubricity, creep resistance and solvent resistance than the amorphous polymers. [7]

Elastomeric materials or elastomers (*elast*ic + poly*mer*, from Latin *elasticus*, "beaten, ductile") are natural or synthetic materials that do not break when stretched 100% and after being held at 100% stretch for 5 minutes then released, they must return to within 10% of their original length within 5 minutes. [8]

Elastomers are rubber-like materials with T_g below room temperature, when the elastomer becomes rigid and loses its rubbery characteristics. Most plastics and elastomeric products are not pure materials but rather mixtures of a basic polymer with a variety of additives, e.g. pigments, lubricants, stabilizers, antioxidants, flame retardants, anti-block agents, cross-linking agents, fillers, reinforcement agents, plasticizers, UV absorbents, foaming agents etc. All these additives need to be incorporated into the polymer prior to the fabrication. The development of quality resins and additives plays an important role in the elastomer production. The exact composition of the end product and the production process are usually unknown and not published. [7]

Natural rubber, based on latex, milky colloidal suspension from the Para rubber tree (*Hevea brasiliensis*) or some other rubber tree, e.g. Gutta-Percha, rubber fig, Panama

rubber tree and other plants, is an elastic hydrocarbon polymer. The purified form of natural rubber is polyisoprene, most often cis-1.4-polyisoprene with molecular weight of 100,000–1,000,000, which can also be produced synthetically. Typically, a few per cent of other materials, e.g. proteins, fatty acids, resins and inorganic materials are found in natural rubber. The name "rubber" was given by Joseph Priestly in 1770, when he noticed that a piece of this material is extremely good for rubbing out pencil marks on paper.

Natural rubber is often vulcanized, i.e. a process in which rubber is heated and sulphur, peroxide or bisphenol are added to improve the resilience and elasticity, and to prevent the rubber from perishing. The vulcanization process is most closely associated with Charles Goodyear, who invented the process in 1830. Carbon black is often used as an additive to rubber to improve its strength and elasticity. [URL5]

Synthetic rubbers are any petrochemical based cross-linkable elastomers. With regard to the basic monomer, butyl rubber, ethylene-propylene rubber, neoprene rubber, nitrile rubber, polybutadiene rubber, polyisoprene rubber, styrene-butadiene and other synthetic rubbers are recognized. [9]

According to Ullmann's Encyclopedia of Industrial Chemistry (ref. to DIN definitions), rubber is not a cross-linked, but a cross-linkable (vulcanizable) polymer. Elastomers are polymeric materials that are cross-linked (vulcanized), they have rubber-elastic properties, particularly from the room temperature up to their decomposition point. [10]

There are often differences in the use of the term "rubber" by different authors of professional and scientific articles. In professional communication, the term "rubber" is almost always used for any material made of natural or synthetic crude rubber by curing or vulcanization process. The term "elastomer" should be reserved for cross-linked elastic material only. To assure a correct scientific approach, the term "rubber" or "crude rubber" for a not cross-linked polymer and "elastomer" for a cross-linked polymer with rubber-elastic properties is going to be used in the thesis, i.e. in accordance with Ullmann's Encyclopedia.

The optimum properties and/or economics of many elastomers are obtained by formulating one or more basic rubbers with reinforcing agents, fillers, extending oils, vulcanizing agents, antioxidants, pigments etc.

The details of the composition and production processes of commercially available rubber and elastomers, including the curing of rubber, are very often unknown despite the strong impact on the physical and chemical properties of rubber. The macromolecules could be bonded directly (C-C), over curing agents (C-S-C, C-S_x-C), or other rubber or elastomer components. The macromolecules are usually not chemically bonded to the fillers; however, strong adhesion forces are present among them, primarily giving the elastomeric properties to the elastomer. The bulk and surface of an elastomer are thus of heterogenic structure, different for each product. [11, 12]

During the investigation, two basic types of synthetic rubbers were used (according to the ASTM nomenclature), namely NBR (nitrile-butadiene rubber) and EPDM (ethene-propene-diene-monomer; ethene-propene copolymer) rubber blend with T (thiokol, polythioether rubber, rubber with sulphur in the polymer backbone) or TM (M – rubber having fully saturated polymer backbone of the polymethylene type; TM – rubber with sulphur in saturated polymer backbone) rubber. [10]

NBR has good resistance to fuels, oils and solvents with improved abrasion resistance with lower resilience, higher hysteresis and is often declared as the polar type of rubber. A variation of ACN (acrylonitrile) units grafted to the basic polymer chain controls the polarity and other properties.

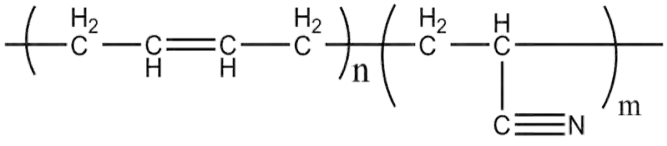

(NBR rubber)

EPDM has good resistance to ozone and weathering, but poor hydrocarbon and oil resistance, and is often declared as the non-polar type of rubber. It is a polymer consisting of ethene and propene units as a part of the main polymer chain. When a non-conjugated diene is grafted onto the main polymer chain, it becomes a terpolymer. The amount and ratio of ethene/propene content and the variety of diene monomer unit gives rubber different properties. [13]

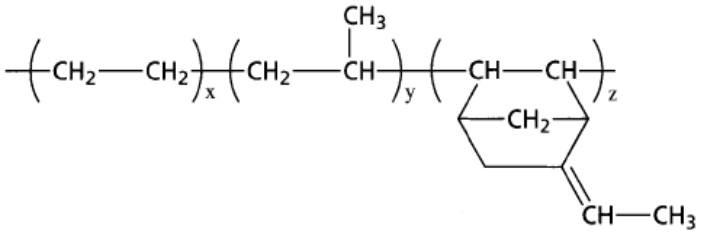

(EPDM rubber)

T rubber has good chemical resistance, resistance to ozone and weathering; it is creep and has low resilience. [10] The polymer varies in radicals and the amount of sulphur used, and it is also used as a curing agent [14]

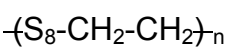

(T rubber)

2.3 Lithographic rubber blankets

A lithographic “rubber blanket” (also called printing blanket, offset blanket etc) is a multi-layered thin composite structure (Figure 3). The term “rubber blanket” is widely accepted by professionals to name the final cured and finished product made of different elastomer and other layers. In general, it consists of a covering surface elastomer layer (also known as face, printing layer, upper layer etc), an elastomeric foam layer (also compressible layer) and several orthotropic tissue layers (cotton fabric, cotton/polyester fabric, cord etc).

The first patent for offset lithographic printing in metal decoration was given to Robert Barclay and John Doyle Fry in 1875. At the beginning of offset printing, cardboard was used, but was later replaced by a “rubber blanket”. The first lithographic offset press for printing on a paper substrate was invented by Ira Washington Rubel in 1903.

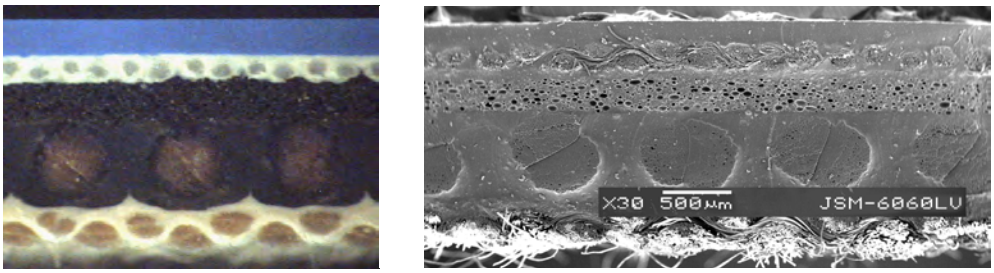

Figure 3: *Cross-section of Advantage Dual “rubber blanket”, image obtained with optical microscope (left), SEM image of Advantage UV Red (right).*

Modern printing presses (Figure 4) are designed for the use of only one “rubber blanket” with an underpacking of dimensional stable plastic film to obtain a total relative overpacking of 0.10–0.15 mm. Typical of offset lithographic presses in a medium format, the overpacking is achieved by setting the surface layer of the blanket over the bearer of the blanket cylinder to the same level (overpacking at 0.00 mm), and with the overpacking setting of the plate over the plate cylinder bearer and paper over the impression cylinder bearer at 0.10–0.15 mm. With a close contact of bearers during printing, typical printing pressure of 150 MPa is achieved. For each press model, detailed instructions for the working pressure settings and overpackings are provided by the press manufacturer.

The overall thickness of "rubber blankets" is either 1.95 mm or 1.70 mm, depending on the press design (undercut on blanket cylinder). For special purposes, blankets in other thicknesses are produced: ~ 1 mm with a pressure adhesive layer for continuous forms and label printing, > 2 mm for no-pack blankets for web presses.

The tissue layers provide elastomeric layers with high tenacity and stabilize the blanket against relaxation. Most modern printing blankets include one or even more compressible layers of different thickness, made with different production processes. Compressible layers could be made using the salt leach process, microspheres or the blowing process with overpressure.

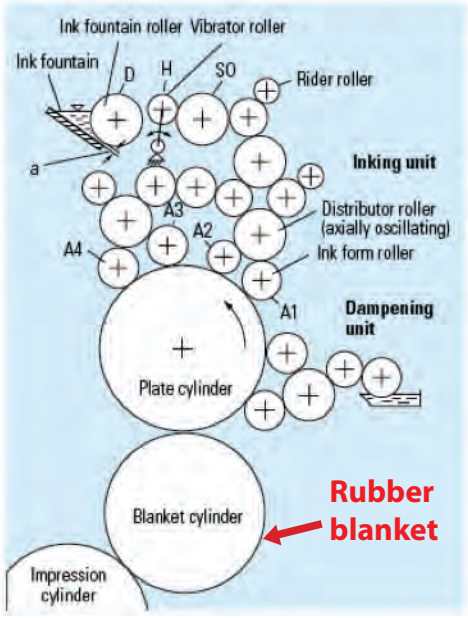

Figure 4: *Cross-section of printing unit of modern offset lithographic press.* [15] *Printing plate is mounted on the plate cylinder and "rubber blanket" on the blanket cylinder.*

The main subject of the investigation was a thin covering elastomer layer with the thickness of typically ~ 0.1 mm. It consisted of an elastomer with good resistance to the fountain solution, printing inks, paper abrasion and cleaning solvents with a proper dampening solution and ink transfer properties. The polar NBR elastomer is in use with conventional oil based printing inks, while the EPDM elastomer is appropriate for UV printing inks based on acrylates. For a mixed production (conventional and UV inks) or special printing conditions, different blends (EPDM/NBR, NBR/T), other types of elastomers (PVC blends), curing agents, fillers

and additives are used. The surface of the covering layer should have appropriate QR (quick release) properties, depending mainly on the elastomer composition and surface finishing, for the given ink formulation and the print substrate (paper) properties.

In the cast finishing process, the elastomer surface is tightly pressed against a layer of paper during curing. When the paper is removed, an imprint of its surface is left on the blanket.

Mechanical finishing includes buffing and grinding using different grades of sandpaper. The blanket is thus reduced to the final thickness with controlled roughness. The buffing and grinding surface layer treatment was used for the majority of “rubber blanket” samples used in the present work.

In chemical etching, the blanket surface is dusted with starch instead of talc, prior to the vulcanization. Following the curing, the residual starch is removed with chemical etching to produce a surface consisting of tightly packed shallow holes. [4, 16, 17]

2.4 Surface free energy

The surface free energy is a measure of the difference in the attractive forces between the molecules on the surface and molecules in the bulk. In the interior of a material, each molecule is acted on equally in all directions, while this is not true for the molecules on the surface, which are in contact with air (gas, vapour etc) or other media.

For liquids, the cohesive forces between the liquid molecules are responsible for the phenomenon known as surface tension. The cohesive forces for the molecules in bulk liquid are equally distributed on all sides, while the molecules on the surface cohere more strongly to those directly associated with them on the surface. This forms a "virtual film" on the surface, which makes it more difficult to move an object through the surface than when it is completely immersed. The surface tension is typically measured in mN/m, i.e. the force in mN to break a film of 1 m length. Pure water at 20 ºC has the surface tension of 72.8 mN/m.

The surface free energy may be defined as the excess energy on the surface of a material compared to the bulk. The surface energy quantifies the disruption of intermolecular bonds which occurs when the surface is created. It is typically measured in mJ/m^2; for liquids, the numeric value is the same as for the surface tension. The mobility of the surface molecules of solid is exceedingly low when compared to any liquid, thus the term "surface tension" should not be used to describe the surface property of solid and the measurement methods should be adjusted.

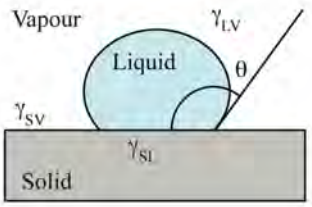

Figure 5: *Sessile drop of liquid on solid surface.*

In 1805, T. Young was the first to describe the contact angle equilibrium. The vectorial summation of forces (Figure 5) at the three-phase intersection point gives:

$$\gamma_{SV} = \gamma_{LV} \cos\Theta + \gamma_{SL} \quad (1)$$

where γ is the surface tension or the surface free energy, γ_{SV} is the interfacial tension of solid and vapour, γ_{LV} is the interfacial tension of liquid and vapour, γ_{SL} the interfacial tension of solid and liquid, and Θ the contact angle.

There are many measurement methods based on the contact angle of a test liquid with a solid material, including the static and dynamic measurements of sessile drop, sliding drop on an inclined plate method, drop form and drop dimension method. To measure the advancing or receding contact angle, hysteresis has to be taken into consideration in the calculations. The measurements using a volatile test liquid and a porous, rough or non-homogenous solid surface are difficult and often lead to errors. Other methods include a dynamic or static Wilhelmy plate, inverse gas chromatography etc.

The calculation of the surface free energy using the Young's equation (1) was not accurate enough and additional methods were discovered. Fowkes assumed that the surface free energy is a sum of independent components, associated with specific interactions:

$$\gamma_S = \gamma_S^d + \gamma_S^p + \gamma_S^h + \gamma_S^i + \gamma_S^{ab} + \gamma_S^o \qquad (2)$$

where γ_S^d, γ_S^p, γ_S^h, γ_S^i and γ_S^{ab} are dispersion, polar, hydrogen (related to hydrogen bonds), induction and acid-base components, while γ_S^o refers to all the remaining interactions.

According to Fowkes, the dispersion component of the surface free energy is connected with the London interactions, arising from electron dipole fluctuations. They result from the attraction between adjacent atoms and molecules, and are independent of other types of interactions. The remaining van der Waals interactions were considered by Fowkes as a part of induction interactions. Fowkes investigated mainly two-phase systems containing a substance in which only a dispersion interaction appears.

Owens and Wendt significantly changed Fowkes's idea with the assumption that all components in Equation (2), except γ_S^d, can be considered as polar interactions γ_S^p and consequently obtained the following equation:

$$\gamma_{SL} = \gamma_S + \gamma_L - 2(\gamma_S^d \gamma_L^d)^{0.5} - 2(\gamma_S^p \gamma_L^p)^{0.5} \quad (3)$$

The polar interaction definition by Owens and Wendt differs from Fowkes's; therefore, the meanings of γ_S^p differ in Equations (2) and (3).

Wu accepted the same idea as Owens and Wendt; however, he used harmonic instead of geometric means::

$$\gamma_{SL} = \gamma_S + \gamma_L - 4[\gamma_S^d \gamma_L^d / (\gamma_S^d + \gamma_L^d) + \gamma_S^p \gamma_L^p / (\gamma_S^p + \gamma_L^p)] \quad (4)$$

Wu's approach has not been widely used in the studies on the wettability and surface free energy of polymers.

Van Oss, Chaudhury and Good introduced a similar idea, dividing γ_S into two components, one including long-range interactions (London, Keesom and Debye), called the Lifshitz-van der Waals component (γ^{LW}), and the other containing short-range interactions, called the acid-base component (γ^{AB}). The latter component is considered to equal $2(\gamma^+\gamma^-)^{0.5}$, where γ^+ and γ^- are associated with the acid-base interactions.

$$\gamma_{SL} = [(\gamma_S^{LW})^{0.5} - (\gamma_L^{LW})^{0.5}]^2 + 2[(\gamma_S^-)^{0.5} - (\gamma_L^-)^{0.5}] \cdot [(\gamma_S^-)^{0.5} - (\gamma_L^-)^{0.5}] \quad (5)$$

The Owens-Wendt and Wu theories, and Van Oss acid-base theory are widely accepted and used methods for the calculation of different components (disperse, polar, acid-base etc) and total surface free energy. For the contact angle measurements, two or more test liquids with different polarity and other properties are used. There have been several improvements of these methods in the published studies, where proper methods concerning a solid material and test liquids were investigated, and corrections of test liquid (water, by Della Volpe) values of the surface free energy components were suggested. The results obtained with different methods are not unique; hence, there are no absolute values of the surface free energy or its components. Some methods are more convenient for the measurements of contact angles and calculations of surface free energy than others for some groups of solid materials (e.g. metals, minerals, polymers etc); however, there is no general agreement or proposal for a standard determination of the surface free energy of elastomers.

There are other methods, e.g. equation of state, as empirically upgraded Young's equation for the measurements with only one liquid. The Neumann method is also based on only one liquid. Both methods are empirical and give useful results only under corresponding conditions and only within a limited range of measured contact angles. The empirical Zisman method is used for the determination of the critical surface free energy γ_c of a solid, the value of which equals the value of γ_L of the liquid being in contact with this solid at a zero contact angle. The critical surface free energy γ_c does not equal γ_S. [18, 19, 20, 21, 22, 23, 24]

Table 5: *Critical surface energy of common organic surfaces.*

Surface constitution		γ_c (mJ/m^2), at 20 ºC
-CF_3	Fluorocarbon surfaces	6
-CF_2H		15
-CF_3 and CF_2-		17
-CF_2-		18
-CH_2-CF_3		20
-CF_2-CFH-		22
-CF_2-CH_2-		25
-CFH-CH_2-		28
-CH_3 (crystal)	Hydrocarbon surfaces	22
-CH_3 (monolayer)		24
-CH_2-		31
-CH_2- and ..CH..		33
..CH.. (phenyl ring edge)		35
-CClH-CH_2-	Chlorocarbon surfaces	39
-CCl_2-CH_2-		40
=CCl_2		43
-CH_2ONO_2 (crystal)	Nitrated hydrocarbon surfaces	40
-$C(NO_2)_3$ (monolayer)		42
-CH_2NHNO_2 (crystal)		44
-CH_2ON_2 (crystal)		45

In Table 5, critical surface tensions of organic compounds are presented according to Zhang, the data being compiled by Tillman and co-authors. γ_c obviously increases with complexity, the presence of oxygen and double bonds of organic compound surfaces and could be useful to predict the γ_S of materials [25, 26]

All well-known and established methods for the surface free energy determination of solids enable useful results under the following conditions: pure, flat, smooth, homogeneous, solid sample; pure test liquids with known properties; standard climatic conditions in a laboratory during the contact angle measurements; standard procedure according to the chosen measurement method.

The contact angle measurements of a rough solid surface were investigated by many authors. The contact angle depends among other factors on roughness. This phenomena was observed and reported by Wenzel (1936, Wenzel state) for a rough hydrophilic surface with a close contact of a drop of liquid with a solid surface. The hydrophobic rough surface where the contact of liquid with the surface is observed only at the top of "pillars", with a layer of vapour (air) at the rest of the surface under a liquid drop, was investigated by Cassie and Baxter (1944, Cassie-Baxter state). According to the theory describing the Wenzel state, a higher contact angle and lower surface free energy of a rough solid sample is attained compared to a smooth solid surface and a much higher contact angle at the Cassie-Baxter state (Figure 6).

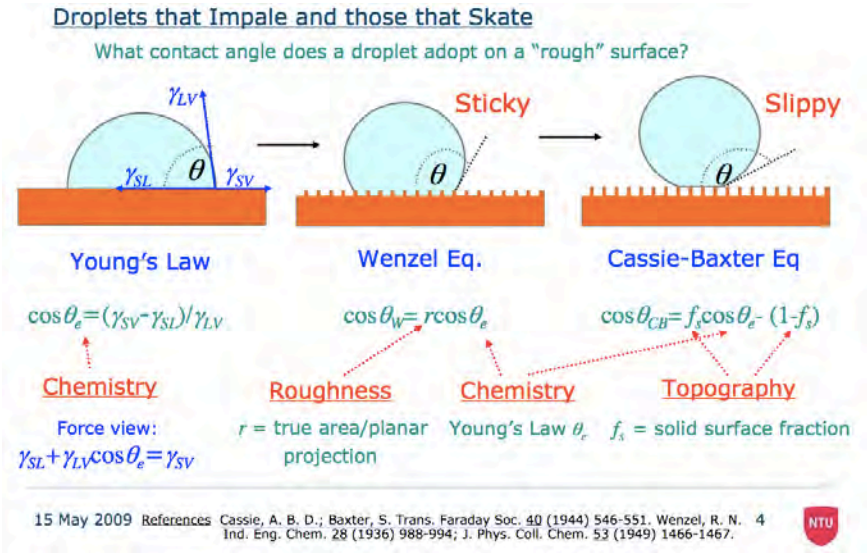

Figure 6: *Liquid drop on smooth and rough surface.* [27]

2.5 Modification of surface properties of elastomers

In the past three decades, many surface treatment methods of polymers have been used in the plastic manufacturing processes, plastic decoration, printing of labels, flexible packaging, and other research fields and manufacturing technologies. Elastomers are rarely present among the surface treated polymers. In most cases, they are used as medical accessories and implants, sealants and coatings. The adhesion of elastomers to other materials and biocompatibility has been according to the literature the main issue. The basic treatment methods include mechanical, chemical and physical cleaning, ablation, deposition and other modifications of surface properties.

Water washing utilizes alkaline cleaning agents to remove the dirt and oils, and an aqueous emulsion of hydrocarbon solvents to remove the mould release agents. This method is used mainly before the painting or coating of plastic objects.

Solvent cleaning may be achieved with wiping, spraying or immersing in vapour to degrease polymer objects. Most effective is bathing the plastic parts in solvent vapours, where the solvent condenses on a polymer and runs off, taking the surface contaminants with it.

Mechanical cleaning involves mostly sandblasting and other abrasive techniques of the polymer surface treatment.

Chemical etching with chromic and sulphuric acid chemically changes, cleans or roughens the polymer surface.

Chemical priming can provide improved surface characteristics by applying a chemically distinct layer on the substrate. Polyethyleneimine, polyurethanes, acrylates, chlorinated polymers, solvent based solutions of nitrocellulose and other materials are in use for chemical priming.

Evaporated acrylate coating is the evaporation process of an acrylate monomer in a reactor, where it is deposited as a thin smooth layer on the substrate surface.

Wet chemical treatment with acids, amines, caustic and phenols enhances the wettability and other surface properties by chemically changing the polymer surface.

Fluorination treatment process involves continuous exposing of polymeric webs to a fluorine gas diluted with an inert gas (nitrogen) inside a reaction chamber, giving the web surface high surface adhesion properties.

Flaming oxidizes the polymer surface, thus a higher surface free energy is achieved with the formation of polar groups and changing the chemical composition. Heat mainly causes a chain scission.

Corona discharge involves exposing the polymer surface to many electric discharge sparks, it becomes oxidized, forms polar groups and causes roughness. The corona treatment could add or remove the material and cause bond scission. The corona treatment of a plastic film print substrate is a frequently used method in the modern label and packaging printing industry.

Plasma treatment involves exposing the polymer to ionized gas, usually oxygen, in an evacuated chamber to oxidize the polymer surface and form polar groups. The plasma treatment of a plastic print substrate is in use by the packaging printing industry as well.

Sputter-etching is an ion bombardment in a reactor causing roughness of the polymer surface with ablation and changes in the chemical composition of the material surface.

High intensity e-beam is used for the bulk and thick layers of the polymer treatment with a chain scission and cross-linking.

High intensity UV irradiation causes rough surface with ablation and the change in the chemical composition with a chain scission.

Laser treatment can change the surface from rough to smooth. Depending on the type and power of a laser, it causes ablation, chemical changes with photolysis and chain scission, and other surface modifications.

Electrostatic discharge treatment of a polymer with the humidification of the work area or applying antistatic organic compounds, e.g. non-ionic ethoxylated alkylamine, anionic sulphonate/phosphates and cationic quaternary ammonium compounds, can change the surface properties. [28, Pat.21, URL6]

In the present study, a modification of elastomer surface properties using the plasma and laser treatment was studied, thus a more detailed overview of both methods is presented. The preliminary investigations indicated a possible role and influence of surface roughness; therefore, some findings from the literature are presented below.

2.5.1 Functionalization by mechanical modification of surface roughness

The modification of the surface free energy of polymers using sandpaper of different grain sizes is reported in the literature.

Guo Chaowei and co-authors got a higher contact angle with water using the **rubbing technique by applying different grades of sandpaper** for polycarbonate (grade #240, rubbing 10 ×, changes in contact angle with water from 86º to 136º), for polymethyl-methacrylate (#240, 10 ×, from 75º to 131º), for polystyrene (#240, 10 ×, changes from 78º to 140º), for poly-tetrafluoro-ethylene (#240, 10 ×, changes from 108º to 150º), while the contact angle after the rubbing was lower for polyvinyl-alcohol (#240, 10 ×, changes from 45º to 15º). [Pat.22] For other grades of sandpaper and rubbing intensities, the results were similar in most cases. This method gives a wide range of surface wettability from superhydrophilicity to superhydrophobicity.

Encinas and co-authors reported about by an approx. 10 mJ/m^2 lower value of the surface free energy at the R_a value increased by 1 µm for silicone. For LDPE (low density polyethylene), the surface free energy was higher by approx. 15 mJ/m^2 at the R_a value increased by 4 µm. The surface free energy remains almost unchanged at HDPE (high density polyethylene) and PP (polypropylene) elastomer after the **rubbing with sandpaper**. [29]

The published papers by other authors mostly deal with hard solid materials (metal, silicon, ceramics) or with a very rough surface, typical of road surface and are thus not of interest for this investigation.

2.5.2 Surface functionalization with modification of macromolecular structure

The defunctionalization with heat was reported by Khontong, who first treated the dicumyl peroxide (Dicup) cross-linked natural rubber (elastomer) with $KMnO_4$ and

K_2CO_3 oxidizing agents to get a functionalized hydrophilic elastomer surface. After the heating in hot water (for at least 10 minutes at 50, 70, 90 ºC), the samples became hydrophobic again. The same effect of defunctionalization was observed when using water at room temperature for 24 h. The defunctionalization was interpreted as the result of recoiling of entropic unfavourably uncoiled chains induced when the rubber surface was oxidized. [30]

The switchable "contraphilic" surface of polyurethane was reported by Makal and Wynne with amide inter/intramolecular hydrogen bonding proposed for the hydrophilic (dry) state, while the surface-confined, amide-water hydrogen bonding "releases" semifluorinated groups, giving the hydrophobic state. The hydrophilic wetting behaviour was observed when the samples were dry and hydrophobic when wet. The changes were explained with the nanoscale changes in the chemical composition (on the order of 1 nm) overweighting surface topology with a semifluorinated side chain "release", where the surface became more hydrophobic by pulling the hydrophilic groups away from the polymer-water interface for the polymer immersed in water. [31]

2.5.3 Plasma treatment of elastomers

Plasma (from Greek *πλάσσειν – plassein*, "to mold") is an ionized gaseous medium, which consists of electrons, ions and possibly of neutral particles and photons. Most of the universe is plasma and several natural phenomena, e.g. solar corona, lightning and *Aurora Borealis* are recognized as plasma effects. [32]

The gas plasma surface treatment process was firstly used in 1956 by K. Rossman to introduce polar oxygen-containing groups onto the polyolefin surface [33]. Today, it is a well-suited tool for modifying polymer surfaces. Depending on the process parameters, the material loss or material deposition can predominate.

Plasma activation is an alteration of polymer surface characteristics with a substitution of chemical groups or moieties of groups normally present on the polymer chain being modified. It is a result of bombarding the surface with photons, ions and neutral particles, all of the active species in the plasma reacting with the polymer surface. In low-pressure reactors, the by-products, typically CO_2, H_2O, and low molecular weight hydrocarbons, are readily removed by the vacuum system. The use of co-reactants

like oxygen contributes to an accelerated breaking of bonds and forming of new functional groups. The ionization of oxygen into various species typically gives:

$$O_2 + e \rightarrow O_2^- \rightarrow O + O^-$$

$$O_2 + e \rightarrow O_2^- \rightarrow O + O + e$$

$$e + O \rightarrow O^* + e$$

$$e + O \rightarrow O^+ + 2e$$

$$e + O_2 \rightarrow O_2^+ + 2e$$

$$e + 2O_2 \rightarrow O_2^- + O_2$$

$$O_2^- + O \rightarrow O_3 + e$$

where O^+ and O^- are ionized forms of oxygen and O^* is excited form of oxygen, capable of producing light by releasing a photon.

In an oxygen glow, discharge components formed during the ionization recombine, releasing the energy and photons, emitting a red glow and radiation. [34] The photons in the UV region have enough energy to break the C-C and C-H bonds and the resulting lower weight materials are removed from the surface, together with the products induced directly by the plasma.

Using other gases, different groups and thus different functionalities of the polymer surface are attained. The depth of the surface functionalization is very low, up to a few molecules. In general, gases such as O_2, N_2, He, Ar, NH_3, N_2O, CO_2, CF_4 and air, or some combinations of these gases are used. In a low-pressure oxygen plasma, the following oxidation reaction schemes for polyolefin are expected:

$$RH + O \rightarrow R + OH$$

$$R + O_2 \rightarrow RO_2$$

$$RO_2 + R'H \rightarrow RO_2H + R'$$

$$RO_2 + R' \rightarrow RO_2R'$$

where RO_2H and RO_2R' indicate the formation of acids and esters. A possible formation of alcohols, ethers, peroxides and hydro-peroxides is not indicated. [URL7]

In Figure 7, the plasma phase species with the polymer surface is presented according to Gilliam, the data being compiled from different sources.

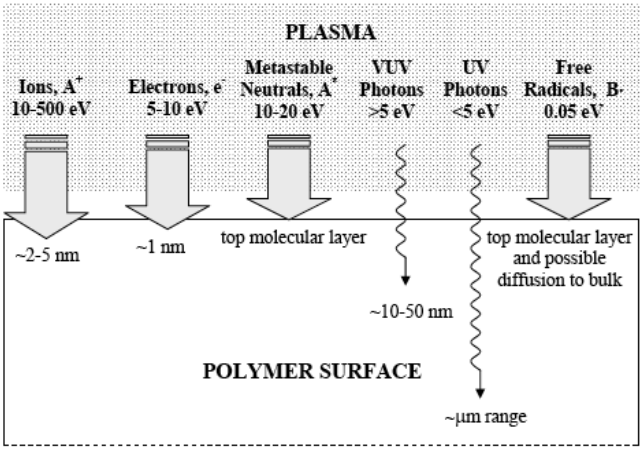

Figure 7: *Interaction of plasma phase species with polymer surface.* [35]

The surface of a polymer is distinguished from the bulk. During the manufacturing process and in use, the polymer is in contact with other materials and air. Several layers of different thickness are thus formed with a strong impact on the surface characteristics (Figure 8).

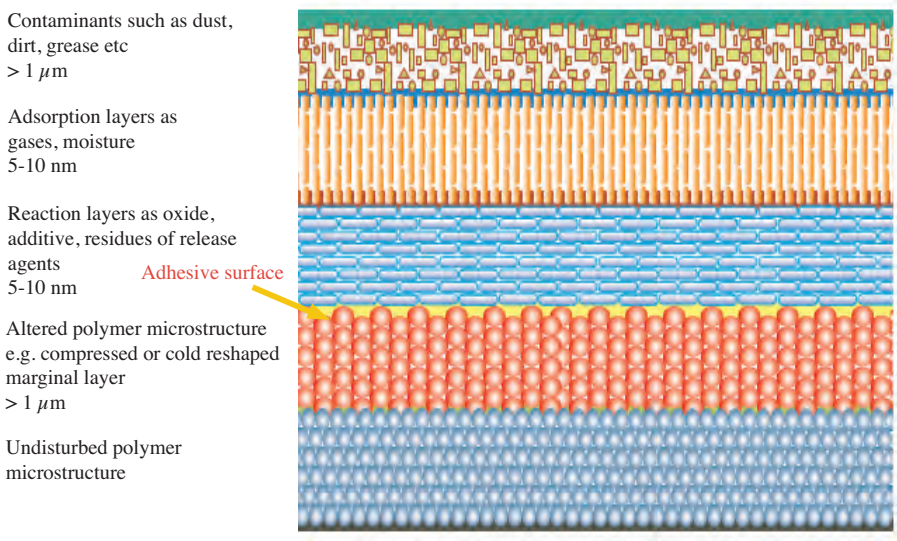

Figure 8: *Surface layers of polymer with different thickness and capability to absorb or react with various gases, contaminants and chemical agents.* [36]

The surface characteristics of polymers and their modification by using a plasma has been continuously studied by many authors for more than 50 years. The majority of published scientific papers deal with polymers for medical use [37], particularly their biocompatibility and adhesiveness to metal and other materials. The printability and surface properties of plastic films used in the packaging printing are typically published as technical papers. In the following overview, only short abstracts of papers and other publications of possible importance for the present investigation, dealing with a plasma modification of the surface free energy of various polymers, esp. elastomers, are presented.

Etching of PTFE (poly-tetra-fluoro-ethylene) and PE (poly-ethylene) polymers by using a plasma consisting of atomic and molecular oxygen, atomic fluorine, CF_x radicals, ions, high-energy metastable species and photons was studied by Egitto. Polymer etching was achieved with fluorine containing gases and oxygen. An important impact of polymer structure on etching, specifically its degree of unsaturation, was reported. The explanation is that unsaturated polymers have a higher affinity for atomic fluorine than the saturated polymer surfaces. The fluorine abstraction of hydrogen atoms from the polymer surface and incorporation of fluorine and/or CF_x radicals into the polymer was observed. The polymer surface was also modified with plasma high-energy metastable species and UV radiation. [38]

Chen et al studied superhydrophilic and superhydrophobic switchable surfaces, formed on a photoresist polymer applied on Si wafer. They used the **all-plasma modification process** based on a different plasma chemistry. This process included a plasma-induced formation of nano-patterns, substrate etching and surface chemical modification. The surface treated with a fluorocarbon plasma becomes superhydrophobic, while the surface treated with an oxygen plasma becomes superhydrophilic. By using a stencil mask, they achieved areas with both characteristics on the same polymer surface. [39]

Kim et al reported on the reduction of adhesion forces between CIIR (chloride-isobutene-isoprene rubber) and stainless steel ball, for the rubber surface excited by plasma treatment with oxygen and argon gases, explained with an **increased Young's modulus and surface roughness** of the rubber after the plasma treatment. [40, 41]

Vesel et al investigated the surface modification of PTFE by using the oxygen and nitrogen RF (radio-frequency) plasma treatment. The **new functional groups** were detected only when using the nitrogen plasma treatment, while the oxygen plasma treatment did not cause any noticeable chemical changes of the surface. [42]

The use of carbon-dioxide gas or liquid with an atmospheric plasma **pre-treatment to remove the micron and submicron particles** from the surface of plastic and other material was reported by Wolf. [43]

The treatment of polyolefins, PET (poly-ethylene-terephthalate) and PMM (poly-methyl-methacrylate) with an atmospheric pressure non-equilibrium plasma developed for the surface **modification including cleaning, degreasing, oxidation, reduction, grafting, cross-linking (carbonization), etching and deposition** was studied by Shenton and Stevens. They made a comparison of a well-known vacuum plasma and an atmospheric pressure non-equilibrium plasma. They achieved many similar surface modifications by using both types of plasma; however, in several cases, e.g. at the surface free energy and roughness, the results were different. [44]

The surface properties of poly(1-butene) were modified by Chvátalová et al, namely by using various RF plasmas based on air, argon, argon then allylamine, argon wearing ammonia and argon with octafluorocyclobutane. All types of plasma except for fluorocarbon cause an **increase in the polar functional groups and hydrophilicity** of the surface, while the fluorocarbon plasma causes increased hydrophobicity. [45]

Friedrich et al reported on a **pulsed plasma polymerization** for producing adhesion-promoting plasma polymer layers with a high concentration of exclusively one sort of functional groups, e.g. OH, NH_2 or COOH, by using allylalcohol, allylamine and acrylic acid. [46]

Joshi studied a selective surface functionalization process, which preferably forms one type of functional groups on the surface in a high and variable concentration. He used the under-water plasma process as one of the most attractive processes to solve the problem of a monotype functionalization. Such a plasma is an efficient source of ions, electrons, UV-radiation, high frequency shock waves, radicals, e.g. hydroxyl radical, and reactive neutral molecules, e.g. hydrogen peroxide, hydrogen and oxygen. It was

established that the **underwater plasma and the closely related glow discharge electrolysis** are interesting new methods for the polymer surface functionalization. An underwater capillary discharge was seen more effective in the -OH functionalization and was largely seen as a flow dominated process due to the shock wave turbulences. By using such a water based plasma, approx. 25–40% of all O-functional groups were produced as OH-groups in comparison to < 10% OH produced in the oxygen low-pressure plasma. The variety of plasma-produced species in the water-phase is also much smaller due to the limited reaction possibilities of a plasma with water. [47]

Zhang et al studied the **deposition of plasma polymers** from di-ethylene-glycol, mono-vinyl-ether and allylamine monomers in a plasma reactor at continuous-wave and pulsed plasma conditions. For different settings of input power and pulse duration in a plasma reactor, a different density of chemical groups was achieved. [48]

The atmospheric pressure plasma achieved by using a corona treatment of PP and the resulting modification of its surface properties, while varying the energy deposition, relative humidity, web speed and gas temperature, was studied by Dorai and Kushner. Significant amounts of gas phase O_3 and N_xO_y were produced. They found out that increasing the energy **deposition increased the densities of alcohol, carbonyl, acid, and peroxy radicals** on the PP surface. Increasing the relative humidity increased the production of peroxy and acid groups, while the decreasing increased the production of alcohol and carbonyl groups. Increasing the temperature decreased the concentrations of alcohol, carbonyl and acid groups on PP, while those of peroxy radicals increased. For a given energy deposition, higher web speeds resulted in decreased concentrations of alcohols, peroxy radicals, carbonyl and acid groups on PP. [49]

The treatment of natural vulcanized rubber by using an atmospheric plasma caused with a dielectric barrier discharge with acetic acid and allylalcohol was studied by Moreno-Couranjou et al. The modification of the surface properties with a **raised total oxygen amount** was confirmed. The C=O bonds might explain stronger adhesion to the silicon adhesive. [50]

The **plasma-source ion implantation technique** was applied as the surface modification method for PET, PVC, PA (polyamide) and PMMA (poly-methyl-methacrylate) films by Tanaka et al. The plasma source was Ar, N_2 and C_2H_2. The

surface of polyester materials was successfully modified with an ion implantation. The process was controlled with a regulation of correct energy of accelerated particles. Low energy ions can catalyse the surface chemical reactions to modify the physical and chemical properties of polymer surfaces. [51]

Pelletier and Anders made an overview of the PBII (plasma based ion implantation), and PBIID (plasma based ion implantation and deposition) methods for a **surface modification and thin film deposition**. They compared the advantages and disadvantages of their method with a conventional ion beam implantation and physical vapour deposition for PBII and PBIID, respectively. Both methods are used for machine parts production, for surgical implants, bio- and blood-compatible surfaces, and coatings etc. With limitations, also the non-conductive materials, e.g. plastic sheets, can be treated. The major interest in the PBII processing originates from its flexibility in the ion energy (from a few eV to up to about 100 keV). [52]

The RF tetrafluoromethane plasma treatment of PDMS (poly-dimethylsiloxane) was studied by Cordiero et al. The smooth PDMS **coatings with fluorine** content up to 47% were attainable. The tetrafluoromethane plasma generated a harder, non-brittle, chemically stable layer without any surface morphology changes. The surface became more hydrophilic after the treatment. That surprising phenomena may be explained with an increased exposure of oxygen containing moieties towards the surface upon the reorientation of fluorinated groups towards the bulk or as a consequence of oxidation effects associated with the plasma treatment. [53]

The **mechanism of fluorination** of the NBR polymer in the RF plasma of fluorinated gases (CF_4, CHF_3) was reported by Tressaud et al. The enhanced fluorination (with CF_2-CH_2, CHF-CF_2 or CF_n groups) of the surface was observed after the treatment at 90 ºC, at room temperature only a small amount of polymer was fluorinated, most fluorine species reacting with inorganic cations (e.g. Ca_2^+, Zn_2^+). [54]

Kitova et al studied the influence of argon, argon/water and argon/ethanol **soft plasma treatment** to the surface free energy of PMMA and PC (polycarbonate). They found out the same effectiveness of short time Ar/H_2O and Ar/C_2H_5OH plasma treatment compared to a long time pure Ar plasma treatment. The ethanol in the plasma resulted in a more uniform, detect free and undamaged surface. [55]

Increasing the surface free energy and decreasing the surface roughness of the EPDM elastomer treated with a nitrogen/argon and nitrogen/hydrogen/argon RF induced plasma was reported by Moraes et al. [56]

The effectiveness of nitrogen, oxygen and air RF plasma treatments on two styrene-butadiene vulcanized rubbers with a different formulation was studied by Ortiz-Mágan and Pastor-Blas. They found out that an extended plasma treated time is required to **remove the sulphur-rich vulcanization agents and wax** from the surface first. Afterwards, a shorter treatment time is enough to increase its polarity with the **creation of C-O and C=O polar groups** on the surface. An air and oxygen plasma proved to be more aggressive than the nitrogen plasma. [57]

For the study of the functionalization of PET, a weakly ionized, highly dissociated RF nitrogen plasma, was used by Vesel and Mozetič. The XPS (X-ray photoelectron spectroscopy) results showed the **appearance of new functional groups**, e.g. amine and amide. [58]

The relationship of the surface polarity, the chemical structure and composition, and the crystalline/amorphous phase contribution in the surface modification mechanisms of plasma-exposed polymers was explored by Borcia et al. The highest degree of modification was obtained for the PA-6 and HDPE samples, where PA-6 is the sample with the highest polarity, whereas HDPE has the simplest structure. The modification was higher for polymers with a lower crystallinity index and lower average size of the crystalline regions. Under the He-N_2 plasma treatment, **free radicals and polar groups were created with a combined functionalization and cross-linking**. The surface treatment resulted in **increased roughness**, accompanied with the formation of a granular ordered structure. [59]

Kumar et al studied the RF **plasma "polymerization"** of PEG (poly-ethylene-glycol) on the PET surface. The modified surface was found to be highly hydrophilic, smooth, thin, pin-hole free as a result of strongly adherent PEG film on the PET substrate. [60]

Avram et al studied Ar and CF_4 or CF_4 with O_2 RF plasma for a surface treatment of the SU_8 photoresist, PDMS elastomer, SiO_2 and Si. An **Ar plasma was used to generate hydrophilic surfaces, and CF_4 or CF_4 with O_2 was used for the creation of hydrophobic surfaces**. [61]

The modification of friction in correlation with adhesion, wettability and surface chemistry changes for the Ar plasma treated PET was studied by Beake et al. They found out that the plasma modified surfaces exhibit higher friction and are more easily disrupted by the movement. The calculations on the contact angle data with a combination of polar and non-polar liquids showed that the argon plasma treatment considerably enhances the work of solid/polar-liquid adhesion and the surface free energy of the films due to the **creation of acidic and base functions** on the polymer surface. In contrast, Lifshitz-van der Waals (non-polar) interactions decrease slightly as a consequence of the **plasma-induced chain-scission**. [62]

The study by Guo et al describes the **surface modification of elemental sulphur with a plasma polymerization** with acetylene, perfluorohexane and acrylic acid. Significant improvements were obtained in dissimilar elastomer blends using a modified encapsulated sulphur powder which was used in the vulcanization reaction. [63]

Grythe and Hansen studied the effect of argon, oxygen and nitrogen plasma treatment of the solvent cast EPDM rubber. They found out that up to 20 % of **oxygen** can be easily **incorporated into hydroxyl groups, but also as carbonyl and carboxyl**. At short times, the surface energy changes were much faster than the changes in the surface structure, and both can be controlled during the treatment. [64]

The EPDM **surface architecture manipulation** with a spin coated and cross-linked monomer-multifunctional acrylate under the impact of an RF oxygen gas plasma was studied by Dessai et al. They established that long term hydrophilic surfaces can be achieved with suitable combinations of N-vinyl pyrrolidone, glycidyl methacrylate, allyloxy-1,2-propanediol monomers and diallyl amine and ethylene glycol dimethacrylate as cross-linkers. [65]

The atmospheric nitrogen plasma activation and polymerization of the EPDM, NBR and SBR (styrene-butadiene rubber) elastomers enormously affect the surface properties by improving the separation force in the case of gluing; the friction properties could decrease with a plasma polymerization, the barrier properties could improve, and the **plasma could clean-up the surface contaminated with the blooming of zinc-stearate**. The elastomer was found to be **chemically functionalized** by the plasma treatment. [66]

2.5.4 Laser treatment of elastomers

Laser (light amplification by stimulated emission of radiation) was invented and patented by Gordon Gould in 1958. His work was based on Einstein's predictions and was conducted at the same time with the work of Townes, to whom the patent for an optical maser, today known as laser, was granted, and simultaneously with Schawlow, Lebedev, Maiman and many other researchers. Most modern laser types were proposed and invented in the following decade after the first laser was built by Maiman in 1961. [67]

Lasers have several impacts on the surface of treated polymer samples, depending on the laser type and settings, polymer material composition, environment and other conditions. Lasers can cause plasma, ablation, deposition, polymerization, other chemical reactions, heating, roughness and other changes on the sample surface, in more detail described below upon few selected publications.

Ahmad et al reported on the **plasma** induced with a Q-switched ruby laser in as early as 1969. They studied a laser induced breakdown of a gas, where two phases in the plasma evolution occurred – the first one was the formation of radiation driven breakdown wave and the second was a purely thermal driven expansion. The ionization was only of secondary importance. [68]

The main mechanisms involved in the generation of the **laser-induced plasma** are multiphoton ionization and electron impacts leading to a cascade breakdown and material ablation. A laser pulse of irradiance higher than certain threshold (generally > 0.9 GW/cm^2) properly adjusted to the considered material produces its breakdown. During the ns irradiation, only a portion of the laser pulse directly interacts with the sample, while, depending on the pulse duration, most of the pulse energy is spent on the heating the ejected free electrons and inducing photoionization of the ablated material. [69]

Laurens et al made a **comparison of the low-pressure plasma and excimer laser** (248 nm wavelength and 30 ns pulse duration) **treatment** of PET. They concluded that extremely significant improvements of the adhesion were obtained in a very short time for both treatment methods. In the case of plasma treatment, the surface

oxidation and increased wettability associated with the surface cross-linking were probably responsible for the reinforcement of the Al-PET strength. In the case of laser treatment, the surface oxidation had a deleterious effect on the adhesion due to an accelerated degradation of the surface with the UV photons irradiation. [70]

Kawamura and Srinivasan issued the first reports on the laser ablation of polymers almost simultaneously in 1982, when the terms "laser ablation", "ablative photodecomposition" and "laser fluence" (energy per unit area) were introduced. The threshold fluence is material and wavelength dependent and can vary from tens of mJ/cm^2 to more than 1 J/cm^2. A chemical surface modification during the laser ablation depends strongly on whether the fluence is above or below the ablation threshold. Lippert reported on the Si-O species ejected from a silicone rubber surface treated by using a laser at the wavelength of 193 nm. On the same rubber, the OH and Si-O groups were formed during an incubation (first pulses under ablation fluence threshold) at the wavelength of 266 nm. [71, 72]

Bityurin et al prepared an overview of models describing laser ablation of polymers. They distinguished between the **photochemical, photothermal and subpicosecond ablation,** and provided a detailed mathematical model of the surface photochemical and photothermal etching, ablation, broken bonds, melting and other phenomena, depending on the laser light properties and polymer substrate characteristics. The subpicosecond ablation was explained with a multiphoton ionization and absorption of radiation with chromophore groups in the polymer. The phenomena of coincidence impact of photochemical and photothermal models were explained, as well as the role of mechanical stresses. [73]

PMMA, PI (polyimide) and specially designed polymers were used by Lippert to show that an ablation mechanism is **a mixture of photochemical and photothermal** features closely related to the polymer structure and properties. Photoactive groups were introduced into the polymer structure to improve the quality of ablation. The complexity of interactions between the polymer and laser photons was illustrated with the photokinetic etching with continuous wave UV lasers, the probably pure photochemical ablation for VUV (vacuum UV) lasers, the mixed photothermal-photochemical laser ablation for other irradiation wavelengths, shock assisted photothermal ablation on ps (picosecond, 10^{-12} s) time scales, the wavelength and

polarization dependent ablation with fs-lasers (femtosecond, 10^{-15} s), and the influence of exciting various functional groups for a mid-IR ablation. [74]

Lippert studied the **UV laser ablation** as a method to structure polymers with a high resolution. Photochemical and photothermal reactions are strongly dependent on the type of polymer, laser wavelength, pulse length and the substrate. The UV laser ablation can also be utilized to deposit thin polymer films with a "pulsed laser deposition"; however, this is limited to certain polymers. An alternative "laser-induced forward transfer" technique utilizes the decomposition of a thin layer to transfer complete layers of sensitive materials to a substrate with a high spatial resolution. [75]

The investigation by Subedi et al of a PC (polycarbonate) surface treatment using two UV lasers with 254 nm and 365 nm wavelengths showed that the treatment performed with a **shorter wavelength resulted in a higher wettability** compared to the treatment with a longer wavelength. Similar results were obtained by Laurens et al, who investigated the impact of two excimer lasers with the irradiation wavelengths 193 nm and 248 nm on PEEK (polyether-etherketone) PC (polycarbonate) and epoxy resin. The results indicate that a much stronger reactivity was obtained after the treatments at 193 nm for all the investigated polymers. At this wavelength, the original polymer surfaces were strongly modified by UV photons; the surface reorganization occurred and polar groups induced an increase in the surface wettability. [76, 77, 78]

The excimer KrF fs-pulsed laser with 248 nm of wavelength gives no hydrogen, oxygen or carbon containing groups below the ablation threshold, indicating a chemically clean processing PTFE film, in contrast to the excimer **ns-pulsed laser** which **chemically degrades** the surface. [79]

Sohn and Lee reported the results of an excimer laser (193 nm) treatment of an SBR elastomer. Upon increasing the energy density, the adhesive strength **increases up to the highest value and decreases** by further increasing the number of irradiation pulses due to increased roughness. [80]

Nearly 80 samples of EPDM, SBR, NR (natural rubber), NBR, and MVQ (methyl-vinyl silicone) sleeves, differing in the rubber composition and additives were treated using an atmospheric plasma, CO_2 laser and electron beam. The results indicated that

a laser beam treatment has a **substantial impact on the surface free energy, ink transfer efficiency and roughness properties** of elastomers. [81]

Graft copolymerization of acrylamide onto PET using a CO_2 pulsed laser was performed to **improve wettability**. After the laser irradiation in air, the films were placed into an aqueous solution of a monomer and then heated to decompose peroxides formed on the irradiated PET film. [82]

The PE **surface in water** was **photochemically modified to be hydrophilic** using an ArF laser. The hydrogen atoms were pulled out from the surface by the hydrogen atoms which were photodissociated from the water and replaced with OH radicals, which were also photodissociated. [83]

Lippert studied the incorporation of photochemically active groups, i.e. chromophore groups to **lower the threshold of laser ablation** caused with photochemical and photothermal reactions of the specially designed polymers and polyimide. [84]

The surface modification of PET with the irradiation with a 193 nm **excimer laser in a vacuum chamber filled with different flux of ammonia** was studied by Wu et al. The hydrophilicity of the surface increased after the patterning and there were no significant change in the roughness. The chemical analysis using different methods showed the grafting of amino groups and C-N bond formation on the surface. [85]

The surface photo-transformation reactions using only photons as reagents were studied by Park et al to create specific surface functional groups to change the surface friction or surface tension, or to covalently bind a wide variety of organic molecules and bio-macromolecules onto the surface. A simple exposure to light through a mask allows for spatial patterning of the surface functional groups and associated surface properties. They found out that the **cis-trans isomerization** is by far the most useful photochemical rearrangement reaction. Azobenzene and stilbene derivatives can be reversibly **switched between the cis and trans forms** by using light. When located on the surface, the cis isomer has a higher dipole moment and greater wettability with water. [86]

The surface properties of PDMS irradiated with an excimer lamp (172 nm) or proper UV laser was studied by Graubner et al. The irradiation in combination with the

formed ozone results in the oxidation of PDMS to SiO_2 at the polymer-air interface. The **photochemical conversion** of surface methylsilane groups to silanol groups is responsible for the large **increase in the surface free energy**. The strict linearity of the contact angle versus the irradiation time and the clear dependence from irradiation intensity allows the tuning of the chemical surface functionalities. [87, 88]

Reif reported on the **impact of pulse duration** on the response of a material. At ns pulses, the surface relaxation/reorganization is present with atom and ion emission that is visible as plasma plume. At ps pulses, the core energy dissipation, core motion and bond breaking is present in the material. At fs pulses, an electronic excitation end electron emission can be observed. After the ablation, the surface relaxes with a self-organized formation of regular nanostructures for a 150 fs pulsed laser treatment of a solid material like Al_20_3, BaF_2 and CaF_2. [89]

2.6 Research challenge and hypothesis

A professional challenge follows the main principle of any modern production process, i.e. the reduction of material, energy, production time at a higher quality, speed, low-cost and environment-friendly manufacturing of goods. Observing the modern offset lithographic press, it can be seen that the blanket cylinder has only one basic functionality, i.e. transferring the ink from the printing plate to the print substrate, usually paper. By rendering the blanket surface with the printing (ink accepting) and non-printing (ink repelling) areas, the printing plate becomes obsolete. The annual worldwide consumption of lithographic printing plates is approx. 50 billion m^2, and even a small percentage of substituting conventional plates with the rendered "rubber blanket", containing the printing and non-printing areas, presents a great advantage regarding the costs and environmental sustainability. [90]

An important breakthrough in such an approach was the plasma functionalization of the material and a discrete defunctionalization of the same material by using electron-beam invented by Mozetič et al. [Pat.23]

The merging of the functionality of the printing plate and "rubber blanket" thus became a serious challenge. The first analysis and treatment of commercially available blankets was performed to get a technically appropriate "window", limited with the surface properties of a functionalized and defunctionalized surface. An overview of published papers and patents in Chapter 2.5, dealing with the treatment of polymers offers an appropriate background for the beginning of experimental work. The preliminary tests of commercially available blanket samples with an oxygen plasma were promising and the investigation continued by using different "rubber blanket" samples and some typical raw materials, e.g. crude rubber and fillers.

There are other possibilities to use a rendered elastomer surface in different conventional or digital printing techniques where similar advantages are expected. The same solutions should be useful in microlithography as well, where the "rubber" stamps are already used in a high-speed mass production of electronic elements on silicon chips or even in nanolithography. [91, 92]

The scientific approach assumes well-known sample properties, controlled processes and proper measurement methods, giving the opportunity to draw grounded scientific conclusions and contributions. The surface layer of each type of the "rubber blanket" used for the investigation is a technical material with unknown (unpublished) technical properties. For each type of the "rubber blanket", a proper blend of crude rubbers from different suppliers was used with different curing agents and additives; hence, an exact chemical composition is unknown. The manufacturing process parameters, e.g. processing temperatures and time, for each operation are an industrial secret. The surface roughness, hardness, elasticity, resistance to solvents and cleaning agents, and other properties are controlled and measured at the end of the manufacturing process to provide the final product for the market according to the producer's internal or published technical specification.

The initial **scientific research challenge** was to study the physical and chemical properties of an oxygen and nitrogen plasma treated "rubber blanket" surface compared to the untreated samples. The functionalization should be determined by measuring the contact angle with different liquids and using proper calculation methods to attain the total, disperse and polar components of the surface free energy that correlate with the hydrophilicity/ hydrophobicity or oleophilicity/oleophobicity of samples. The changes in the chemical composition of probably only a few nm thick functionalized surface layers should be measured. Typical methods introduced in the published papers and other references for the surface chemical structure analysis of polymers are XPS, FTIR-ATR and AFM (atomic force microscope). Other methods were rarely used by other authors and were also less accessible in available laboratories during the investigation.

The determination of surface properties of raw materials was limited to the commonly used crude rubbers and silica fillers. The same or comparable methods of the treatment and measurements as methods used for the study of elastomers should give an overview of the contribution of ingredients to the surface properties of final products.

The functionalization of a polymer surface should be achieved with an oxidation using an oxygen or nitrogen plasma treatment, while the defunctionalization was expected to be achieved using opposite chemical reactions, i.e. reduction and/or

resetting of the macromolecular structure of a polymer by heating using a laser treatment. The rubber or elastomer surface should be defunctionalized by using proper laser heating for only discrete areas to achieve the desired rendering. The macromolecular structure and chemical composition of a laser rendered surface was expected to recover the surface properties of an untreated sample, taking into account some minor chemical or structural differences caused with a plasma or laser cleaning, and ablation effects. The use of lasers which differ in wavelength, frequency, specific power and other properties should result in different effects of defunctionalization. With a short wavelength UV laser, a direct impact on the chemical structure was expected, caused with a bond breaking.

The scientific curiosity was not limited only to the surface free energy and polarity or hydrophilicity/hydrophobicity and oleophilicity/oleophobicity of the untreated, plasma treated and plasma followed by laser treated, or only laser treated sample surfaces. An additional challenge was to identify and interpret the chemical reactions and structural changes on the surface of functionalized and defunctionalized rubber and elastomer samples.

The research **hypotheses** were as follows:

The surface energy of blankets can be increased significantly with a treatment with a low-pressure gaseous plasma.

The increased surface energy occurs due to the formation of surface functional groups.

The surface energy increases by increasing the dose of O or OH radicals until the saturation is achieved at a certain dose.

By increasing the surface energy the adsorption capacity of treated surface increases.

Local heating with an appropriate laser allows for a selective defunctionalization of the surface.

3 MATERIAL SPECIMENS

The samples for the investigation were supplied by Savatech d. o. o. Kranj, a producer of “rubber blankets” for lithographic offset printing and other printing techniques. All “rubber blanket” samples are commercially available and were supplied in January 2009. For all treatments and measurements, samples cut from the same piece of a “rubber blanket” were used for each type. An additional set of “rubber blanket” samples was supplied in March 2010; however, it was used only for additional measurements in certain cases. The measurement results from the new lot were labelled as NEW.

The crude rubbers and silica fillers were supplied in May 2009 by the Central laboratory of Savatech d. o. o. in the same form as they are used in the production process. Only a limited selection of crude rubbers and silica fillers used in the production of the surface layer of “rubber blankets” were supplied.

All liquids used for the sample preparation and measurements were in the p.a. quality.

3.1 Rubber blankets

The trade names, specifications and research labels of "rubber blankets" are presented in Table 6. All samples were used for only some basic measurements. For most of the research, the blanket samples labelled RED, BLACK, BLUE and LIGHT BLUE were used, while for the treatment and measurement methods with a limited accessibility, the selection of samples was even narrower.

Table 6: *Samples of "rubber blankets" used for investigation (producer's data)*.

Blanket trade name	Label	Crude rubber	Polarity	Filler	Curing agent
Advantage UV Red	RED	EPDM	Non-polar	Silica	Sulphur
Advantage UV Black	BLACK	EPDM	Non-polar	Carbon black	Sulphur
Advantage Plus	LIGHT BLUE	NBR/TM 90/10	Polar (NBR)	Silica	Sulphur
Advantage DUAL	BLUE	NBR/TM 90/10	Polar (NBR)	Silica	Sulphur, stronger crosslinking
Advantage Expression	CYAN	NBR/TM 90/10	Polar (NBR)	Silica	Sulphur
Advantage 8848	8848	BR/XNBR 90/10	Non-polar (BR) Polar (XNBR)	Silica	Sulphur

Each type of "rubber blankets" is most suitable for particular printing conditions including the press construction, print substrate, ink, solvents, durability, print quality, and printing speed. The EPDM non-polar rubber based blankets are suitable for the printing with UV polar type printing inks, the NBR polar rubber based blankets are suitable for the use with non-polar vegetable or mineral oil based printing inks. The properties of the NBR rubber were improved by using a blend with the TM rubber. For the mixed printing production with UV and oil based inks, blankets with stronger cross-linking are recommended by Savatech d. o. o.

Sample 8848 is made of BR (butadiene rubber) with a XNBR (carboxylated acrylonitrile rubber) blend and is designed to have a minimum surface wear of the "rubber blanket" for the use in plastic pot and conical shape containers printing.

A thin film of the substances diffusing out subsequently covers the surface of blanket samples, especially the surface of BLACK and BLUE. It is a result of undissolved excess particles of the curing agent and/or additives known as blooming. [14, 93]

The surface of all blankets was buffed (grinded and polished according to specification), with the exception of sample 8848 with a cast surface. Sample 8848 had the nominal thickness of 1.69 mm, while all other samples had the nominal thickness of 1.95 mm.

The technical specifications of samples were obtained by Savatech d. o. o., while additional information is available on their website and in their internal technical documentation. [URL8]

For the measurement and/or treatment, the samples were cut into pieces of a suitable dimension of approx. 10 × 50 mm. The surface plaques caused by blooming, residual rubber dust after grinding and polishing, and other impurities have to be removed prior to the surface treatment and measurements to get reliable results. Every sample was thus wiped with a paper tissue soaked with ethanol and dried for at least 15 minutes prior to the first treatment or measurement. For a subsequent handling, i.e. treatment and measurement, the sample surface remained untouched for another 24 hours. The cleaning of samples took place in accordance with the industrial praxis, where a brand new blanket mounted in a press often gives acceptable functionality and print quality after intensive initial washing, cleaning and a few hundred or even a few thousand impressions.

During the investigation, some less important differences in the measurement results occurred within one set of measurements or between the tests made under different climate conditions (transportation of samples between laboratories, some laboratories without air condition), or due to the time delay from the treatment to measurement. In all cases, the measured effects between the untreated and plasma or laser treated samples were much more significant comparing to the differences between the repeated measurements of the same set of samples within a period of investigation.

For the measurements of the mechanical and structural properties of RED, BLACK, LIGHT BLUE and BLUE blanket surface elastomer properties, special samples of elastomer plates made from the same material (same composition of crude rubber, filler, curing agents and additives) under the same conditions (curing time and

temperature) were prepared and cut into a double paddle form – homogeneous plates of 2 mm in thickness and 75 mm in length, normally used in the production process control (Figure 9).

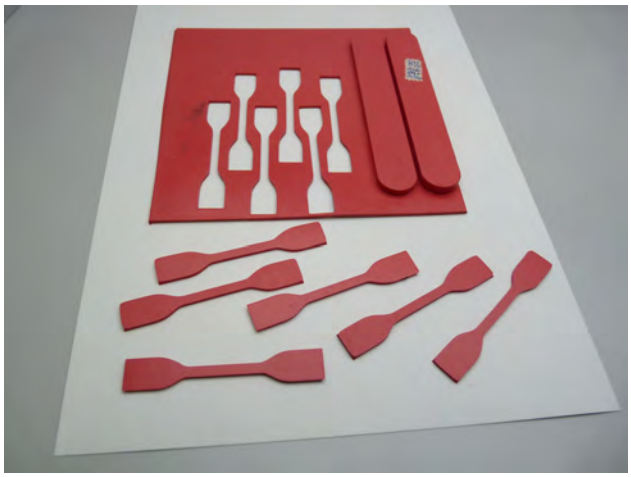

Figure 9: *RED samples of homogeneous elastomer plates die-cut into double paddle form*.

3.2 Crude rubber

Four different pieces of crude rubber were obtained. They were cut from bales, which are most probably used as the basic raw material in the production of the surface layer of the blankets used in the investigation (Table 7). The NBR crude rubbers are transparent, yellowish, tough, elastic and sticky. They have strong adhesion to the surface of other materials and after being cut into small pieces or slices, they tend to "glue" back into one piece of material. The EPDM crude rubber is opaque, white, porous, very tough, however, not sticky.

Table 7: *Crude rubber samples (specifications from producer/supplier data sheets)*. [URL9, URL10, URL11, 94]

Trade name	Label	Savatech code	Specification
Europrene 19.45 GRN	Glass 2	1047	NBR, Polimeri Europa, Italy 19 % acrylonitrile, Mooney viscosity 45 MU (internal)
Krynac 33.30 F	Glass 1	2215	NBR, Bayer Elastoméres, France 33 % acrylonitrile, Mooney viscosity 30 MU (ISO 289)
Europrene 45.60 N	Glass 3	7167	NBR, Polimeri Europa, Italy 45 % acrylonitrile, Mooney viscosity 60 MU (internal)
Keltan 8340 A	Glass 4	7394	EPDM, DSM Elastomers 55 % ethylene, 5.5 % ENB (ethylidenenorbonene) termonomer Mooney viscosity 80 MU (ISO 289)

Due to their physical properties, crude rubbers are unsuitable for a plasma and laser treatment, and for the measurements of their surface properties. Crude rubber was cut into small pieces, dissolved in toluene and applied as a viscous liquid on the glass micro-slides to get a thin polymer film (Figure 10). After the drying of a wet > 0.2 mm thick layer, a dry ~ 0.1 mm thick dry polymer film on a glass appeared. For Glass 1 and Glass 4, the results were satisfactory with a flat smooth homogeneous surface. Glass 1 remained sticky even after the evaporation of toluene. For Glass 2 and Glass 3, the obtained dry surface was rough, the roughness being caused by knot-like forms of the

collapsed polymer. Glass 2 and Glass 3 were used carefully, taking most of the smooth parts for the treatment and measurements. Some influences of the surface structure and unevenness on the measurements were thus possible.

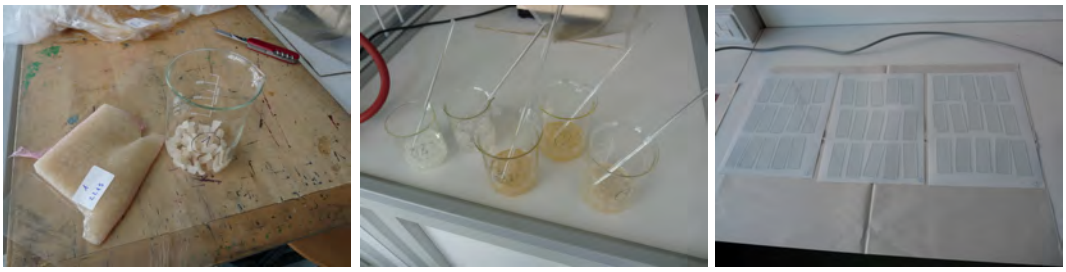

Figure 10**:** *Preparation of crude rubber samples from cut (left), dissolving (middle) to final, prepared samples at glass-slides (right).*

3.3 Silica filler

Two different silica fillers were obtained from Savatech d. o. o. to compare their surface properties and particle sizes (Table 8). Carbon black, as a traditional filler material, was not investigated. The basic silica is SiO_2 dust; however, silica fillers are often modified by using different additives to improve their properties.

Table 8: *Specifications of silica filler samples*. [URL12]

Trade name	Label	Savatech code	Specification
Ultrasil 7000 GR	A	6577	White granules, synthetic amorphous silicon dioxide (SiO_2) content > 97 %, spec. surface area 175 m^2/g
VP Coupsil 6508	B	7112	White powder, reaction product of organosilane VPSi 225 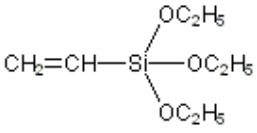 (vinyltriethoxysilane) and precipitated silica ULTRASIL® VN 2, silane content 6.9 %, rest is silica, volatiles 3.5 %, spec. surface area 220 m^2/g

The role of the silica filler is to control viscosity, elasticity and to enhance the elastomer performance by attaching silica to the polymer. The final elastomer products thus become composites with inorganic fillers of nanometer size. The particle sizes are not published in the technical specifications by the producer and depend on proper dispersion and mixing techniques. In the published papers, they are recognized as particulates silica (10–100 nm), aggregates of different structure (100–1000 nm) and agglomerates (1–1000 μm) [95]. For Ultrasil 7000 GR, the primary particle size is 14 nm [96]. Using the de-agglomeration with an ultrasonic technique with a simultaneous laser diffraction, it is possible to detect particle sizes (aggregates) of silica between 40 nm and 500 μm [97].

4 RESEARCH METHODS AND EQUIPMENT

The treatment of samples and the measurement of their properties were performed at different locations. The plasma treatment, initial contact angle measurements and XPS analysis were performed at the "Jožef Stefan" Institute in Ljubljana. The laser treatment of samples was possible at LPKF Laser & Elektronika d. o. o. in Naklo. Most of the contact angle measurements and surface free energy calculations were performed at the Faculty of Pharmacy, University of Ljubljana. An inverse gas chromatography and silica filler particle size measurement was conducted at the same location, and with their support also the AFM and SEM-EDS (scanning electron microscopy – energy dispersive spectroscopy) analysis was possible. An additional SEM-EDS analysis, UV-VIS (ultraviolet-visual) spectroscopy and an interpretation of the FTIR-ATR spectra were performed at the National Institute of Chemistry, Ljubljana. At the Faculty of Natural Sciences and Engineering, University of Ljubljana, where the preparation of all samples was carried out, a part of the UV-VIS measurements, SEM (scanning electron microscope) and optical microscopic analysis were performed and the DMA (dynamic mechanical analysis) was made. With the help of Savatech, d. o. o., sample specimens were obtained and prepared for the measurements. A part of the surface free energy determination based on the contact angle and ink trapping measurements, as the reference to the measurements performed in Ljubljana, was done at the University of Pardubice, the Czech Republic.

In some cases, the equipment was available for only a very limited time. With a schedule coordination and a lot of understanding of all involved colleagues, the most important results of time dependent measurements of physical and chemical properties were obtained within a very short time, by rule within one day. For some very expensive measurements and the use of less available equipment, only a limited number of treatments or measurements was performed, but enough to complete the investigation in the initial stage and to make basic conclusions.

4.1 Plasma treatment

Plasma is used for changing the surface chemistry and morphology by increasing the roughness, cleaning of impurities, etching and plasma polymerization on numerous substrates. Typically, the hydrophilicity increases by using an oxygen, nitrogen or argon plasma, while the hydrophobicity increases with a treatment using a tetrafluoromethane plasma. An oxygen and nitrogen plasma were used for the treatment of hydrophobic elastomer samples to get a functionalized hydrophilic surface.

4.1.1 Plasma reactor

For the plasma treatment of samples, a laboratory plasma reactor with a vacuum pump and an inductively coupled RF generator at the power of approx. 200 W was used. The plasma reactor consisted of a closed glass tube, connected to a vacuum pump on one side and a gas inlet on the other side (Figure 11). A precise valve allowed for fine adjustments of vacuum pressure, controlled by a pressure gauge. The RF generator gave an initial pulse using 14 loops of a copper wire coiled around the glass tube. The treatment time was controlled with a stopwatch and a switch at the RF generator.

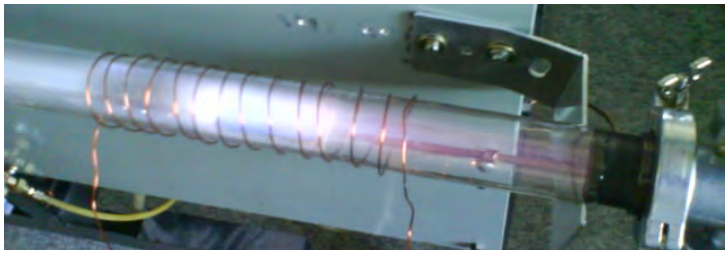

Figure 11: *Plasma reactor during sample treatment.*

4.1.2 Treatment with oxygen and nitrogen plasma

Each sample was exposed to the oxygen plasma with the neutral atom density of 5×10^{21} m^{-3} (4×10^{21} m^{-3}), electron density of 8×10^{15} m^{-3} and electron temperature of about 45000 K for 0, 3, 9, 27, 81, 243 and 729 s. The samples were kept at the floating potential of –15 V. The pressure for the low-vacuum plasma was 75 Pa.

In the preliminary treatment, the influence and dose of the plasma treatment was established. The surface energy remained stable after the oxygen plasma treatment of

the “rubber blanket” samples for 24 h, thus additional treatments and measurements were possible within one day. For all samples, the treatment time of 27 s was used to achieve a low contact angle with water on the rubber and elastomer samples.

For the nitrogen plasma treatment, the same treatment time (27 s) and pressure (75 Pa) were used with the neutral atom density of 1×10^{21} m^{-3}, electron density of 8×10^{15} m^{-3} and electron temperature of 45000 K. [98, 99, 100]

4.2 Laser treatment

For the defunctionalization of the plasma treated rubber and elastomer samples, different types of lasers were used. The first laser treatment to achieve JND (just noticeable difference) between the untreated and treated surface was investigated, and controlled with an optical microscope. Using a low-cost red laser with the power of 100 mW, a green laser with the power of 50 mW and a green laser pointer with the power of 100 mW for the purpose of preliminary tests, no measurable results at the treatment time of 5 minutes were obtained.

A successful treatment of rubber and elastomer samples was achieved by using precise, powerful professional equipment, designed and built for the marking, ablation and cutting systems by LPKF Laser & Elektronika d. o. o. Two devices, one with an IR laser and one with a UV laser, were available for a limited period of time at the producer's laboratory. Both were of similar construction, using the laser beam positioning with a computer-controlled scanner/mirror system and focusing through telekinetic lens that allow for the beam to maintain the right angle towards the material (Figure 12). This scanning process allows the use of software to generate a vector pattern for the surface rendering. [URL13]

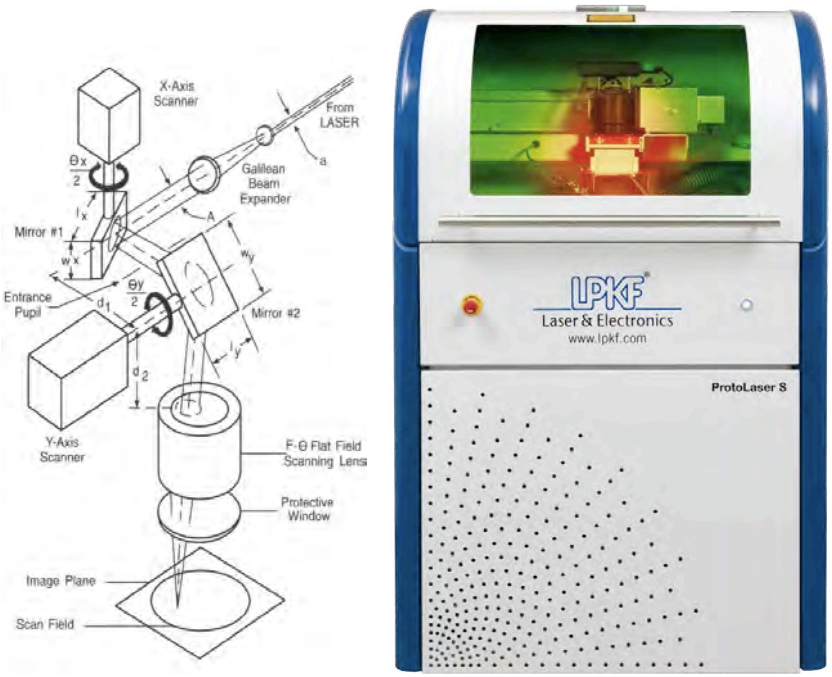

Figure 12: *Schematic presentation of laser imaging system (left)* [URL14], *and device from LPKF (right).*

The main parameters of lasers used in this investigation and their relations were as follows:

$$E_p = P / f , \quad (6)$$

where E_p is the pulse energy (μJ), P the average power (W), f the frequency (kHz), and

$$P_p = E_p / \tau , \quad (7)$$

where P_p is the peak power of pulse (kW) and τ pulse duration (ns).

A professional IR Nd:YAG (neodymium-doped yttrium aluminium garnet, Nd:$Y_3Al_5O_{12}$) laser device, operating at 1064 nm, has the average power of 17.5 W at 200 kHz frequency and 85 ns pulse duration. The pulse energy at this condition is 87.5 μJ and the peak power 1029 W at the theoretically full efficiency. The output peak power setting of this type of an IR laser device is possible by adjusting the current at the LED (light emitting diode) light source or by adjusting the frequency or other parameters. The spot size, normally (in focus) of 25 μm in width, is empirically determined as the width of one ablation line in a thin copper layer on the polymer substrate (used in circuit board production). The energy profile of the spot is in the Gaussian shape.

For the IR laser treatment of RED, LIGHT BLUE and BLUE blanket samples, the average power adjusted to 16 W at the frequency of 200 kHz and 85 ns of pulse duration to achieve 80 μJ of pulse energy and 941 W of pulse power was appropriate for the initial settings of the laser device. An additional adjustment included a new setting of raster (distance between spots) to 35 μm with the spread spot to approx. 50 μm with the out-of-focus setting. Taking into account the efficiency loss (including the optical system and raster setting) by factor 0.66, the more real pulse power rated 621 W was attained.

For the BLACK blanket sample, a very deep surface engraving, caused by ablation, occurred using the same settings. Even in the CW (continuous wave) mode at the average power of 1 W (lowest possible power setting), a strong ablation occurred and the JND sample treatment was impossible.

The UV laser device was based on the frequency-tripled Nd:YAG laser, operating at 355 nm and average power up to 5 W, repetition rate 20 kHz to 100 kHz and spot size

20 μm. The adjustments of the peak power for this type of UV lasers are provided by the frequency settings and adjustments of raster, spot size and focus of the laser beam. The CW operation mode was not possible.

For the RED, LIGHT BLUE and BLUE blanket samples, the UV laser average power was adjusted to 0.17 W (measured with an Ophir Nova II laser power/energy meter; theoretically, it was calculated to only 0.1 W and the difference is explained due to the non-sufficient reliability beyond the normal working range of the device) at the frequency of 100 kHz and 8 ns of pulse duration to achieve 1.7 μJ of pulse energy and 212 W of pulse power. With the efficiency loss factor 0.66, the rated pulse power was calculated to be 140 W. An additional adjustment included the out-of-focus setting by 1.9 mm to spread the spot size to 35 μm.

For the BLACK blanket sample, the basic setting remained the same with the out-of-focus setting being 4.95 mm.

For the crude rubber samples applied on slide-glass, the UV laser was adjusted to the average power of 3.8 W at 100 kHz frequency and 29 ns pulse duration to achieve 38 μJ of pulse energy and 1310 W of pulse power. With the efficiency loss factor 0.66, the pulse power rated 865 W was attained. For different samples, the out-of-focus was adjusted within the range 0.5–2 mm

Several steps were necessary to achieve proper JND for the IR and UV laser devices used in an unusual or beyond normal work area. The process of approaching JND is presented in Figure 13. The system was very sensitive to the out-of-focus adjustments. The same procedure was repeated for each sample. The efficiency loss factor is an approximation, based on the observation of initial results and should be approved and corrected in the future.

During the IR and UV laser treatment of samples, the plasma was observed as a bright white or bluish light with small sparks at the point where the laser beam treated the surface, especially at higher pulse power settings.

Figure 13: *Steps to achieve JND on RED plasma treated sample by rendering 8 × 1 mm area with different settings of UV laser device (top) and rendered surface 8 × 40 mm for final sample (down).*

4.3 Surface free energy determination

For solids, especially polymers with a low surface free energy, direct measurements were not possible, thus the contact angles of solid samples with polar and non-polar liquids, i.e. water, diiodomethane, formamide and ethylene-glycol, were measured first, followed by the calculations using different equations to get the total surface free energy with disperse and polar components. Additional information on acid and base components of surface free energy was obtained using the calculations based on the van Oss theory.

An alternative method based on ink trapping was used only for some samples due to the additional control and confirmation of results, based on the contact angle measurements and calculations.

4.3.1 Contact angle measurement

A Krüss DSA100 apparatus with appropriate software DSA1 v. 1.9 was used for the contact angle measurements (Figure 14). The climatic conditions, measured with an Oregon RMR203MG instrument, were near the standard, the temperature ranging 21–26 ºC and the relative humidity ranging 31–38 %. The image of a static sessile drop was taken at approx. 20 s after the deposition when the drop shape became stable. The drop image was analysed using the "circle fitting" option from the software menu to a prior "manual with line fitting" baseline setting option from the program, and then the contact angle was calculated. The measurements of an unstable, "movable" drop and consequently incorrect results (contamination of the surface and impurities on the surface, technical problems with air bubbles in the syringe pump system, or other reasons) were excluded and the measurements were repeated if that was possible.

For each sample, at least 10 measurements were taken and the average value was calculated and reported. For some sets of treated samples, only the measurements with water or a reduced set of liquids were conducted to finish the measurements within one day (24 h).

Figure 14: *Krüss DSA 100 apparatus during measurement of RED sample*.

The specifications of IFT (interfacial tension) of test liquids, used for the calculations according to the database included in the software, and the drops volume are presented in Table 9. The terminology is in compliance with the original Krüss database, where the data with different values for the same standard liquids, but from different sources, are available as well.

Table 9: *Specification of test liquids*. [URL15]

Liquid	Volume	IFT (total)	Disperse	Polar	Acid	Base
	µl	mN/m				
Water (Ström)	1.0	72.8	21.8	51.0	25.5	25.5
Diiodomethane (Ström)	0.5	50.8	50.8	0.0	0.0	0.0
Formamide (AB)	1.0	58.0	39.0	19.0	2.3	39.6
Ethylene-glycol (AB)	1.0	48.0	29.0	19.0	1.92	47.0

4.3.2 Calculation of surface free energy

The **Owens, Wendt, Rabel, Kaelble** method (extended Owens-Wendt calculation method for measurements with more liquids), **Wu** method and the acid-base method according to **van Oss & Good** were used to determine the surface free energy. For some measurements with only one liquid (water), the **EOS** (equation of state) method was used.

All four methods are supported by the DSA1 software used for the calculations. The calculated surface free energies using different methods and their components are presented in the Appendix in the published contributions at scientific conferences.

The contact angle measurements on a rough and heterogeneous surface are not reliable according to the published references and the used calculation methods are not very precise or generally applicable for all substrates. The final results of the calculated surface free energy according to different methods vary and should be used only as a relative evaluation within one set of measurements and one method of determination of the surface free energy.

4.4 Scanning electron microscopy – SEM

SEM JEOL JSM-6060LV was used for the visual observations of the surface structure and Carl Zeiss FE-SEM SUPRA 35 VP, equipped with EDS Oxford Instruments Inca 400 unit, was used for the chemical analysis.

All samples were sputter coated with a thin Au/Pd layer prior to the observation and chemical analysis to improve the surface conductivity and thus the image quality. For a chemical analysis, these two elements should be subtracted (excluded).

SEM-EDS provides a chemical analysis using the interaction between the primary electron beam and atoms in the sample, which results in the emission of an X-ray. The emitted X-ray has the energy which is characteristic of a parent element. The detection and measurement of the energy permits a qualitative and quantitative analysis of the elemental composition with a sampling depth of approx. 1 µm (Figure 15). It is suitable for the elements with a high atomic mass and is therefore useful for the analysis of fillers and additives in the elastomer, but not for the organic polymers. [101, 102]

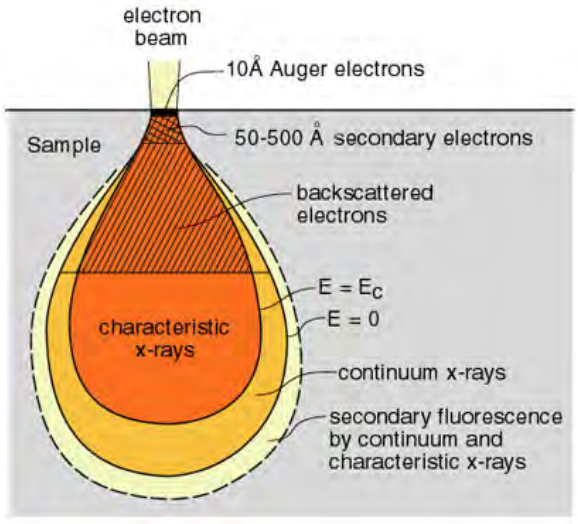

Figure 15: *X-ray escape depth presented in "interaction volume" of SEM*. [URL 16]

4.5 Fourier Transform Infrared – Attenuated Total Reflectance – FTIR-ATR

Perkin Elmer, Spectrum GX1, FTIR-ATR spectrometer (Figure 16) in the mid IR area (wavenumber 500–4000 cm^{-1}) was used to get the IR spectra of the untreated and treated samples. The KnowItAll Academic Edition software, from Bio-Rad Laboratories, was used for the spectra analysis. The software module AnalyseIt IR with an IR spectra database was used to interpret the spectra.

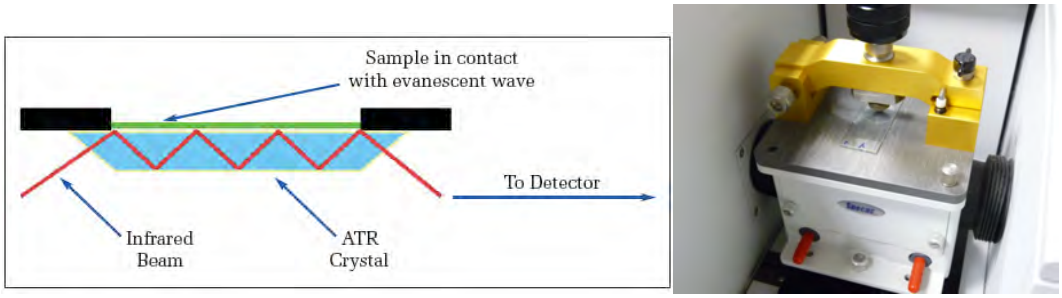

Figure 16: *Schematic presentation of FTIR-ATR measurement principle (left) and slide-glass with crude rubber sample in measuremnt position (right).*

In the ATR mode, the sample is placed in contact with a high refractive index crystal. The IR beam enters the crystal and the rays at or beyond the critical angle to the sample interface are reflected. At each reflection, some energy is effectively absorbed by the sample, the resulting spectrum is measured by the spectrometer in a normal way and the system then generates the IR spectrum. Typical peaks of the absorption spectra provide information on the chemical groups or bonds on the sample surface.

The IR beam depth of the penetration on FTIR-ATR was calculated using the Harrick's method [103] for the diamond crystal refractive index ($n_1 = 2.4$), incident angle 45º, wavelength 1000 cm^{-1}, typical polymer refractive index ($n_2 = 1.5$), and gave 1.176 µm with the highest response from the surface of the sample.

The formula for the depth of penetration d_p is given with:

$$d_p = \lambda_1 / 2\pi(\sin^2 \phi_1 - n_{21}^2)^{1/2}, \qquad (8)$$

where λ_1 ($=\lambda_0 / n_1$) is the wavelength of the incident light in medium 1 (crystal) and λ_0 the wavelength in vacuum, ϕ_1 is the angle of incidence of the IR beam on a plane

interface, and n_{21} (= n_2 / n_1) the quotient calculated from the refraction indexes of medium 2 (sample) and medium 1 (in this case, diamond crystal).

At d_p, the amplitude of the evanescent wave falls to e^{-1} of its value at the interface.

4.6 X-ray photoelectron spectroscopy – XPS

XPS, also known as ESCA (electron spectroscopy for chemical analysis), was used to determine the quantitative atomic composition and chemical structure of a sample surface (Figure 17). It is a surface analysis technique with a sampling volume that extends from the surface into the depth of up to approx. 5 nm, some authors report an even lower penetration depth of 2 nm for electrons, 1 nm for ions and 1 µm for photons. [104]

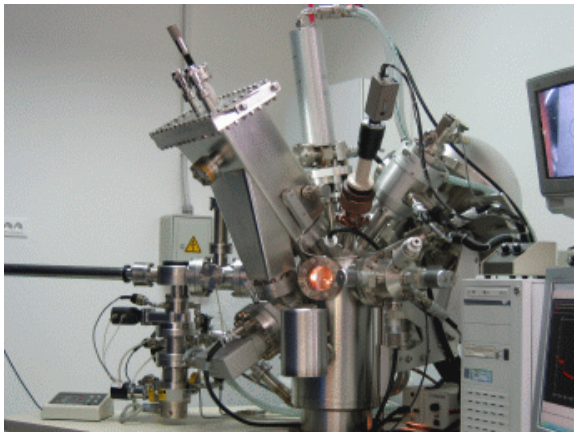

Figure 17: *XPS apparatus at "Jožef Stefan" Institute in Ljubljana used in the research.*

Physical Electronics Inc., model TFA XPS spectrometer was used in the investigation. The process works by irradiating a sample with monochromatic X-rays, resulting in the peaks of the emission of photoelectrons the binding energies of which are characteristic of the elements within the sampling volume in a high vacuum.

An ultra-high vacuum at 10^{-7} Pa was used for the XPS measurement. The power of the X-ray source was 200 W, with the X-ray energy 1486.6 eV, the energy resolution was 0.6 eV. The aperture diameter of 4.0 mm on a sample holder was used. First, the overview spectra in the wide range 0–1100 eV were measured and afterwards, the high energy resolution C1s and S2p spectra were measured.

The method is advanced, high-tech, highly specific, expensive and time consuming; therefore, only a few measurements were performed to attain precise, reliable reference results and to find the correlations with other methods for the chemical analysis of the surface, especially with the FTIR-ATR method.

4.7 Other measurement methods

A short overview of methods supporting or upgrading the primary performed measurements or presenting an alternative to the confirmation of results is presented as follows.

4.7.1 Optical microscopy

Different optical microscopes, conventional or equipped with a digital camera, were used during the investigation. The images were taken on a Leica microscope at an optical magnification of 35×.

4.7.2 Roughness measurement

A Mahr M1 perthometer (Figure 18), a stylus based instrument, was used for the roughness measurements. The stylus with a fine tip slides on the surface of a sample and consequently, a profile of the surface is obtained. From the surface profile, the R_a, R_z, R_{max} and other geometric characteristics of the surface were calculated.

The mean values and standard deviation of 20 measurements performed in different directions on the untreated and treated blanket samples led to the information on surface roughness, caused by a plasma or laser treatment of the surface.

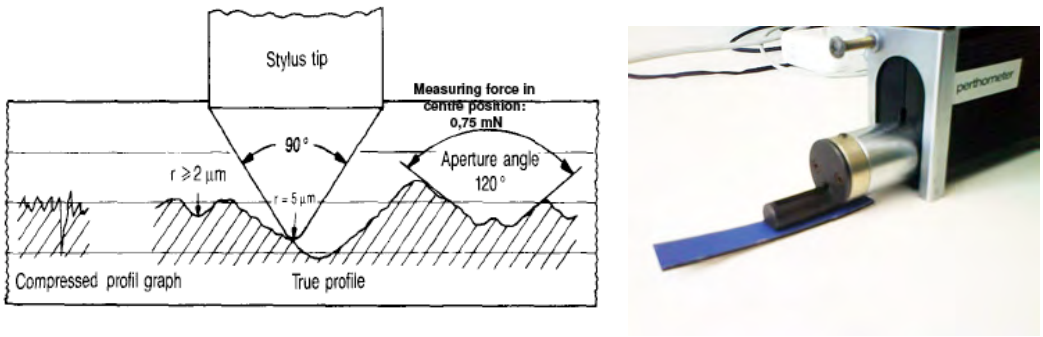

Figure 18: *Principle of roughness measurement with stylus-based instrument* [URL17] *(left), and Mahr M1 measuring head (right).*

4.7.3 Dynamic mechanical analysis – DMA

A TA Instruments model Q 800 instrument (Figure 19) was used for DMA. Crude rubbers and specially prepared elastomer probes were cut to get appropriate sample

stripes, clamped into the device. The settings of measurement parameters followed the technical specifications for each material from the published literature. Each sample was mechanically treated, the response of the probe to the impact forces under a wide range of temperatures in the measurement chamber was recorded and then used for the calculation of material properties, e.g. T_g and tan δ (ratio of loss modulus to storage modulus), using appropriate software provided by the supplier. [105]

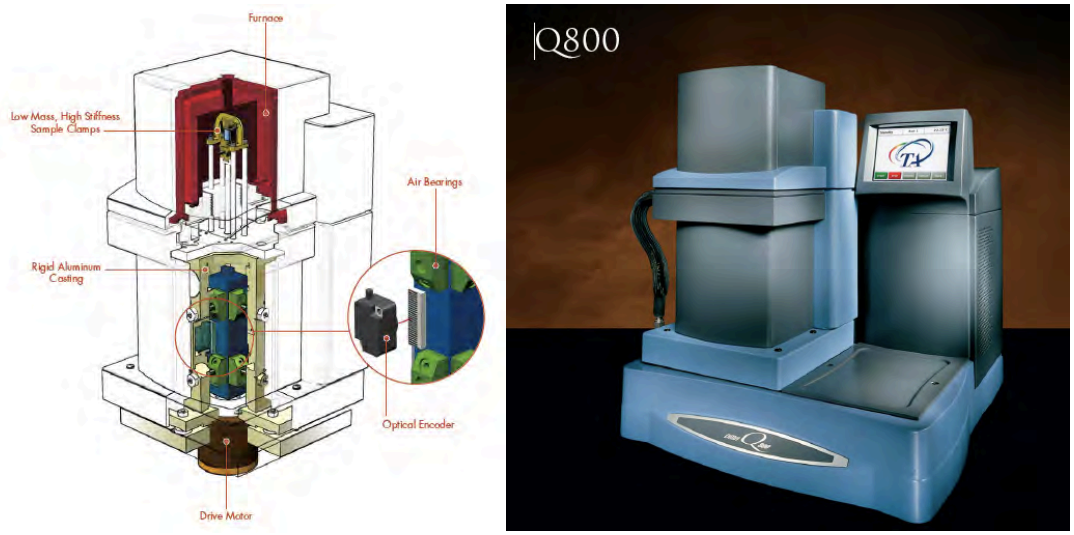

Figure 19: *Schematic presentation of measuring chamber (left), and DMA apparatus TA Instruments Q800 (right)*. [URL18]

4.7.4 UV-VIS spectrophotometry

The reflection spectra of blanket samples were measured first on a Perkin Elmer Lambda 800 UV-VIS spectrophotometer (Figure 20) in the range 175–900 nm to get an overview of the spectral absorbance of different rubber samples before the laser treatment. Due to the wavelength of the IR laser beam being 1064 nm, all the measurements within the range 200–2000 nm on a Perkin Elmer Lambda 950 UV-VIS spectrophotometer were repeated later.

.

Figure 20*: Lambda 800 UV-VIS spectrophotometer*.

A conversion of the measured reflection spectra to the absorption spectra was made using the Beer-Lambert law:

$$A = -\log (I_r/I_0) , \quad (9)$$

where A is absorbance, (I_r/I_0) is reflectance, the quotient of intensity of reflected and incident light (measured value with UV-VIS spectrophotometer)

4.7.5 Inverse gas chromatography – IGC

The measurements with an IGC (inverse gas chromatography) apparatus Agilent Technologies 6890N (Figure 21) were performed to get an overview of the surface properties of the silica filler samples that could not be measured using the contact angle method. The tablet made of a silica filler (samples A and B, Table 8), prepared for the contact angle measurements, absorbed the drop of water immediately and was thus characterized as superhydrophilic.

IGC is a gas phase technique for characterizing the surface and bulk properties of solid materials. The cylindrical column of the IGC apparatus was uniformly packed with silica powder samples. A pulse or constant concentration of acetone vapour was then injected down the column at a fixed carrier gas flow rate and the time taken for the pulse or concentration was measured with a detector on the other side of the column.

Only two measurements were performed to confirm the difference between two silica fillers.

Figure 21: *Measuring chamber of Agilent Technologies 6890N, glass cylinder filled with silica, connected to gas inlet and measurement sensor is visible.*

4.7.6 Particle size measurement

The particle size measurements of silica powder samples were performed on a Malvern Instruments Master Sizer 2000 apparatus based on a laser beam diffraction, represented in Figure 22.

The agglomerates of silica samples A and B were very rigid, and any attempt of breaking them apart into basic particles using an ultrasound treatment in an ethanol bath was not very successful.

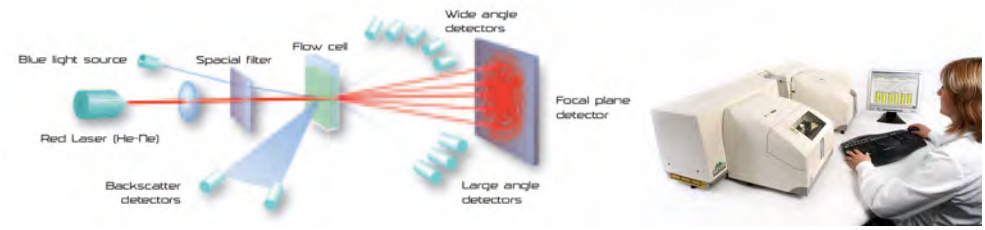

Figure 22: *Presentation of laser beam diffraction measurement principle (left), and Master Sizer 2000 apparatus (right).*

4.7.7 Atomic force microscopy – AFM

The sub-nanometer characterization of the probe surface is possible with AFM. The measurement principle is based on a very precise tip, scanning a small area of the probe surface where the atomic force of a sample leads to the deflection of cantilever. Depending on the situation, the forces that are measured include the mechanical contact forces, van der Waals forces, capillary forces, chemical bonding, magnetic forces etc. [URL19]

Only two samples were measured using the AFM method to get an initial overview into the measurement technique and to compare the AFM nano-topographic image of the surface with the images obtained using SEM and an optical microscope.

4.7.8 Ink trapping

The modified method by Kang [106] was used for the ink transfer/trapping measurement on a proprietary build instrument (at the University of Pardubice, Figure 23), where the amount of a drop of ink, transferred from the donor "rubber blanket" to a piece of standard paper was weighed and the relative trapping of different samples was calculated. The water based printing ink for flexographic printing was used according to the internal specifications..

Figure 23: *Process (from left to right) of weighing, splitting flexographic printing ink droplet and projection of split droplet onto the screen to control the experiment.*

5 RESULTS OF THE STUDY

Only the key results of the study are presented. Other results are available in the papers published at international research conferences (cf. Appendix).

5.1 Contact angles and surface free energy

The results of contact angles with water to determine the stability of achieved changes in hydrophilicity after the oxygen plasma treatment are presented in Figures 24–29. The contact angles for the treatment times longer than 80 s were not measured, as the samples showed visible traces of thermal degradation and burning. All measurements were performed immediately after the treatment, and repeated after 3 h and after 24 h.

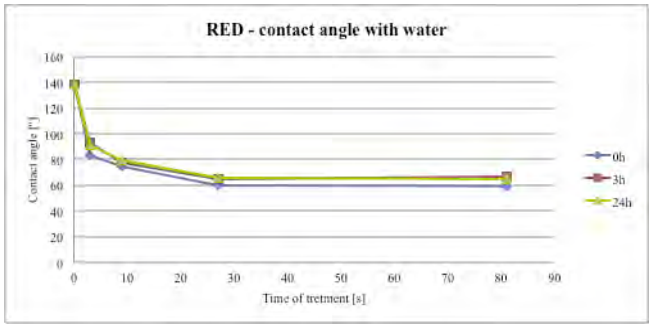

Figure 24: *Contact angles with water for RED sample, as function of time taken for oxygen plasma treatment.*

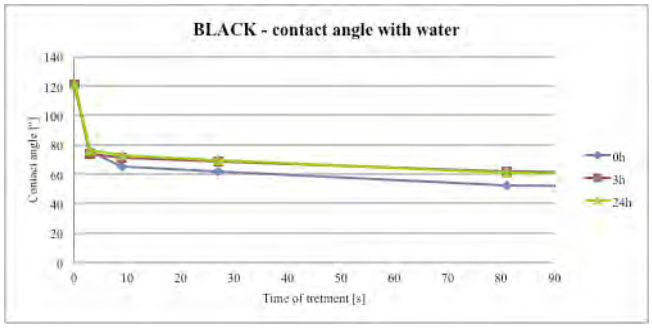

Figure 25: *Contact angles with water for BLACK sample, as function of time taken for oxygen plasma treatment.*

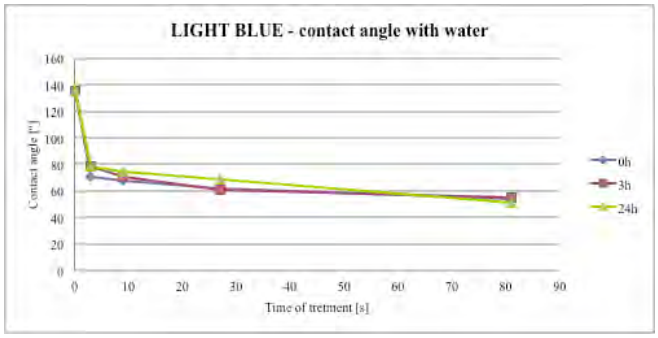

Figure 26: *Contact angles with water for LIGHT BLUE sample, as function of time taken for oxygen plasma treatment.*

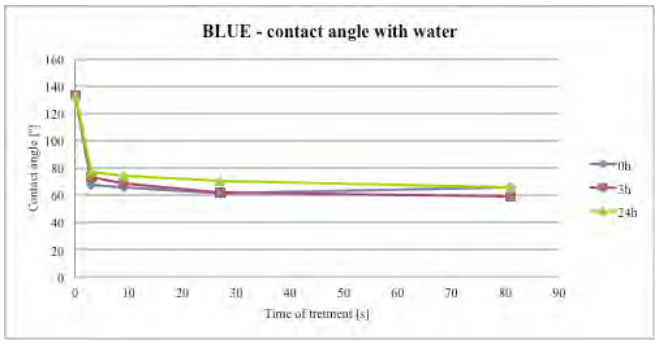

Figure 27: *Contact angles with water for BLUE sample, as function of time taken for oxygen plasma treatment*.

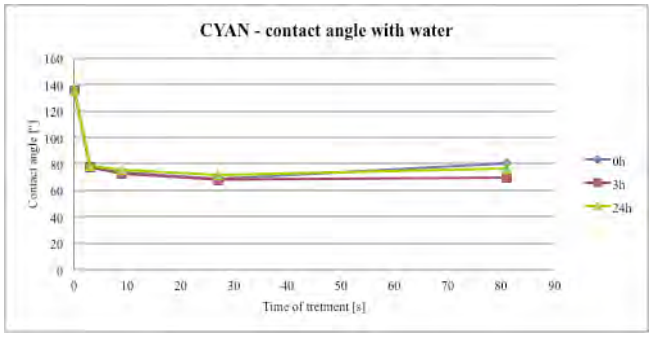

Figure 28: *Contact angles with water for CYAN sample, as function of time taken for oxygen plasma treatment*.

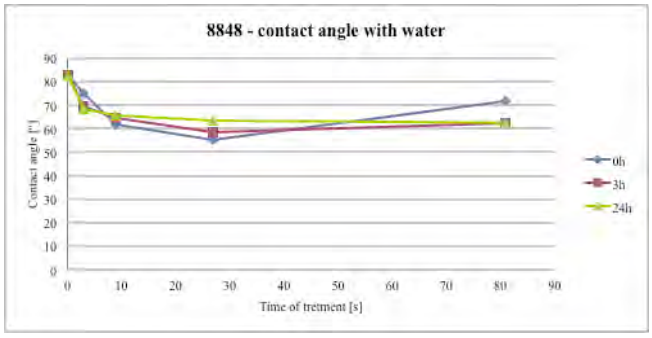

Figure 29: *Contact angles with water for sample 8848, as function of time taken for oxygen plasma treatment*.

In Figure 30 surface free energies with disperse and polar components of 'rubber blankets' are presented for untreated, oxygen plasma treated and nitrogen plasma treated samples. Nitrogen plasma treatment was not applied to CYAN and 8848 samples.

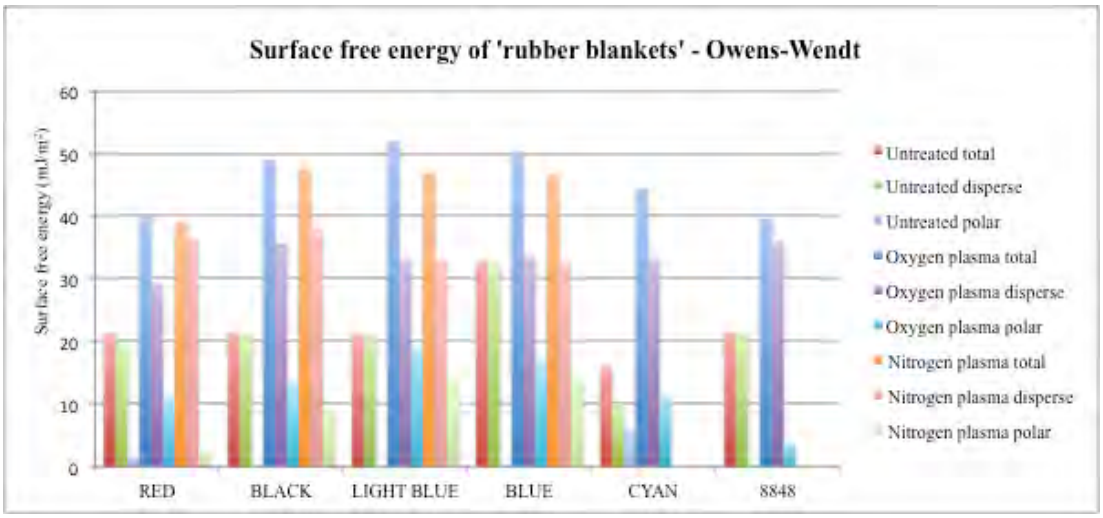

Figure 30: *Surface free energy of "rubber blanket" samples, treatment time being 27 s for all samples*.

In Figure 31, the surface free energy of the untreated and oxygen plasma treated crude rubber samples are presented.

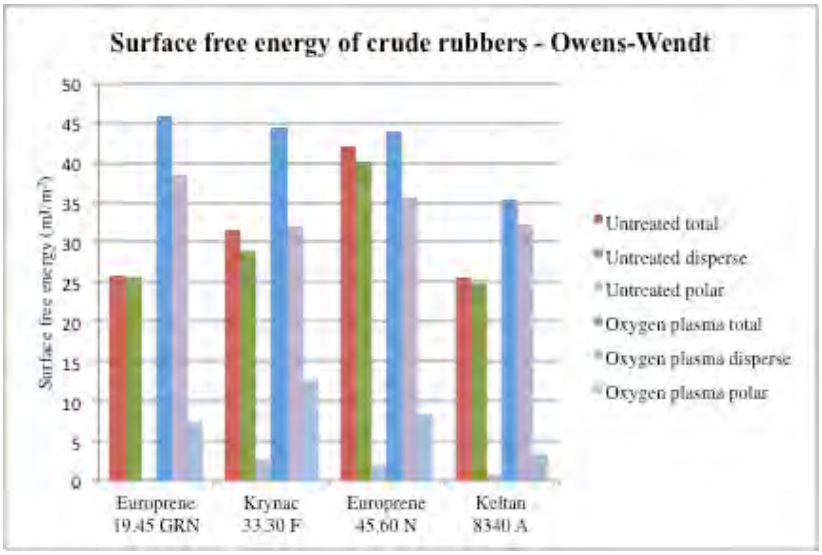

Figure 31: *Surface free energy of crude rubber samples, treatment time being 27 s for all samples*.

The changes in the contact angle with water for the untreated, and after the oxygen plasma and laser treatment are presented in Figure 32. A significant difference (lower values) in the contact angle with water, comparing Figure 32 to Figures 24–27, could be a consequence of different measuring conditions (difference in drop volume 1 µl vs. 3 µl, at unknown temperature and relative humidity) and apparatus (reading and

calculating contact angle from drop shape)

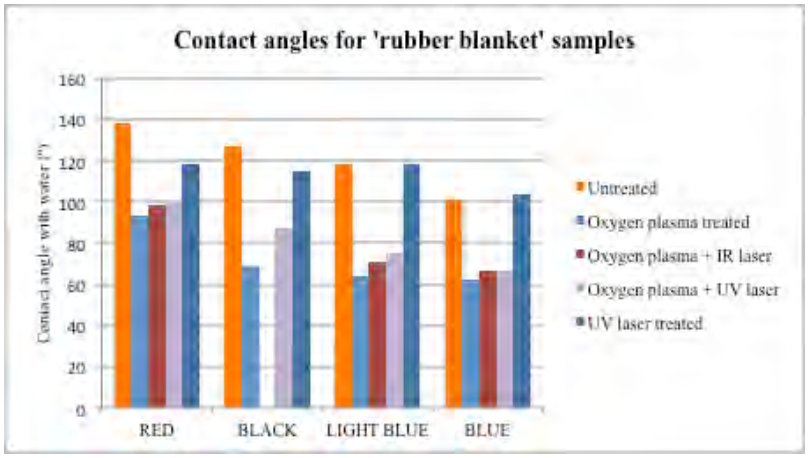

Figure 32: *Contact angles with water for "rubber blanket" samples after oxygen plasma, IR laser and UV laser treatment. Time for oxygen plasma treatment was 27 s for all samples, laser was set to achieve JND.*

In Figure 33, the contact angles with water for the untreated, plasma and UV laser treated crude rubber samples are presented.

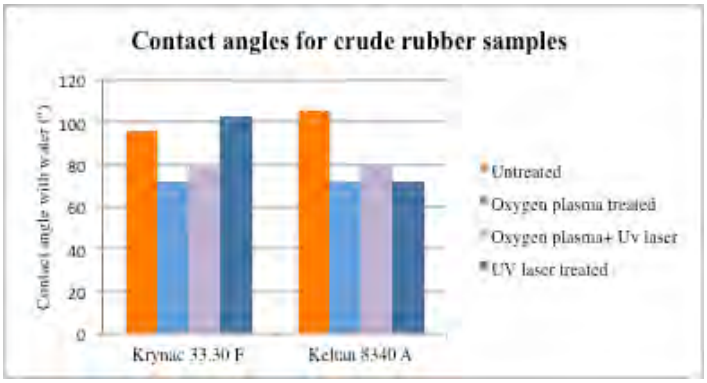

Figure 33: *Contact angles with water for two crude rubber samples after oxygen plasma and UV laser treatment. Time for oxygen plasma treatment was 27 s for all samples, laser was set to achieve JND.*

5.2 SEM images

The impact of the oxygen plasma treatment on the "rubber blankets" for 27 s is presented in Figures 34–36.

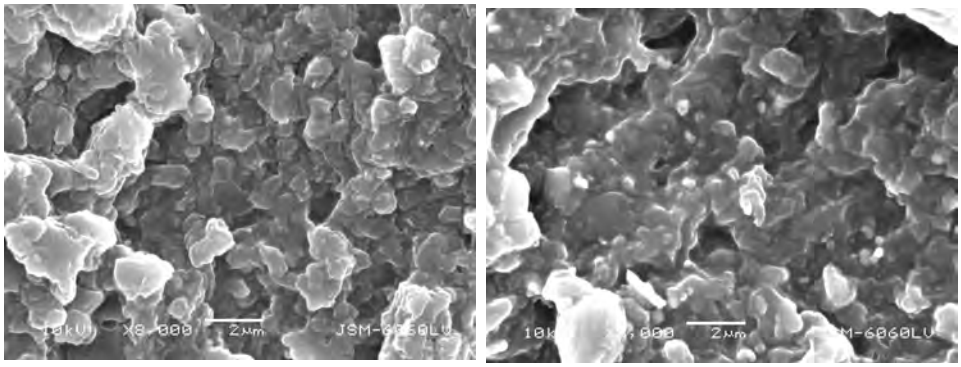

Figure 34: *RED "rubber blanket" samples, untreated (left) and oxygen plasma treated for 27 s (right).*

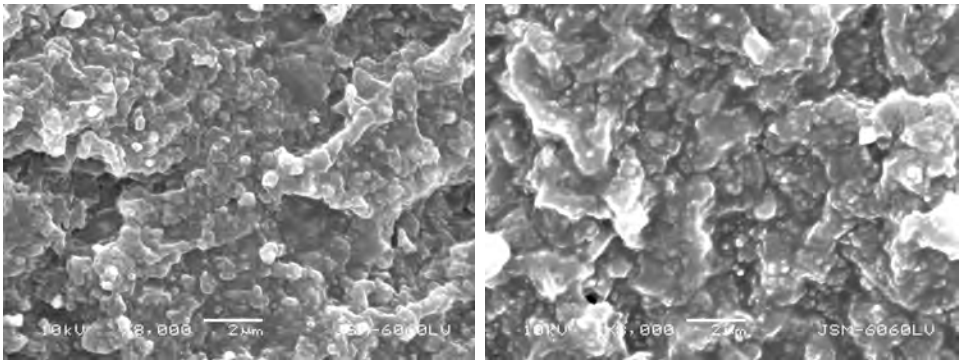

Figure 35: *BLACK "rubber blanket" samples, untreated (left) and oxygen plasma treated for 27 s (right).*

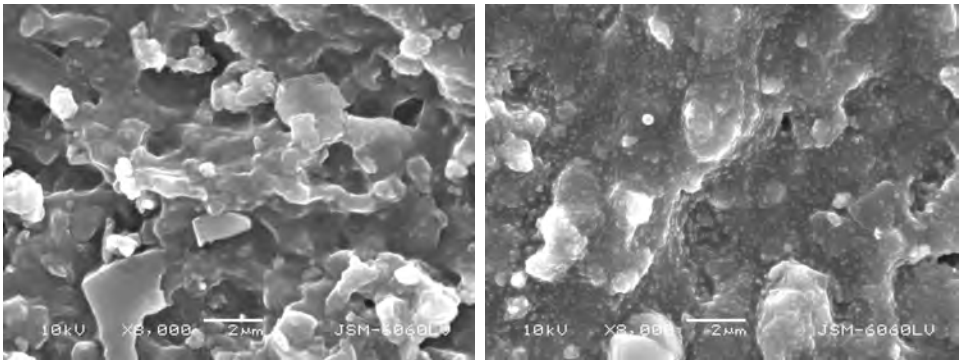

Figure 36: *BLUE "rubber blanket" samples, untreated (left) and oxygen plasma treated for 27 s (right).*

The SEM images of the untreated, UV laser treated, oxygen plasma treated (27 s) and oxygen plasma with UV laser treated BLUE samples are presented in Figure 37.

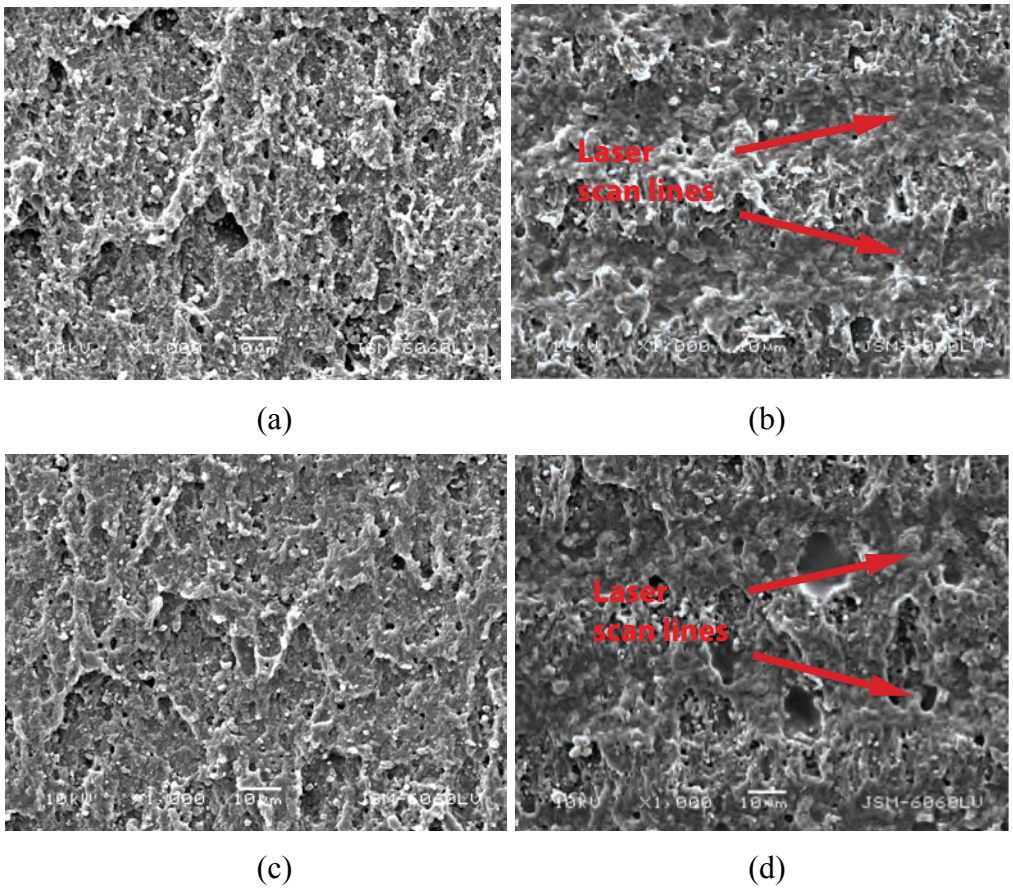

Figure 37: *BLUE "rubber blanket" samples, untreated (a), UV laser only treated (b), oxygen plasma treated (c) and oxygen plasma treated with UV laser treatment (d).*

The SEM images of crude rubber applied on glass are presented in Figure 38.

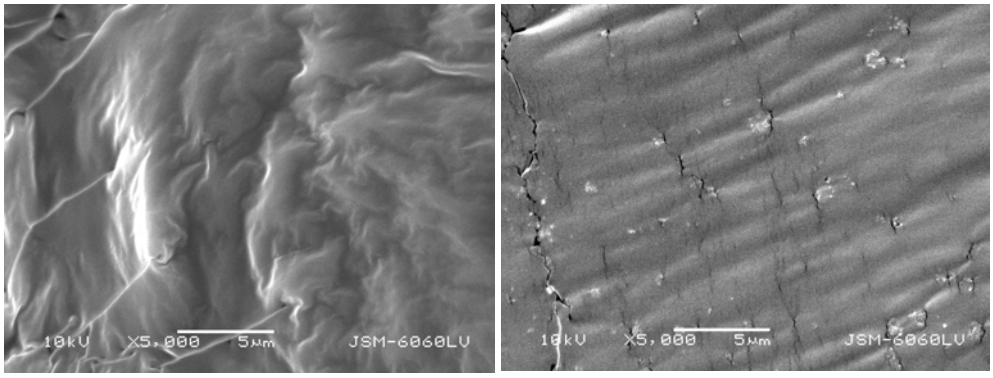

Figure 38: *Crude rubbers Krynac 33.30 F (left) and Keltan 8340A (right), applied on glass-slide, untreated.*

5.2.1 Results of SEM-EDS analysis

The results of the SEM-EDS analysis of BLUE untreated and treated samples are presented in Table 10. An original report obtained with software gives many numerical data and graphical presentations of the amount of elements detected, here only the weight in % was chosen. The total does not equal 100%, as the Au/Pd measured weight was subtracted.

Table 10: *Results of SEM-EDS analysis of elements on surface of untreated and treated BLUE samples*.

Element	Untreated	Oxygen plasma treated	Oxygen plasma + UV laser tr.	UV laser only treated
	Weight (%)			
C	37.49	38.03	37.80	36.43
O	8.02	8.47	7.43	6.97
Al	0.57	0.67	0.57	0.58
Si	4.22	4.36	4.20	4.09
S	2.67	2.54	2.50	2.39
Ti	0.96	1.00	0.89	0.89
Zn	1.32	1.47	1.10	1.12
Totals	55.23	56.54	54.50	52.46

In Figures 39 and 40, the results of the SEM-EDS analysis of BLUE samples are presented.

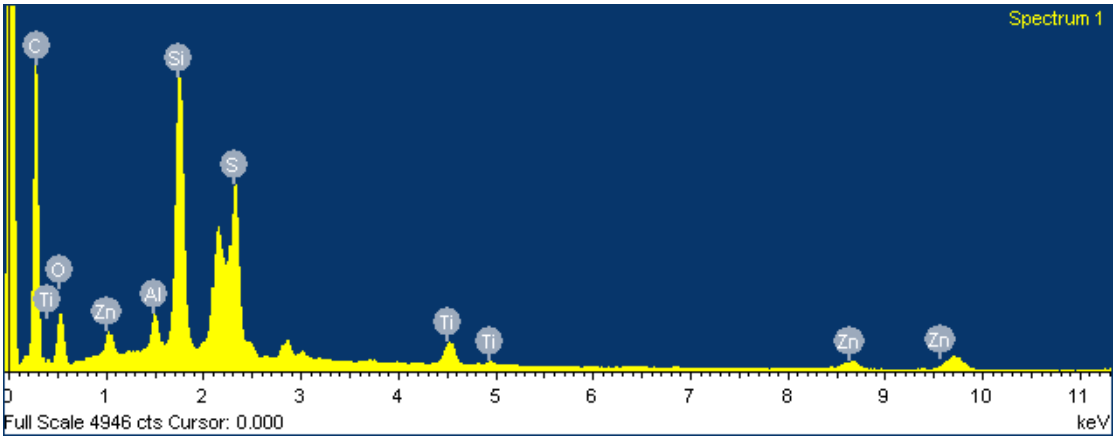

Figure 39: *Graphic presentation of SEM-EDS analysis of untreated BLUE "rubber blanket" sample.*

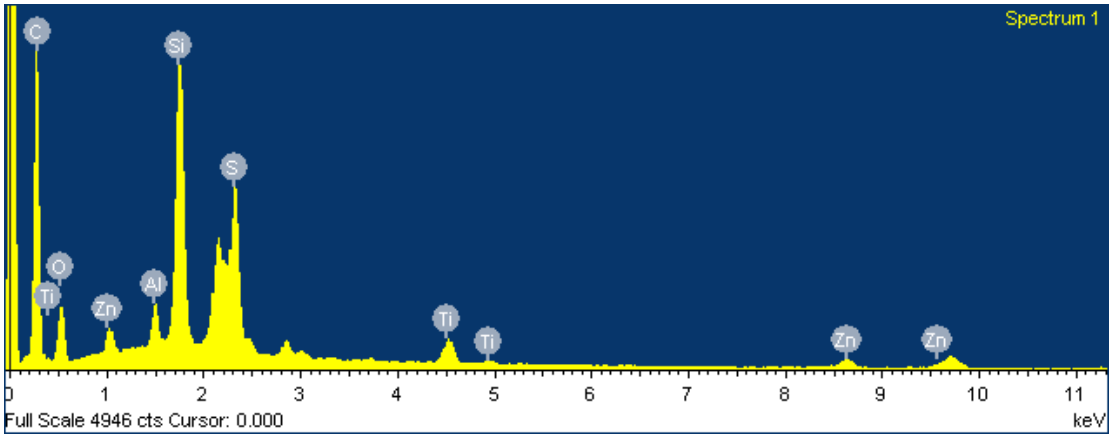

Figure 40: *Graphic presentation of SEM-EDS analysis of oxygen plasma treated BLUE "rubber blanket" sample. Plasma treatment was applied for 27 s.*

5.3 FTIR-ATR spectra and interpretation of results

Figures 41–45 present the FTIR-ATR spectra of the RED and BLUE "rubber blanket" samples with the magnifications of the areas where changes occurred after the treatments. An interpretation of the spectral data follows the graphical presentations of the spectra.

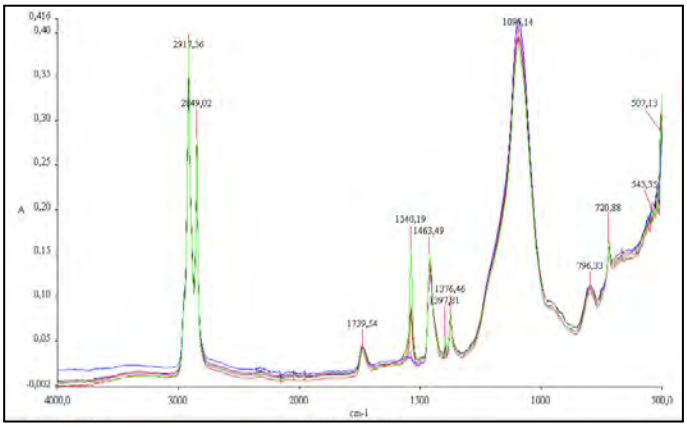

Figure 41: *Absorption spectra of RED "rubber blanket" spectra (green – no treatment, red – oxygen plasma treatment, blue – oxygen plasma and IR laser treatment, violet – oxygen plasma and UV laser treatment, brown – UV laser treatment). Plasma treatment was applied for 27 s.*

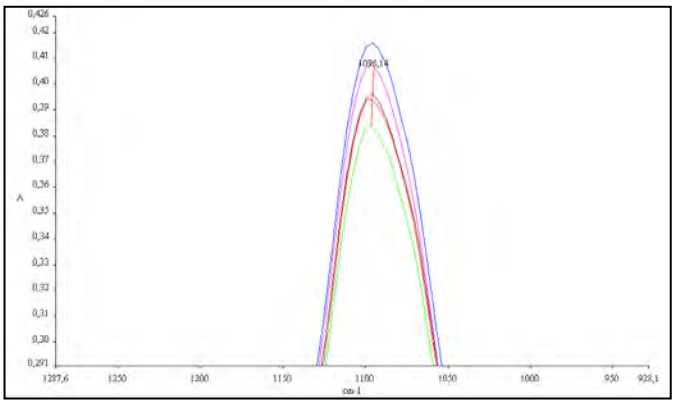

Figure 42: *Zoomed part of absorption spectra of RED "rubber blanket" spectra with top of peak at 1096 cm^{-1} due to silica filler. Plasma treatment was applied for 27 s.*

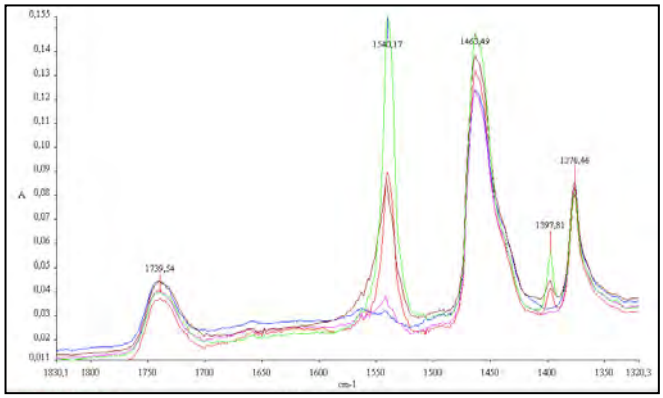

Figure 43: *Zoomed part of absorption spectra of RED "rubber blanket" spectra with significant peaks at 1397 cm^{-1}, 1463 cm^{-1} and 1540 cm^{-1}. Plasma treatment was applied for 27 s.*

Significant changes between the untreated and plasma treated RED samples were achieved at 1096, 1397, 1463 and 1540 cm^{-1}.

The peak at 1096 cm^{-1} has all the characteristics of an asymmetric stretching vibration of the Si-O-Si bonds. Most likely, it is contributed by silica fillers. The changes among the samples are small and could be a result of the treatment. At this peak, the lowest absorption is achieved for the untreated sample and the highest for the oxygen plasma combined with the IR laser treated sample. This effect could be a consequence of removing an amount of the rubber material, which causes a higher amount of silica fillers in the working depth of the FTIR-ATR measurements.

The peak at 1398 cm^{-1} shows the presence of sulphur – it is characteristic for an asymmetric stretching vibration of S in the SO_2 bonds, taking part in the CO-SO_2-OC group. Its intensity diminishes by a similar extent with an oxygen plasma etching and with laser treatments. When the laser treatment was applied on the oxygen plasma treated sample, the peak completely vanished. It shows that the plasma and laser treatment diminishes the sulphur from in the SO_2 bonds in the cured rubber structure.

The peak at 1463 cm^{-1} is composed of at least three contributions, which show a deformation vibration of the CH, CH_2 and CH_3 bonds. The small changes in the peak intensity confirm some diminishing of the amount of these groups with a treatment.

The peak at 1540 cm^{-1} shows the presence of bonded nitrogen and could be contributed to the vibrations of amides (CNH bonds in -CO-NH-C groups), nitro

($C\text{-}NO_2$) groups, or ureas (NH, bonded in some R-NH-CO- group). At this peak, the highest absorption was achieved at the untreated samples and the lowest at the plasma combined with the IR or UV laser treated samples. This shows that considerable differences in the CNH bonds occur in the rubber structure with a treatment.

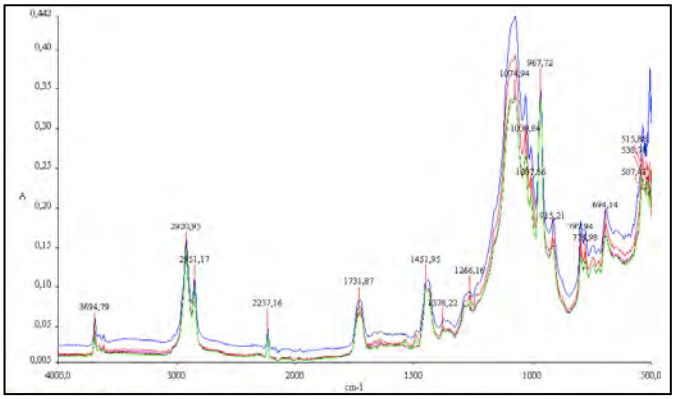

Figure 44: *Absorption spectra of BLUE "rubber blanket" spectra (green – no treatment, red – oxygen plasma treatment, blue – oxygen plasma and IR laser treatment, violet – oxygen plasma and UV laser treatment, brown – UV laser treatment). Plasma treatment was applied for 27 s.*

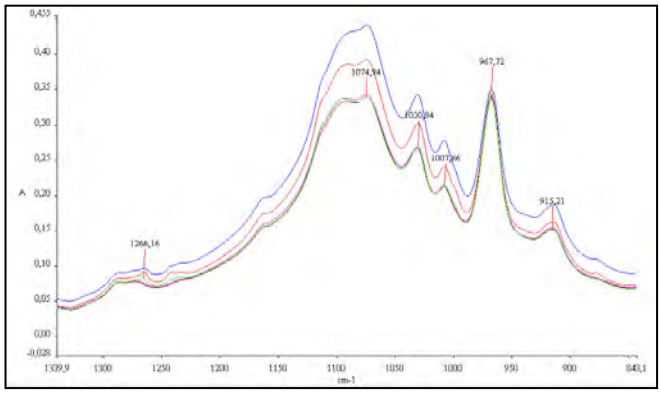

Figure 45: *Zoomed part of absorption spectra of BLUE "rubber blanket" spectra with significant peak at 1074 cm^{-1}. Plasma treatment was applied for 27 s.*

Significant changes between the untreated and plasma treated BLUE samples were at a wide composed peak centred at 1075 cm^{-1}. The main broad peak was caused by the asymmetric stretching vibration of oxygen in a silicone group (Si-O-Si) due to the silica fillers present in the "rubber blanket". This broad peak is overlapped by several, weak narrow side peaks, contributing to the vibrations of various chemical groups in the chemical structure of the elastomer. The overall intensity of this broad absorption

feature rose with the treatment; however, no changes of narrow peaks were obtained. It is reasonable to conclude that the treatment removed some amount of the elastomer material without any noticeable changes in the remaining elastomer. While the silica filler remained untouched in both surface treatments, the ablation of the surface elastomer material induced the presence of a higher amount of silica particles in the penetration depth of the FTIR-ATR experiment. Therefore, the broad absorption peak became higher, while the relative intensities of all overlapped narrow bands remained the same.

The FTIR-ATR spectra of other "rubber blankets" are omitted. There were no significant differences between the untreated and oxygen plasma treated samples, and the treatment with the IR and UV laser was not possible for all samples.

The FTIR-ATR spectra of the untreated and treated crude rubbers are presented in Figure 46.

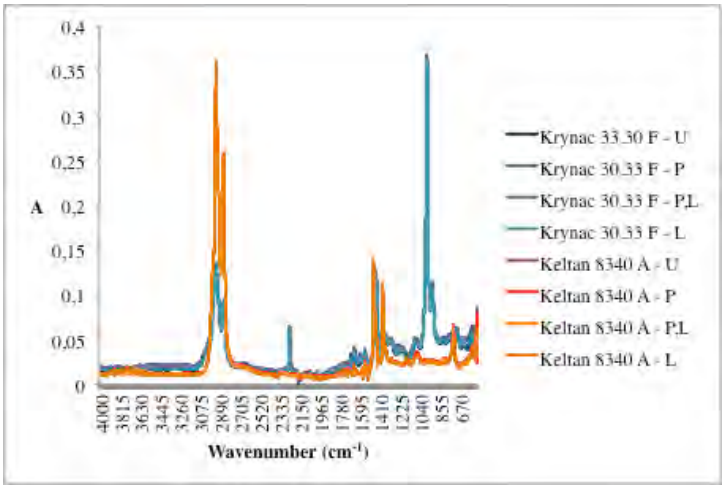

Figure 46: *FTIR-ATR spectra of two untreated (U), oxygen plasma treated (P), oxygen plasma with UV laser treated (P, L), and UV laser treated (L) crude rubber samples. Plasma treatment was applied for 27 s.*

The spectral data are almost identical for the untreated and treated Krynac 33.30 F and Keltan 8340 A crude rubber samples.

5.4 Results of XPS analysis

The chemical composition of the untreated and oxygen plasma treated RED and BLUE "rubber blanket" samples are presented in Table 11 and in Figures 47–54.

Table 11: *Chemical composition of RED and BLUE samples, untreated and oxygen plasma treated, calculated from spectral data, presented in Figures 47 to 50. Plasma treatment was applied for 27 s*

Sample	C1s	N1s	O1s	Si2p	S2p	Zn2p3
RED untreated	88.6	–	7.9	1.1	0.9	1.4
RED oxygen plasma treated	79.9	1.9	12.2	1.3	3.2	1.5
BLUE untreated	79.4	3.0	11.8	1.7	3.3	0.9
BLUE oxygen plasma treated	75.4	1.7	16.0	2.3	3.8	0.9

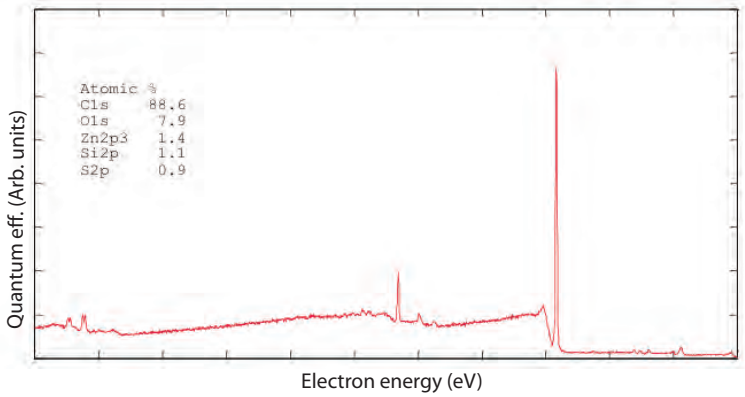

Figure 47: *XPS overview spectra of untreated RED sample*.

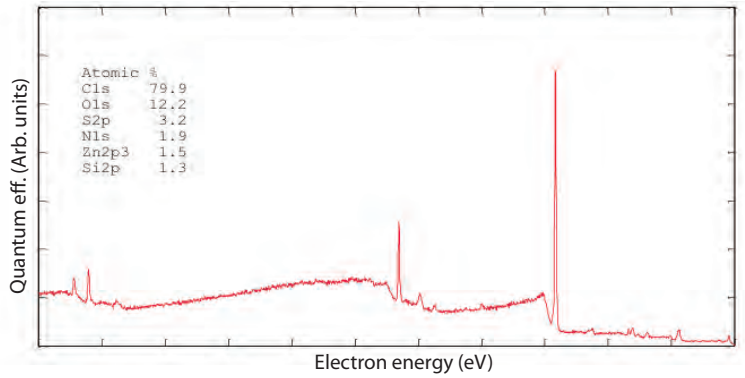

Figure 48: *XPS overview spectra of oxygen plasma treated RED sample. Plasma treatment was applied for 27 s.*

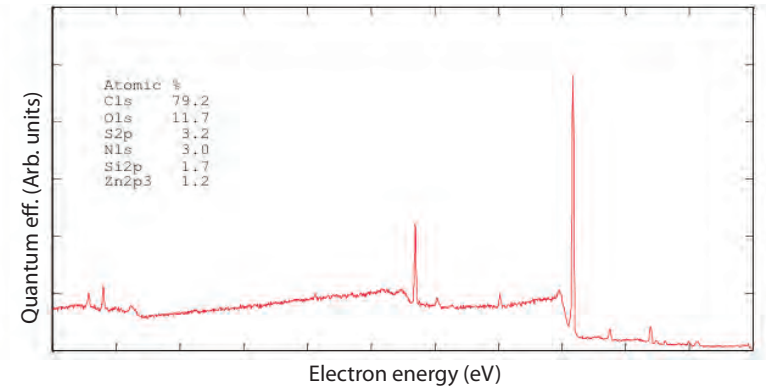

Figure 49: *XPS overview spectra of untreated BLUE sample*.

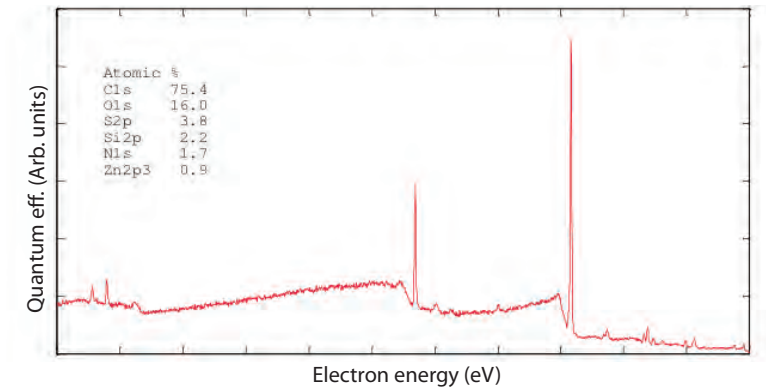

Figure 50: *XPS overview spectra of oxygen plasma treated BLUE sample. Plasma treatment was applied for 27 s.*

Short comments and an interpretation of the results of the XPS analysis are presented in the captions under Figures 51–54.

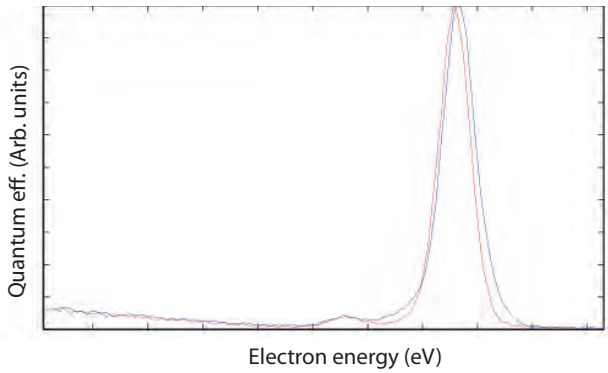

Figure 51: *Carbon spectra comparison of untreated (red) and oxygen plasma treated (blue) RED sample. Plasma treatment was applied for 27 s. Spectrum of oxygen plasma treated sample is slightly wider as a result of charge impact during analysis. There are no additional peaks showing new functional groups.*

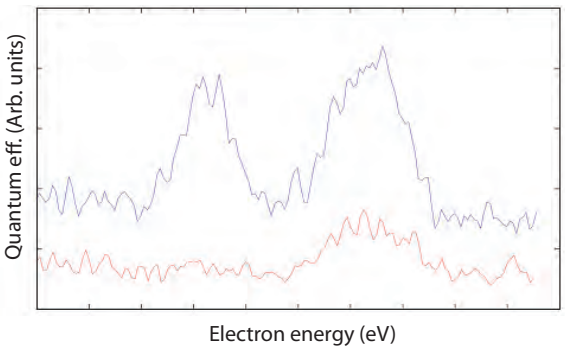

Figure 52: *Sulphur spectra comparison of untreated (red) and oxygen plasma treated (blue) RED sample. Plasma treatment was applied for 27 s. At untreated sample, sulphur is bonded to carbon only (peak on the right at 163.5 eV). After treatment, new peak arises at ~ 169 eV of energy, which belongs to SO_3^- groups, arising as a result of chemical reaction between oxygen from plasma and sulphur from vulcanized rubber.*

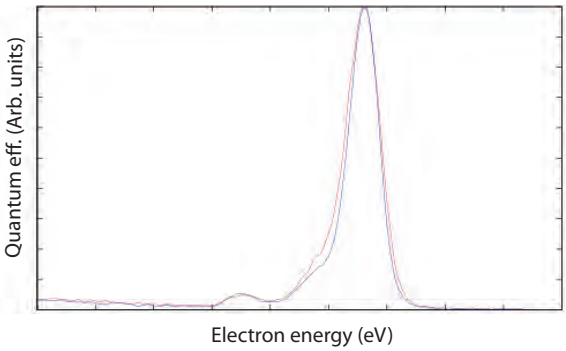

Figure 53: *Carbon spectra comparison of untreated (red) and oxygen plasma treated (blue) BLUE sample, where no additional bonds arise, indicating interaction of carbon with oxygen. Plasma treatment was applied for 27 s.*

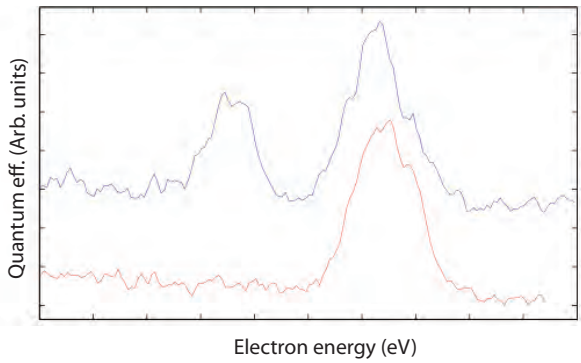

Figure 54: *Sulphur spectra comparison of untreated (red) and oxygen plasma treated (blue) BLUE sample. Plasma treatment was applied for 27 s. Similarly to RED sample, new peak arises as a result of new bonds between sulphur and oxygen.*

5.5 Images taken with optical microscope and camera

A selection of images in Figures 55–59, taken with an optical microscope and digital camera, was chosen to illustrate the physical properties of samples and surface characteristics not clearly visible using SEM.

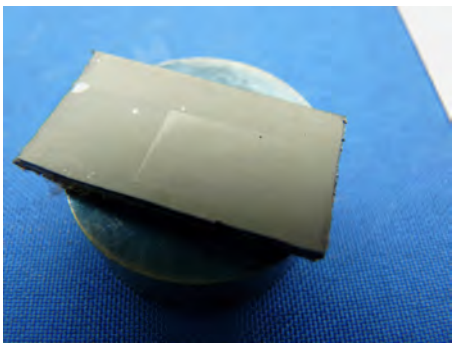

Figure 55: *BLUE sample, prepared for SEM-EDS analysis. UV laser rendered pattern with uneven surface structure (light shadow in the corner) is clearly visible.*

Figure 56: *Thermal degradation of oxygen plasma treated RED (left) and BLUE (right) samples for more than 27 s.*

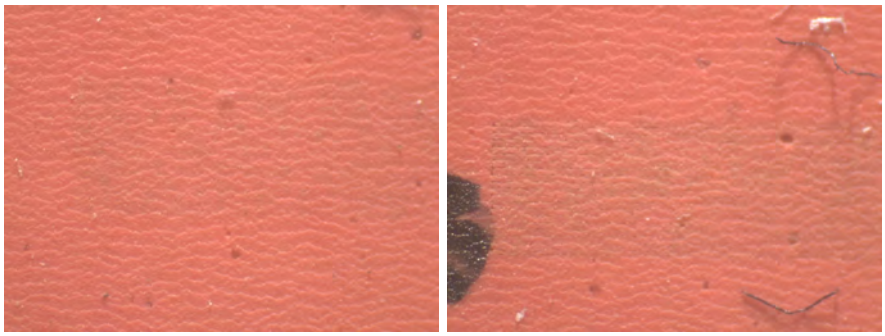

Figure 57: *Rough waviness structure on RED sample, untreated (left), oxygen plasma and JND IR laser treated (right), visible only under narrow lighting angle from side, perpendicular to the waves. Same structure is not visible on SEM images.*

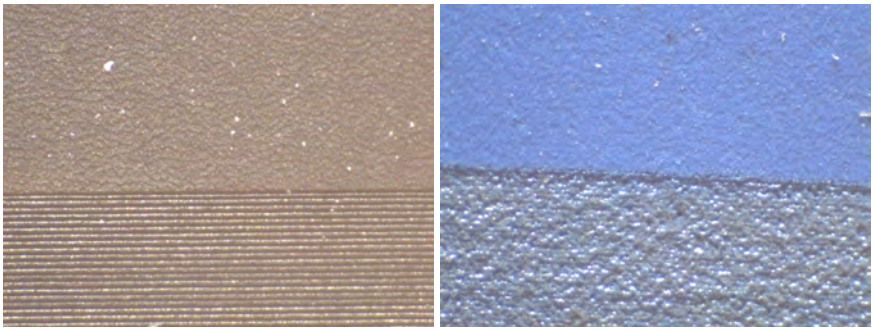

Figure 58: *Strong IR laser ablation on BLACK (left) and LIGHT BLUE (right) oxygen plasma treated samples, achieved during adjustment of IR laser to get JND.*

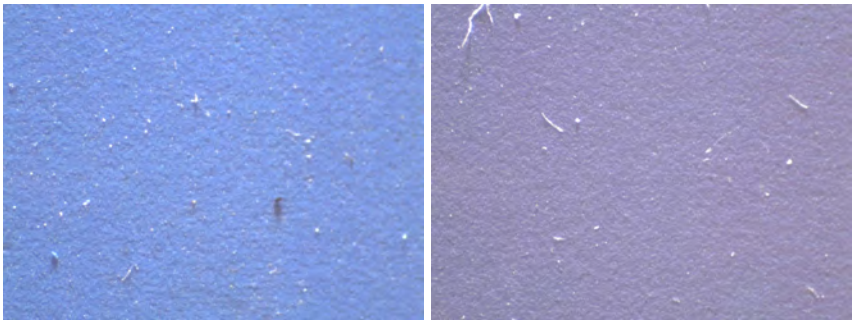

Figure 59: *LIGHT BLUE (left) and BLUE (right) oxygen plasma treated samples with JND pattern (lower side of pictures) achieved using IR laser, which is almost invisible.*

5.6 Results of roughness measurements

The roughness measurements of the untreated and oxygen plasma treated RED and BLUE samples, using Perthometer Mahr M1, are given in Table 12 as the mean values and standard deviation of 20 measurements, performed in different directions. The differences between the untreated and oxygen plasma treated surfaces are very small and therefore negligible. The results for other measurements with similar results are omitted.

Table 12: *Roughness parameters for untreated and oxygen plasma treated RED and BLUE samples. Treatment time was 27 s.*

Parameter	RED				BLUE			
	Untreated		Oxygen plasma tr.		Untreated		Oxygen plasma tr.	
	value	σ	value	σ	value	σ	value	σ
R_a (µm)	1.144	0.143	1.070	0.094	0.675	0.063	0.675	0.049
R_z (µm)	6.109	0.685	5.804	0.404	4.425	0.499	4.348	0.453
R_{max} (µm)	7.442	1.817	6.629	0.569	5.430	1.002	5.506	1.212

5.7 Results of DMA analysis

Figures 60–67 offer a graphic presentation of the DMA analysis of the surface layer elastomer for the "rubber blankets" and of crude rubbers with a short interpretation of important data.

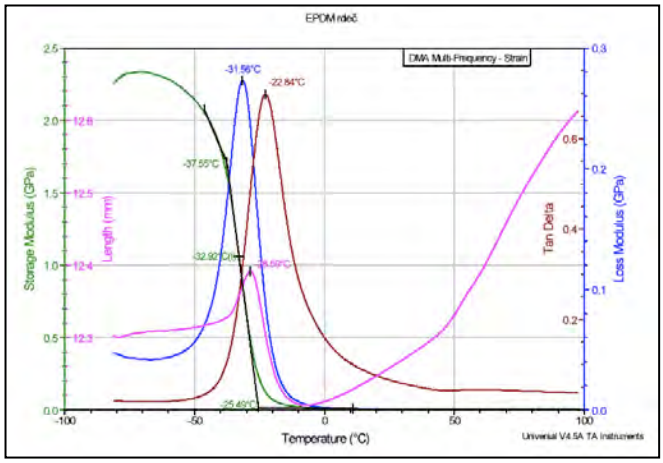

Figure 60: *DMA analysis of RED sample, indicating T_g = –32.92 ºC and tan δ with one peak at –22.84 ºC.*

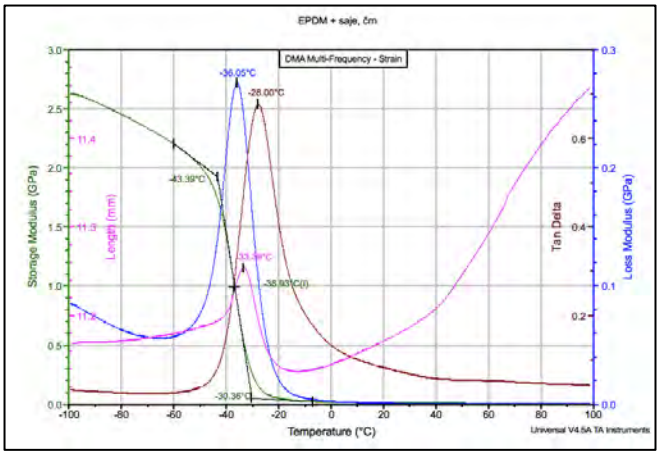

Figure 61: *DMA analysis of BLACK sample, indicating T_g = –36.93 ºC and tan δ with one peak at –28.00 ºC.*

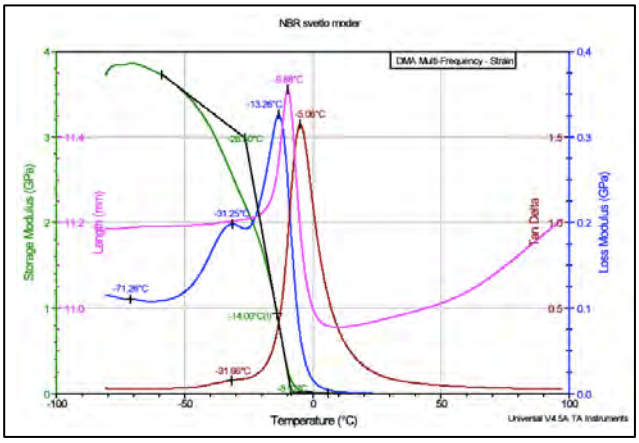

Figure 62: *DMA analysis of LIGHT BLUE sample, indicating T_g = –14.00 ºC and tan δ with one peak at –5.04 ºC.*

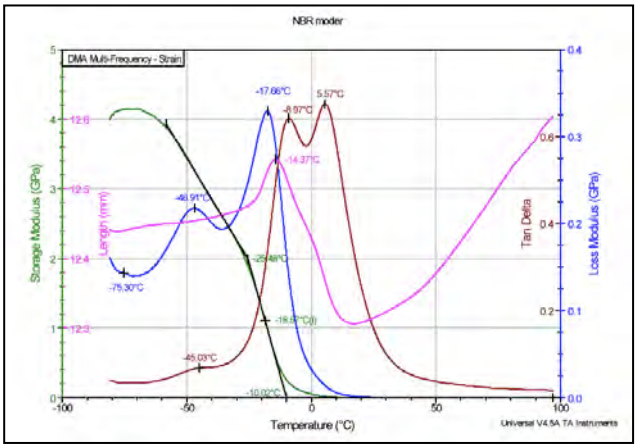

Figure 63: *DMA analysis of BLUE sample, indicating T_g = –18.75 ºC and tan δ with two peaks at –8.97 ºC and 5.57 ºC.*

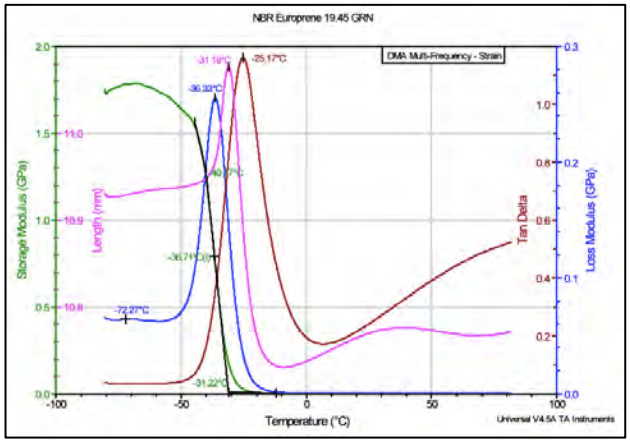

Figure 64: *DMA analysis of Europrene 19.45 GRN sample, indicating T_g = –31.19 ºC and tan δ with peak at –25.17 ºC.*

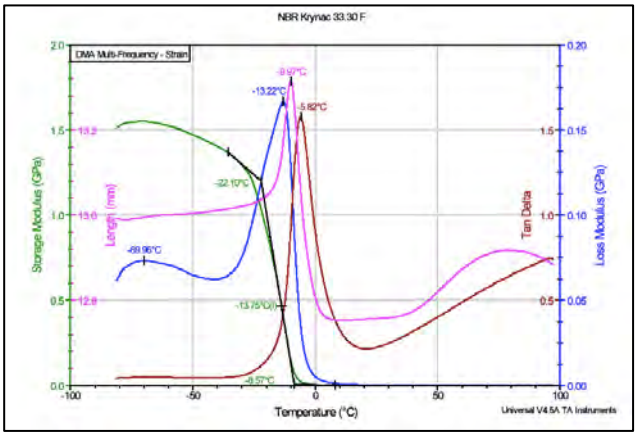

Figure 65: *DMA analysis of Krynac 33.30 F sample, indicating T_g = –13.75 ºC and tan δ with peak at –5.82 ºC.*

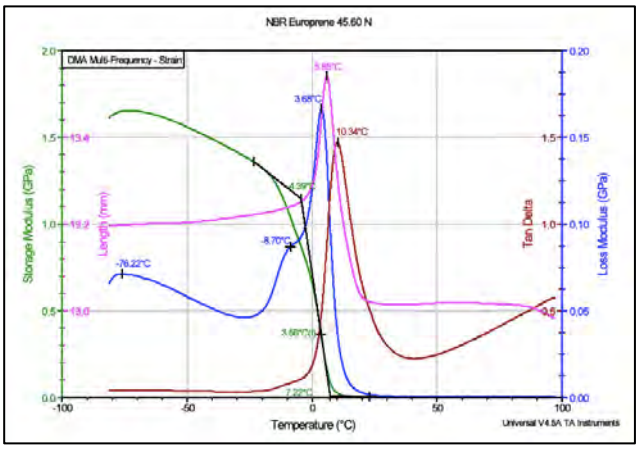

Figure 66: *DMA analysis of Europrene 45.60 N sample, indicating T_g = 3.56 ºC and tan δ with peak at 10.34 ºC.*

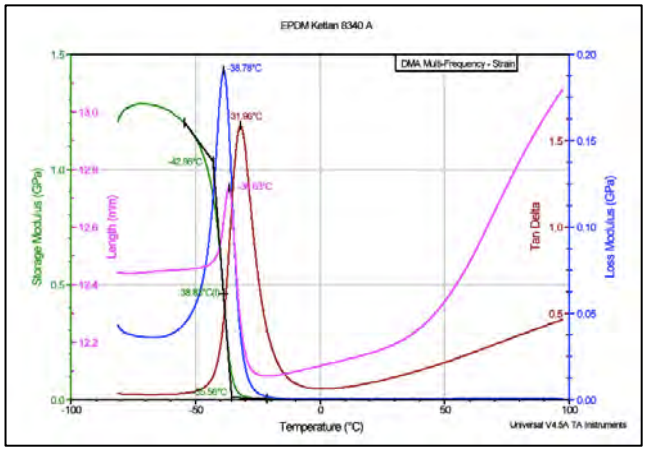

Figure 67: *DMA analysis of Keltan 8340A sample, indicating T_g = –38.83 ºC and tan δ with peak at –31.96 ºC.*

5.8 UV-VIS absorption spectra

In Figure 68, the UV-VIS absorption spectra of four “rubber blankets” are presented.

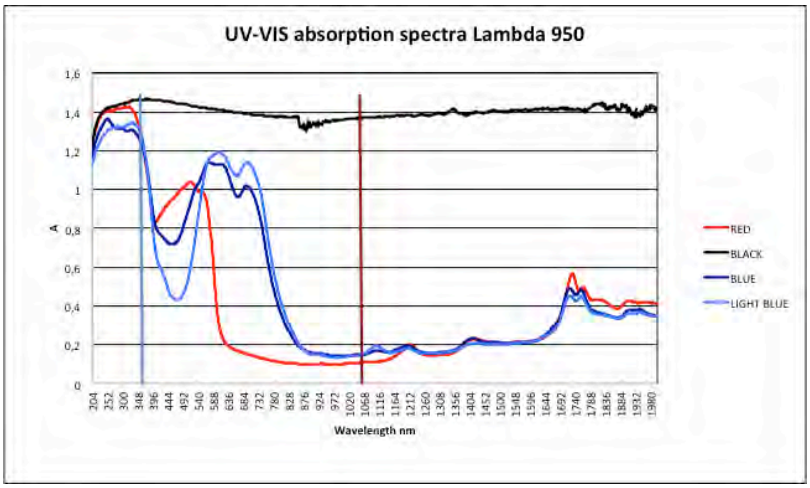

Figure 68: *UV-VIS absorption spectra of RED, BLACK, LIGHT BLUE and BLUE “rubber blanket” samples. Blue and red vertical lines indicate UV and IR laser wavelength used during investigation*.

A high absorbance of all four “rubber blanket” samples in the UV area allows a relatively low fluence for the UV laser treatment. In the IR area, the absorbance of BLACK is much higher and the IR laser treatment to achieve JND for this “rubber blanket” was unsuccessful.

5.9 Results of IGC measurements

The results of the IGC method are given as the retention time under a solvent vapour treatment of a sample (Table 13).

Table 13: *Retention time for two silica samples measured using chloroform solvent.*

Sample	Position	Quantity (mg)	Time (min)
Ultrasil 7000	front	11	1.395
Coupsil 6508	front	10	1.070
Ultrasil 7000	back	16	2.470
Coupsil 6508	back	14	1.263

The modified Coupsil 6508 (A) filler with a shorter retention time has a higher surface free energy compared to the unmodified Ultrasil 7000 (B) filler. The surface free energy was not calculated.

5.10 Particle sizes of silica filler

The results of the particle size and distribution measurement for both silica filler samples are presented in Figures 69 and 70.

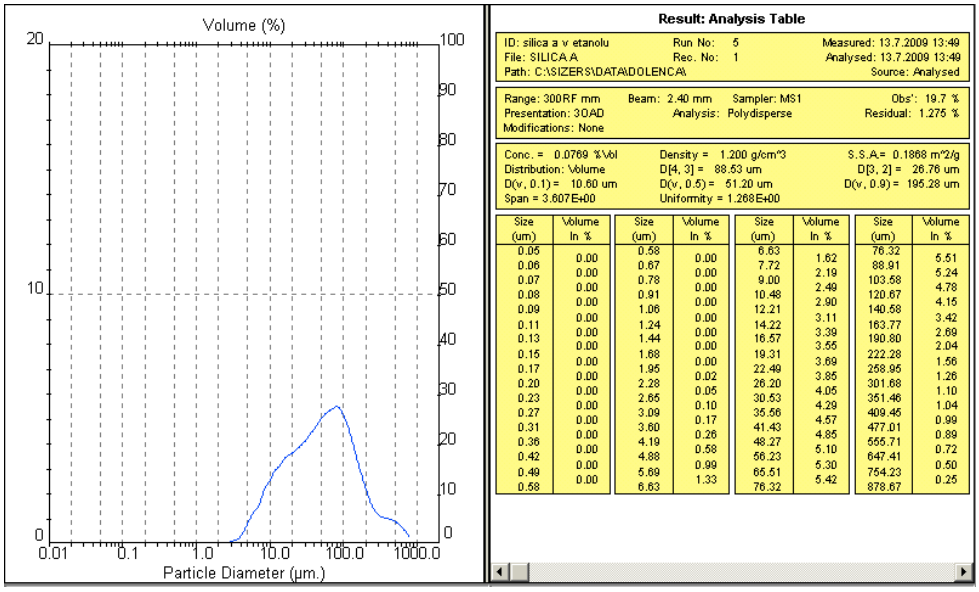

Figure 69: *Particle distribution of unmodified Ultrasil 7000 (A) filler.*

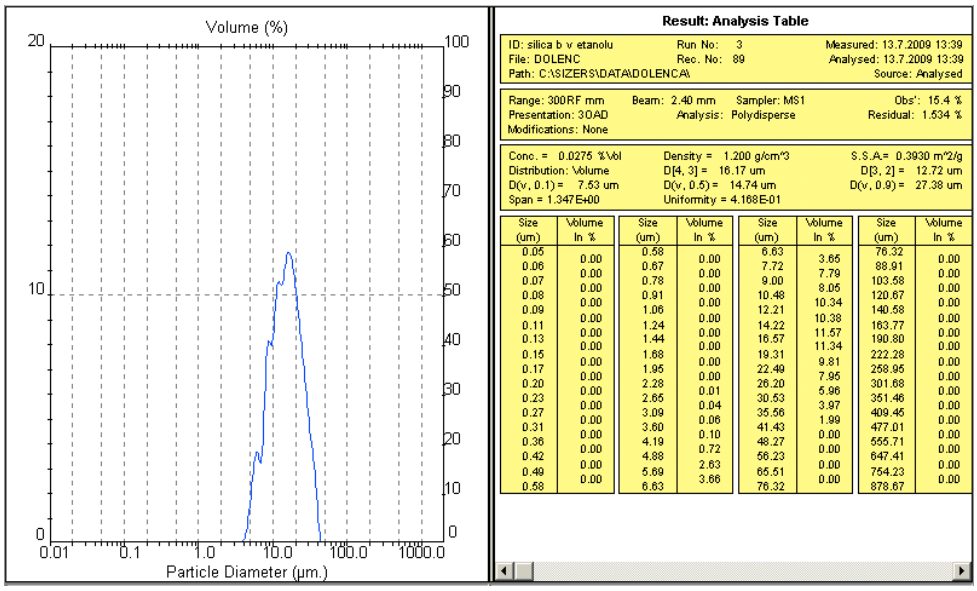

Figure 70: *Particle distribution of modified Coupsil 6508 (B) filler.*

The particle size measurements for Ultrasil 7000 show a wide distribution from approx. 2 µm to up to 800 µm with the peak at 90 µm. For Coupsil 6508, a much narrower distribution in the range 2–40 µm with the peak at 15 µm was attained.

5.11 Results of AFM analysis

The surface topography of two untreated samples is shown in Figures 71–74.

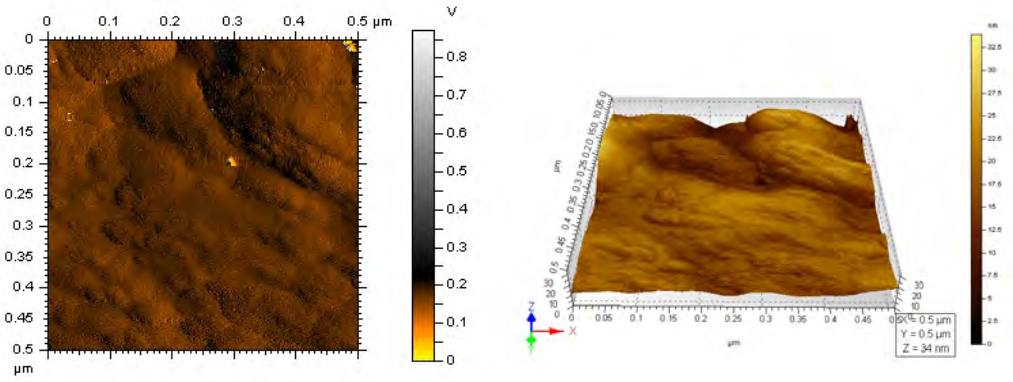

Figure 71: *AFM image of untreated RED "rubber blanket" sample, 2D amplitude (left) and 3D topography (right).*

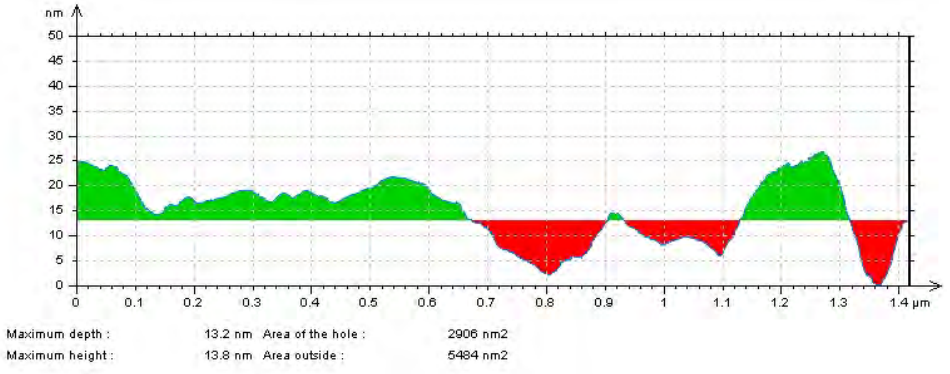

Figure 72: *AFM surface profile of Hole-Peak for RED untreated sample.*

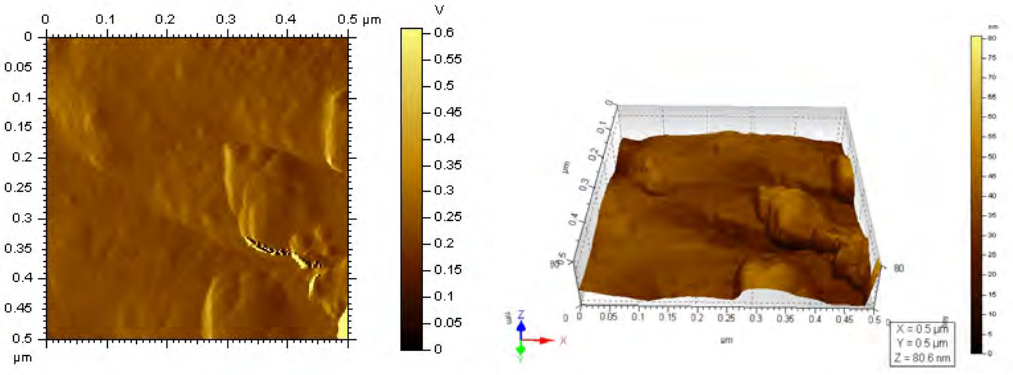

Figure 73: *AFM image of untreated BLUE "rubber blanket" sample, 2D amplitude (left) and 3D topography (right).*

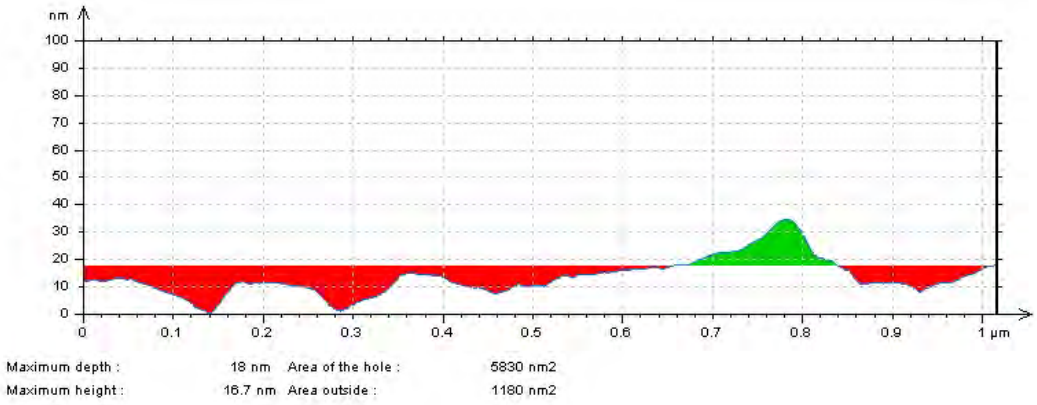

Figure 74: *AFM surface profile of Hole-Peak for BLUE untreated sample..*

5.12 Results of ink trapping measurements

The results of the ink transfer/trapping measurements are presented in Table 14.

Table 14: *Ink transfer/trapping for four new and "old" samples of "rubber blankets"*.

Sample	Ink transfer/trapping (%)
RED NEW	24.5
RED	29.3
BLACK NEW	33.6
BLACK	21.6
LIGHT BLUE NEW	30.1
LIGHT BLUE	27.6
BLUE NEW	29.8
BLUE	28.9

The ink trapping is useful to confirm a lower surface free energy for the BLACK NEW, LIGHT BLUE NEW and for BLUE NEW samples, but not for the RED NEW sample. Obviously, there might be some differences among samples, their preparation or even difficulties in the measurement method.

6 COMMENTS AND CONCLUSIONS

The results of the investigation meet many of the expectations introduced at the beginning of the thesis. After two years of searching for valuable references, the possibilities for the testing and measurements, search for new ideas, materials, methods and accessibility to high-end research equipment with a proper support of specialized top scientists, and interpretation of achieved results, the main goals of the presented work are achieved, and some conclusions are ready to be presented to the scientific community.

The initial comments are given directly with the published results, since they are directly connected to the content of figures and tables. In Chapter 6.1, general findings are commented upon and interpreted to accent the most important findings and correlations between the published results.

6.1 Discussion of results

The methods and samples used during the investigations were very sensitive to the proper preparation of samples, variability of conditions during the treatment, time, temperature and relative humidity in the laboratories, and other influences. The samples themselves were inhomogeneous and rough, in some cases even not flat, some crude rubbers were sticky. The human factor was very important during the investigation and almost all methods depended on human knowledge, experience and decisions. In all cases, the conclusions are based only on the results where the differences in apparent values are clearly visible.

The determination of proper time for the oxygen plasma treatment of samples is presented in Figures 24–29, where the lowest contact angle for different types of "rubber blankets" at 27 s of treatment time can be seen. There are some small deviations, possibly due to the treatment process, measurement errors, improper preparation of samples, or some other reasons. The measured contact angles with water remain stable after 3 h and even after 24 hours after the oxygen plasma treatment; therefore, a further treatment with a laser made sense and the measurement results of the surface properties were a reliable indicator of the state of samples within one day. The same settings of the plasma reactor and treatment time were used for the nitrogen plasma treatment and oxygen plasma treatment of crude rubber.

Figure 30 shows significant differences in the apparent surface free energy with a disperse and polar component between the untreated and plasma treated samples. The achieved values are somewhat lower for the nitrogen plasma treatment compared to the oxygen plasma treatment. It is evident that the untreated "polar" NBR based elastomers have a very low polar component – after the plasma treatment the "polar" component was much higher; nevertheless, it was still lower than the "disperse" component of the surface free energy.

During the investigations of the surface free energy of "rubber blankets", it was confirmed that using an oxygen plasma treatment, the surface free energy of the NBR or EPDM type of "rubber blankets" can be significantly increased. Thus, the established distinction in the total surface free energy between the untreated and oxygen plasma treated surface of samples gives enough difference in hydrophilicity/oleophobicity and

oleophilicity/ hydrophobicity to open the possibility for rendering the surface of a blanket with the printing and non-printing areas. The durability of such an established "rubber printing plate" in contact with the print substrate and other elements, e.g. dampening and inking rollers, still remains unknown and was not the subject of the present investigation. For a specific "window", limited with the surface free energy and polarity, proper liquids (dampening solution, ink) with adopted surface properties (total, polar and disperse part of the surface free energy) should be developed in the future to continue the research in this direction.

The achieved values in the surface free energy on a "rubber blanket" surface, using the nitrogen plasma treatment are lower compared to the oxygen plasma treatment; nevertheless, according to some other authors [42], there are some advantages of using a nitrogen plasma instead of an oxygen plasma in the case of the PTFE polymer. The use of a nitrogen plasma gives some new groups on the PTFE surface. For the EPDM and NBR based elastomers, the influence of the nitrogen plasma treatment is still unknown and should be studied in the future.

The treatment of crude rubbers with an oxygen plasma, presented in Figure 31, reveals significant changes in the surface free energy for the NBR rubber with a small amount of acrylonitrile groups and almost no apparent changes for the NBR rubber with a high amount (45 %) of acrylonitrile groups. After the oxygen plasma treatment, the polar component of the surface free energy was higher. For the untreated samples, the apparent surface free energy has a close correlation with the amount of acrylonitrile groups. The surface free energy of the oxygen plasma treated NBR crude rubber is obviously independent of the amount of acrylonitrile groups in the NBR crude rubber. The oxygen plasma treatment of the EPDM crude rubber shows a higher surface free energy.

The defunctionalization of "rubber blankets" using IR and UV lasers, presented in Figure 32, was successful to only a limited extent, with only partly recovered the surface properties of the untreated samples. It is evident that the UV laser only treatment gives a significantly lower surface free energy for the untreated EPDM type of "rubber blankets" and slightly higher values for the NBR type of "rubber blankets", compared to the untreated samples. The changes caused by the UV laser only treatment are much lower compared to the oxygen plasma treatment.

The treatment with IR and UV lasers gives promising results. The defunctionalization of the plasma treated samples was only partly achieved and thus not applicable for a proper rendering of the functionalized surface. This should be improved by changing the chemical composition of samples, using curing agents or additives, which would give a better response to different plasma and laser treatment methods. The fine-tuning of the functionalization and defunctionalization process was not possible during the present investigation and should be realized in the future.

The SEM images in Figures 34–36 give confirmation of the achieved JND. The changes in morphology are visible. For the plasma treated samples, the traces of melted elastomer are evident, especially for the BLUE sample. Similar changes and the traces of the laser treatment are visible in Figure 37

The SEM images in Figure 38 show the differences in the surface structure of the NBR and EPDM crude rubber. The differences in the surface topography between the two types of rubber are clearly visible.

The results of the chemical analysis of only one NBR sample, using the SEM-EDS method, presented in Table 10 and in Figures 39 and 40, offer no reliable information about the chemical changes using different treatment methods. The differences in the oxygen and carbon content of the untreated and oxygen plasma treated samples show raised values after the oxygen plasma treatment, lower values using the UV laser after the plasma treatment and even lower values after the UV laser only treatment. The changes in the weight of oxygen and carbon could be explained with the oxidation of the surface after the plasma treatment and with the formation of CO or CO_2 gases, evaporating from the surface during the UV laser treatment. The presence of silicon and zinc after the treatment is in correlation with carbon and oxygen. Hydrogen was not detected, thus the SEM-EDS method is not suitable for the analysis of hydrocarbon groups. The measurements using the SEM-EDS method should be repeated in the future to confirm the measured changes in the weight of the present chemical elements within the thickness of the sample surface layer > 1 μm. The results should be compared to the results obtained using other methods.

The FTIR-ATR chemical analysis of the surface of the “rubber blanket” samples, presented as the IR spectra in Figures 41–45, shows the changes in the chemical

composition during the treatment. For the EPDM type of “rubber blanket”, the changes occurred at two peaks with a loss of SO_2 and CNH bonds, and some diminishing of CH, CH_2 and CH_3 groups. For the NBR type of “rubber blanket”, the raised absorbance could be a result of removing the polymer material after the treatment, which causes a higher presence of silica fillers. No chemical changes of the remaining elastomer after the treatment were detected.

The FTIR-ATR spectra of the EPDM and NBR and crude rubbers before and after the oxygen plasma and UV laser treatment, presented in Figure 46, show an almost perfect match of the spectral values. There are no apparent differences in the chemical composition within the thickness of the surface layer ~ 1 mm. This statement is not in correlation with the apparent differences in the surface free energy and polarity of the untreated and plasma and laser treated crude rubber samples, showed in Figure 31. Obviously, the differences in the surface free energy of the untreated and plasma or laser treated EPDM and NBR crude rubber samples are caused by the changes in the surface structure or topography, and not by the formation of new chemical groups or other changes in the chemical composition on the surface. The changes in the surface free energy for the UV laser treated samples could also be explained with the bond scission of the macromolecular structure, where all of the elements and most of the bonds and thus the chemical structure remain unchanged, while the mobility of shorter polymer chains or branches increases. Another reason for such results may also be the large penetration depth of the FTIR-ATR measurement. The chemical structure on the very surface that influences the changes in the surface free energy could not contribute enough to be resolved in the FTIR-ATR spectra.

The results of the XPS analysis of two types of the EPDM and NBR based “rubber blankets” show that only significant changes in the chemical composition on the surface of the untreated and oxygen plasma treated samples are in the bonded oxygen with sulphur, forming the SO_3 groups, while no other significant chemical changes were observed on the polymer surface. The values for oxygen, silicon and sulphur were higher after the oxygen plasma treatment, while the values for carbon (and nitrogen for the NBR sample) were lower for both elastomers. The analysis of only two untreated and treated samples was not enough to make reliable conclusions. The measurements, analysis and interpretation of the results should be extended to other

relevant samples, repeated and compared to the results obtained with other methods, taking into account different depths of penetration for FTIR-ATR, and the excitation depth of the SEM-EDS and XPS experiments.

The results of the roughness measurements, presented in Table 12, show no significant differences between the untreated and oxygen plasma treated elastomer. After the oxygen plasma treatment, the roughness values were slightly lower for the EPDM and NBR samples, with the exception at R_{max} of the NBR oxygen plasma treated sample with a higher value compared to the untreated sample. The apparent values for roughness are given at the precision of 1 nm. For a soft, elastic material, this measurement precision is not realistic. The non-contact high precision method should be used to obtain more reliable results.

The T_g values measured using the DMA method, presented in Figures 60–67, are in correlation with the amount of acrylonitrile groups in the NBR crude rubbers. The changes in the surface free energy with no apparent chemical changes for crude rubbers with low T_g values (under 23 ºC) can be explained with a high amorphous component of the material with a very small crystallinity, enabling a high mobility of the macromolecular structure of the polymer. The nature of mobility and restructuring of the rubber composition is not clear; nevertheless, it could be described with the rotation of parts of macromolecule, reorientation of the shape of macromolecule, mobility of side branches of the macromolecules creating “nano grass” with the plasma treatment, or some other form of mobility caused by one of the treatment methods.

For elastomers (cured rubbers), the mobility of macromolecules could be combined with the changes in the chemical composition on the surface caused by new groups established as the results of the chemical reaction of plasma species, mostly with curing agents, fillers or additives, since the particles only weakly bonded to the basic macromolecular structure and rarely with the polymer itself.

The SEM images of the changed macromolecular structure in the nm scale of mainly amorphous crude rubber samples are difficult to obtain due to the high energy impact of Au/Pd sputtering and electron beam damage on the sample. The AFM method should give better results.

The UV-VIS absorption spectra in Figure 68 show the absorbance of different “rubber blanket” samples in comparison with the IR and UV laser emission spectra. The setting of both the IR and UV laser devices to achieve a proper rendering energy, i.e. laser fluence, was thus partially predictable; however, the final values were obtained with the testing procedure to achieve JND.

The results of IGC in Table 13 and the results of particle size measurements of the silica filler, presented in Figures 69 and 70, are less important for this study. It was found out that the silica filler is a material with a very high surface activity. The particle size and their distribution show a typical tendency to the agglomeration of the filler.

Figures 71–74 give only an overview of the surface topography attained by using the AFM technique. The resolution of the images at a large magnification should give more information about the changes in topography after the treatment. In the future, the AFM analysis will be used to get a more reliable overview of the changes in the surface of the untreated and treated samples.

The results of the ink trapping measurements, presented in Table 14, are only informative. The method is interesting; however, the results are not very reliable. The explanations for the differences for the RED sample, which are contrastive compared to other “rubber blanket” samples, should be found by using other methods.

6.2 Conclusion

The elastomers and crude rubbers with an amorphous character are a promising material to be used for the functionalization by using a plasma and the defunctionalization by using a laser. Both processes should be improved in the future.

The changes in the surface free energy of elastomers most likely occur due to the changes in the surface structure, following the Wenzel model. In this case, it is hard to control and predict the changes in the surface free energy after the functionalization and defunctionalization process by using a plasma or laser treatment.

Hypotesis were partly confirmed as follows:

The surface free energy of offset "rubber blankets" increased by 20 mJ/m^2 to more than 30 mJ/m^2, using the treatment with a low-pressure gaseous oxygen and nitrogen plasma. The differences in the surface free energy between the functionalized and defunctionalized "rubber blankets" are in a good correlation with the printing and non-printing areas of commercially available conventional and waterless printing plates, introduced in Figure 1 and Table 1.

The increased surface free energy of offset "rubber blankets" is partly a consequence of the formation of surface functional groups as the result of a chemical reaction of the plasma species with sulphur (curing agent), fillers and some additives, and partly of the surface structure modification. The plasma treatment of uncured crude rubbers caused no chemical changes on the surface.

The surface free energy increases after the plasma treatment up to a certain value, to approx. 20–30 mJ/m^2. The superhydrophilicity with the contact angles for water near 0º was not achieved. The increasing presence of O and OH radicals was not established; therefore, the effect depends mostly on the presence of curing agents, fillers and additives.

By increasing the surface free energy, the absorption capacity of a treated surface increases. The latter is confirmed by a lower contact angle with water for the plasma treated samples.

7 REFERENCES

Chapter 7 includes the lists of figures, tables and unconventional abbreviations, and is followed by the references of web pages, patents and published papers, books, presentations, lectures and theses, studied and used during the writing of the dissertation. Other published works of general interest in the field of present research, and direct communication with colleagues, involved in the measurements, comments of methods, results and conclusions without reference are not included, despite valuing their contribution to the final results.

7.1 List of Figures

7.2 List of Tables

7.3 List of unconventional abbreviations, acronyms and symbols

ACN	acrylonitrile
ASTM	American Society for Testing and Materials
AFM	atomic force microscope
BR	butadiene rubber
CIIR	chloride-isobutene-isoprene rubber
CtP	computer to plate, computer to press …
CW	continuous wave
DMA	dynamic mechanical analysis
EOS	equation of state
EPDM	ethene-propene-diene-monomer; ethene-propene copolymer
ESCA	electron spectroscopy for chemical analysis
FTIR-ATR	Fourier transform infrared - attenuated total reflectance
HDPE	high density polyethylene
HLB	hydrophilic – lipophilic balance
IGC	inverse gas chromatography
IFT	interfacial tension
JND	just noticeable difference
LDPE	low density polyethylene
LED	light emitting diode
M	rubber having fully saturated polymer backbone of the polymethylene type

MVQ	methyl-vinyl silicone
NBR	nitrile-butadiene rubber
Nd:YAG	neodymium-doped yttrium aluminium garnet, Nd:Y3Al5O12
NR	natural rubber
PA	polyamide
PBII	plasma-based ion implantation
PBIID	plasma-based ion implantation and deposition
PC	poly-carbonate
PDMS	poly-dimethylsiloxane
PE	poly-ethylene
PEEK	polyether-etherketone
PEG	poly-ethylene-glycol
PET	poly-ethylene-terephthalate
PMM	poly-methyl-methacrylate
PMMA	poly-methyl-methacrylate
PP	polypropylene
PTFE	poly-tetra-fluoro-ethylene
PVC	polyvinylchloride
QR	quick release
R_a	roughness average
R_z	mean roughness depth

R_{max}	maximum roughness depth
RF	radio-frequency
SBR	styrene-butadiene rubber
SEM-EDS	scanning electron microscopy - energy dispersive spectroscopy
T	thiokol, polythioether rubber, rubber with sulfur in the polymer backbone
T_g	glass transition temperature
tan δ	ratio of loss modulus to storage modulus
TM	rubber with sulphur in saturated polymer backbone
UV-VIS	ultraviolet-visual
VUV	vacuum UV
XNBR	carboxylated acrylonitrile rubber
XPS	X-ray photoelectron spectroscopy
γ	surface tension or surface free energy
γ_{SV}	interfacial tension of solid and vapour
γ_{LV}	interfacial tension of liquid and vapour
γ_{SL}	interfacial tension of solid and liquid
σ	standard deviation
Θ	contact angle

7.4 References – URL

[URL1] http://en.wikipedia.org/wiki/Lithography, access date: 20. 12. 2010.

[URL2] Nolan Watts: Aloys and All Those Stones,
http://www.hewit.com/sd11-aloy.htm, access date: 22. 11. 2009.

[URL3] http://www.waterless.org/NwhatIs/howItWorks.htm, access date 4.1.2011.

[URL4] Charles E. Ophardt: Virtual Chembook, Elmhurst College, 2003,
http://www.elmhurst.edu/%7Echm/vchembook/213boilingpoint.html,
access date 3. 10. 2010.

[URL5] Natural rubber, http://en.wikipedia.org/wiki/Naturalrubber,
access date 20. 12. 2010.

[URL6] Eric Finson, Stephen L. Kaplan: Surface Treatment,
http://www.4thstate.com/publications/surftreatmentPrint.htm,
access date 20.12. 2010.

[URL7] Stephen L. Kaplan: Plasma: The Chemistry Tool for the 21st Century,
http://www.4thstate.com/publications/21stCentury.htm,
access date 20. 12. 2010.

[URL8] http://www.savatech.eu/offset-printing-blankets.html, access date: 20. 12. 2010.

[URL9] http://www.polimerieuropa.com, access date: 20. 12. 2010.

[URL10] www.lanxess.com, access date: 20. 12. 2010.

[URL11] http://www.ides.com/, access date: 20. 12. 2010.

[URL12] www.evonik.com, access date: 20. 12. 2010.

[URL13] www.lpkf.com, access date: 20. 12. 2010.

[URL14] www.specialoptics.com, access date: 20. 12. 2010.

[URL15] www.kruss.de/, access date: 20. 12. 2010.

[URL16] http://www4.nau.edu/microanalysis/Microprobe-SEM/Signals.html, access date: 5. 1. 2011.

[URL17] www. mahr.com/, access date: 20. 12. 2010.

[URL18] www.tainstruments.com/, access date: 20. 12. 2010.

[URL19] http://en.wikipedia.org/wiki/Atomic_force_microscopy, access date: 20. 12. 2010.

7.5 References – Patents

[Pat.1] Luc Leenders, Michel Werts: US 2006/0236886 A1, Process for the offset printing of a catalitic species via a hydrophilic phase, Agfa-Gevaert, 2006.

[Pat.2] Julius Feinleib, Peter H. Klose, Stanford R. Ovshinsky: US 3,678,852, Printing and copying employing materials with surface variations, Energy Conversion Devices, Inc., 1972.

[Pat.3] Manfred Kuehnle, Ferdinand R. Martinez, Stanley F. Ignasiak,: US 4,204,865, Direct-imaging flexible offset printing plate and method of manufacture, Coulter Systems Corporation, 1980.

[Pat.4] Satoshi Takeuchi, Masanori Akada, Hitoshi Fujii, Takashi Toida, Minoru Takamizawa, Yoshio Inoue: US 4,292,397, Method for preparing dry planographic plates with plasma, Dai Nippon Printing Co., 1981.

[Pat.5] Alfred Hirt, Hartmut Fuhrmann: US 4,833,990, Printing press for modifying hydrophobic and hydrophilic areas of a printing image carrier, Man Technologie GmbH, 1989.

[Pat.6] Thomas E. Lewis, Bradley W. Davidson, Richard A. Williams, Michael T. Nowak, John F. Kline: US 4,958,563, Lithography plate with a chromium surface and method for imaging, Presstek, Inc., 1990.

[Pat.7] Noritaka Egashira, Hitoshi Fujii, Eiichi Inoue, Satoru Kuramochi, Mitsuru Takeda, Minoru Utsumi: US 5,165,343, Printing plate and printing process, Dai Nippon Insatsu Kabushiki Kaisha, 1992.

[Pat.8] Dilip K. Chatterjee, Syamal K. Ghosh, Gregory S. Jarrold: US 5,836,248, Zirconia-alumina composite ceramic lithographic printing member, Eastman Kodak Company, 1998.

[Pat.9] David K. Biegelsen, Ross D. Bringans, Scott A. Elrod, David K. Fork, Jaan Noolandi: US 6,146,798, Printing plate with reversible charge-controlled wetting, Xerox Corporation, 2000.

[Pat.10] Jeffrey W. Leon, James C. Fleming: US 6,447,978, Imaging member

containing heat switchable polymer and method of use, Kodak Polychrome Graphics LLC, 2002.

[Pat.11] Bernd Vosseler: US 6,520,088, Re-usable printing form with a printing surface and method for forming images on the printing surface, Heidelberger Druckmaschinen AG, 2003.

[Pat.12] Yasuharu Suda, Hitoshi Isono, Hiroaki Ikeda: US 6,637,336, Method for producing printing plate, reusing method for printing plate, and printing machine, Mitsubishi Heavy Industries, Ltd, 2003.

[Pat.13] Andreas Schmohl, Peter Hess: US 7,152,530, Printing form and method for modifying its wetting properties, Heidelberger Druckmaschinen AG, 2006.

[Pat.14] Paul R. West, Jeffrey W. Leon, Nicki R. Miller: US 7,250,245, Switchable polymer printing plates with carbon bearing ionic and steric stabilizing groups, Eastman Kodak Company, 2007.

[Pat.15] Satoshi Hoshi, Kazuto Shimada, Gaku Kumada: US 7,462,437, Presensitized lithographic plate comprising support and hydrophilic image-recording layer, Fujifilm Corporation, 2008.

[Pat.16] Yu Yisong: US 2009/0056581, Method to obtain processless printing plate from ionic polymer particles, 2009.

[Pat.17] Bernd Vosseler, Martin Gutfleisch: DE 1012241384 03.09.2009, Verfahren zur Bebilderung und Löschung einer Drucfläche aus Zirkonat, Heidelberger Druckmaschinen AG, 2009.

[Pat.18] John David Adamson, Peter Andrew Reath Bennett, Richard Arthur Hutchinson, Rodney Martin Potts: WO/2010/029342, Improvements in or relating to printing, J P Imaging Limited, 2009.

[Pat.19] John David Adamson, Peter Andrew Reath, Rodney Bennett, Martin Potts: WO/2010/029341, Improvements in or relating to printing, J P Imaging Limited, 2009.

[Pat.20] Suda Jasuharu: EP1084863: Printing Plate Material and Production and

Regenerating Methods Therefor, Mitsubishi Heavy Industries, Ltd. Tokyo, 2000.

[Pat.21] Andrew J. Ouderkirk, Douglas S. Dunn, Robert W. Warner: US 4879176: Surface Modification of Semicrystalline Polymers, Minnesota Mining and Manufacturing Company, 1989.

[Pat.22] Guo Chaowei, Feng Lin, Jiang Lei: US 7288019: Method of changing the surface wettability of polymer materials, Institute of Chemistry, Chinese Academy of Science, Beijing, 2007.

[Pat.23] Miran Mozetič, Alenka Vesel, Uroš Cvelbar: WO /2006/130122, Method and device for local functionalization of polymer materials, Institut Jožef Stefan, 2006.

7.6 References – papers, books, presentations, lectures, thesis

[1] Muhannad S. Bakir: Introduction to Soft & Nanoimprint Lithography (presentation), Microelectronics Research Center - Georgia Institute of Technology, 2007.

[2] John O'Rourke: The Complete Guide to Waterless Printing, Quantum Resources, Chicago, 1997.

[3] M. Lovreček, M. Gojo, K. Dragčević: Interfacial Characteristics of the Rubber Blanket-Dampening Solution System; in Advances in Printing Science and Technology – Advances in Offset Printing, Proceedings of the 25th Research Conference of the International Association of Research Institutes for the Printing, Information and Communication Industries, Pira International, 1998.

[4] John MacPhee: Fundamentals of Lithographic Printing: Volume I, Mechanics of Printing, GATF Press, Pittsburgh, 1998, ISBN 0-88362-214-9.

[5] Olga Korelić : Kemigrafija, Viša grafička škola, Zagreb, 1973.

[6] Krister Holmberg (editor): Handbook Of Applied Surface And Colloid Chemistry, John Wiley & Sons, Ltd, Chichester, 2002, ISBN 0-471-49083-0, page 257.

[7] Myer Kutz (editor): Handbook of Materials Selection, John Wiley & Sons, Inc., New York, 2002, ISBN 0-471-35924-6, page 352.

[8] Technical Reference Bulletin: Glossary of Elastomeric Terms, C&M Rubber Co.

[9] Nicholas P. Cheremisinoff: Polymer Characterization: Laboratory Techniques And Analysis, Noyes Publications, ISBN: 0-8155-1403-4, page 89.

[10] Heinz Hermann Greve: Rubber, 1. Survey, in Barbara Elvers, Stephen Hawkins, William Russey, Gail Schulz (editors): Ullmann's Encyclopedia of Industrial Chemistry, 5th edition, Vol. A23, VCH Verlagsgesellschaft, Weinheim, 1993, ISBN 3-527-20123-8.

[11] Robert L. Bebb: Chemistry of Rubber Processing and Disposal, Environmental Health Perspectives Vol. 17, pp. 95-101, 1976.

[12] Zoran Šušteršič: Fizikalne lastnosti elastomerov (kavčukov, zmesi in gume), 2004.

[13] Andrew Ciesielski: An introduction to Rubber Technology, Rapra Technology Limited, Shawbury, Shrewbury, Shropshire, 1999, ISBN: 1-85957-150-6.

[14] Utpal Kumar Niyogi: Polymer Science: Introduction to Fibre Science and Rubber Technology, B. Rubber Technology, Delhi, 2007.

[15] Helmut Kipphan: Handbook of Print Media, Springer Verlag, Berlin, Heidelberg, New York, 2001, ISBN 3-540-67326-1.

[16] Franz-Georg Heggemann: The World of Böttcher (booklet), Böttcher.

[17] N. G. Chamberlain: Offset Litho Blankets (booklet), Dunlop Limited, 1972.

[18] Yildrim Erbil: Surface Chemistry of Solid and Liquid Interfaces, Blackwell Publishing, Oxford, 2006, ISBN 978-1-4051-1968-9, page 309-337.

[19] Michael J. Owen: Surface Energy; in Robert F. Brady (editor): Comprehensive Desk Reference of Polymer Characterization and Analysis, Oxford University Press, Oxford, 2003, ISBN 0-8412-3665-8, page 361-374.

[20] M. Zenkiewicz: Methods for the calculation of surface free energy of solids, Journal of Achievements in Material and Manufacturing Engineering, Vol. 24, 2007, page 137-145.

[21] Robert J. Good: Contact angle, wetting, and adhesion: a critical review; in K. L. Mittal (editor): Contact Angle, Wettability and Adhesion, VSP, 1993, page 3-36.

[22] Finn Knut Hansen: The Measurement of Surface Energy of Polymers by Means of Contact Angles of Liquids on Solid Surfaces (lecture), University of Oslo, 2004.

[23] K. L. Mittal, Frank M. Etzler: Is the World Basic? Lessons from Surface Science; in K. L. Mittal (editor): Contact Angle, Wettability and Adhesion, Vol 6, Koninklijke Brill NV, Leiden, 2009, ISBN 978-90-04-16932-6, page 111-123.

[24] Manoj K. Chaudhury: Interfacial interaction between low-energy surfaces, Materials Science and Engineering, R16, 1996, page 97-159.

[25] Jinming Zhang: Development of Environmentally Friendly Non-Chrome Conversion Coatings for Cold-Rolled Steel (PhD thesis), Virginia Polytechnic Institute and State University, Blacksburg, 2003.

[26] Nolan Tillman, Abraham Ulman, Jay S. Schildkraut, Thomas L. Penner: Incorporation of Phenoxy Groups in Self-Assembled Monolayers of Trichlorosilane Derivatives: Effects on Film Thickness, Wettability, and Molecular Orientation, J. Am. Chem. Soc., 1988, 110, page 6136-6144.

[27] Glen McHale, Stephen J. Elliot, Michael I. Newton, Neil J. Shirtcliffe: Superhydrophobicity: Localized Parameters and Gradient Surfaces (presentation), Contact Angle, Wettability & Adhesion, University of Maine, 2008.

[28] Larry L. Bradshaw and Gary L. Schnellert: Printing on Plastics, Visual Communications Journal, International Graphic Arts Education Association, Inc., Sewickley, 1997.

[29] N. Encinas, M. Pantoja, J. Abenojar, M.A. Martionez: Control of Wettability of Polymers by Surface Roughness Modification, Journal of Adhesion Science and Technology, 24, 2010, page 1869-1883.

[30] Sureurg Khongtong: A smart surface from natural rubber: the mechanism of entropic control at the surface monitored by contact angle measurement, Songklanakarin J. Sci. Technol. 28(2), 2006, page 351-359.

[31] Umit Makal, Kenneth J. Wynne: Water Induced Hydrophobic Surface, Langmuir, 2005.

[32] Steven C. Cowley, John Peoples, Jr.: Plasma Science : Advancing Knowledge In The National Interest / Plasma 2010 Committee, Plasma Science Committee, National Research Council, The National Academies Press, 2007, ISBN: 0-309-10944-2.

[33] K. Rossman: Improvement of bonding properties of polyethylene, J. Polymer Science, 19, 1956, page 141-144.

[34] Mary A. Gilliam: A Plasma Polymerization Investigation and Low Temperature Cascade Arc Plasma for Polymeric Surface Modification (PhD Thesis), University of Missouri-Columbia, 2006.

[35] Zlatko Kregar, Slobodan Milošević, Alenka Vesel: Optical emission from oxygen plasma in E and H modes (manuscript), 2010.

[36] Markus Lake: Oberflächentechnik in der Kunststoffverarbeitung: Vorbehandeln, Beschichten, Funktionalisieren und Kennzeichnen von Kunststoffoberflächen (excerpt), Carl Hanser Verlag, München, 2009, ISBN 978-3-446-41849-3.

[37] Michael Helmus (Committee chair): Materials and coatings for medical devices: cardiovascular, ASM International, 2009, ISBN-13: 978-1-61503-000-2.

[38] Frank D. Egitto: Plasma etching and modification of organic polymers, Pure & Appl. Chem., Vol. 62, No. 9, 1990, page 1699-1708.

[39] Lei Chen, Gerard Henein, J. Alexander Liddle: Super-hydrophobic and/or Super-hydrophilic Surfaces Made by Plasma Process, Nanotech Conference & Expo 2009, Houston, 2009.

[40] Jong-Hyoung Kim, Noritsugu Umehara, Hiroyuki Kousaka, Mamoru Shimada, Mitsuru Hasegawa: Effect of micro-scale Young's modulus and surface roughness on adhesion property to plasma-treated rubber surface, Journal of Mechanical Science and Technology 24, 2010, page 119-122.

[41] Jong-Hyoung Kim, Isami Nitta, Noritsugu Umehara, Hiroyuki Kousaka, Mamoru Shimada, Mitsuru Hasegawa: Relationship between Real Contact Area and Adhesion Force of Plasma-Treated Rubber Sheet Against Stainless-Steel Ball, Tribology Online, 3, 7, page 361-365.

[42] Alenka Vesel, Miran Mozetič, Anton Zalar: XPS characterization of PTFE after treatment with RF oxygen and nitrogen plasma, Surface and Interface Analysis, Vol. 40, Issue 3-4, 2008, pages 661–663.

[43] Rory A. Wolf: Advances in Adhesion with CO_2-based Atmospheric Plasma Surface Modification, Process Cleaning Expo 2010, Louisville, 2010.

[44] M J Shenton and G C Stevens: Surface modification of polymer surfaces: atmospheric plasma versus vacuum plasma treatments, Journal of Physics D: Applied Physics, 34, 2001, page 2761–2768.

[45] L. Chvátalová, R. Čermák, A. Mráček: Surface Properties of Plasma-Modified Poly (1-butene), Latest Trends on Engineering Mechanics, Structures, Engineering Geology, 3rd WSEAS International Conference on Engineering Mechanics, Structures, Engineering Geology, Corfu Island, Greece July 22-24, 2010, ISBN: 978-960-474-203-5.

[46] J. Fiedrich, G. Kühn, R Mix: Polymer Surface modification with Monofunctional Groups of Different Types and Density, in Ricardo d'Agostino et al (editor): Plasma Processes and Polymers: 16th International Symposium on Plasma Chemistry, Taormina, 2003, Willey-VCH Verlag GmbH & Co. KGaA, Weinheim, 2005, ISBN 3-527-40487-2, page 3-21.

[47] Ranjit Sharad Joshi: Polymer surface modification using novel underwater plasma (UWP) technique, BAM Dissertationsreihe, Band 59, BAM – Bundesanstalt für Materialforschung und –prüfung, 2010, ISBN 978-3-9813550-2-4.

[48] Z. Zhang, R. Foerch, W. Knoll: Surface Modification by Plasma Polymerization and Application of Plasma Polymers as Biomaterials, European Cells and Materials, Vol. 6. Suppl. 1, 2003, page 52.

[49] Rajesh Dorai, and Mark J Kushner: A model for plasma modification of polypropylene using atmospheric pressure discharges, Journal of Physics D: Applied Physics, 36, 2003, page 666–685.

[50] Maryline Moreno-Couranjou, Patrick Choquet, Jerôme Guillot, Henri-Noël Migeon: Surface Modification of Natural Vulcanized Rubbers by Atmospheric Dielectric Barrier Discharges Plasma Treatments, Plasma Processes and Polymers, 2009, 6, page 397–400.

[51] T. Tanaka, K. Vutova, E. Koleva, G. Mladenov, T. Takagi: Surface Modification of Plastic Films by Charged Particles: in K. Mittal (editor): Polymer Surface

Modification: Relevance to Adhesion, Vol. 5, Koninklijke Brill NV, Leiden, 2009, ISBN 978-90-04-16590-8, page 95-106.

[52] Jacques Pelletier, André Anders: Plasma-based ion implantation and deposition: A review of physics, technology, and applications, Invited Review for IEEE Transactions on Plasma Science, Special Issue on Ion Sources, Vol. 33, No.6, 2005.

[53] A. L. Cordeiro, M. Nitschke, A. Janke, R. Helbig, F. D'Souza, G. T. Donnelly, P. R. Willemsen, C. Werner: Fluorination of poly(dimethylsiloxane) surfaces by low pressure CF4 plasma – physicochemical and antifouling properties, eXPRESS Polymer Letters, Vol.3, No.2, 2009, page70–83.

[54] A. Tressaud, E. Durand, C Labrugre: Plasma-Enhanced Fluorination of Nitrile Butadien Elastomer: an XPS Study, in Ricardo d'Agostino et al (editor): Plasma Processes and Polymers: 16th International Symposium on Plasma Chemistry, Taormina, 2003, Willey-VCH Verlag GmbH & Co. KGaA, Weinheim, 2005, ISBN 3-527-40487-2, page 223-232.

[55] S. Kitova, M. Minchev, G. Danev: Soft Plasma Treatment Of Polymer Surfaces, Journal of Optoelectronics and Advanced Materials Vol. 7, No. 1, 2005, p. 249 – 252.

[56] J. H. Moraes, A. S. da Silva Sobrinho, H. S. Maciel, J. C. N. Dutra, M. Massi, S. A. C. Mello, W. H. Schreiner: Surface improvement of EPDM rubber by plasma treatment, Journal of Physics D: Applied Physics, Volume 40, Number 24, 2007.

[57] Ana B. Ortíz-Magán, Mercedes M. Pastor-Blas: Influence of Rubber Formulation on Surface Modifications Produced by RF Plasma, Plasma Chemistry and Plasma Processing, Volume 30, Number 2, 2010, page 311-332.

[58] A. Vesel, M. Mozetic, Modification of PET surface by nitrogen plasma treatment, Journal of Physics: Conference Series 100, 2008, 012027.

[59] C. Borcia, G. Borcia, N. Dumitrascu: Plasma surface modification in relation to polymer properties, 28th ICPIG, July 15-20, Prague, 2007.

[60] D. Sakthi Kumar, Masayori Fujioka, Kentaro Asano, Atsumu Shoji, Athipettah Jayakrishnan, Yasuhiko Yoshida: Surface modification of poly(ethylene terephthalate) by plasma polymerization of poly(ethylene glycol), J Mater Sci: Mater Med 18, 2007, page 1831–1835.

[61] Marioara Avram, Andrei Marius Avram, Adina Bragaru, Andrei Ghiu, Ciprian Iliescu: Plasma Surface Modification for Selective Hydrophobic Control, Romanian Journal of Information Science and Technology, Volume 11, Number 4, 2008, page 409-422.

[62] Ben D. Beake, John S. G. Ling and Graham J. Leggett: Correlation of friction, adhesion, wettability and surface chemistry after argon plasma treatment of poly (ethylene terephthalate), Journal of Material Chemistry, 8, 1998, page 2845–2854.

[63] Rui Guo, Auke G. Talma, Rabin N. Datta, Wilma K. Dierkes, Jacques W. M. Noordermeer: Novel Surface Modification of Sulfur by Plasma Polymerization and its Application in Dissimilar Rubber-Rubber Blends, Plasma Chem. Plasma Process, 2010.

[64] Kai Frode Grythe, Finn Knut Hansen: Surface Modification of EPDM Rubber by Plasma Treatment, Langmuir 22, 2006, page 6109-6124.

[65] Shrojal M. Desai, Dhananjay S. Bodas, R.P. Singh: Fabrication of long-term hydrophilic elastomeric surfaces via plasma induced surface cross-linking of functional monomers, Surface and Coatings Technology 184, 2004, page 6–12.

[66] A. Wildberger, H. Geisler, R. H. Schuster: Atmosphärendruckplasmaverfahren: Modifizierung der Elastomeroberflächeneigenschaften, KGK, Januar/Februar 2007, page 24-31.

[67] Melinda Rose: A History of Laser: A Trip Through the Light Fantastic, Photonics Spectra, May, 2010, page 58-70.

[68] N. Ahmad, B. C. Gale and M. H. Key: Experimental and Theoretical Studies of the Time and Space Development of Plasma Parameters in a Laser Induced Spark in Helium, Proceedings of the Royal Society of London. Series A, Mathematical and Physical Sciences, Vol. 310, No. 1501, 1969, page 231-252.

[69] M. Capitelli, A. Casavola, G. Colonna, A. De Giacomo: Laser-induced plasma expansion: theoretical and experimental aspects, Spectrochimica Acta Part B: Atomic Spectroscopy, Vol. 59, Issue 3, 31 March 2004, page 271-289.

[70] P. Laurens, S. Petit, P. Bertrand, F. Ar_fi-Khonsari: PET Surface after Plasma or Laser Treatment: Study of the Chemical Modifications and Adhesive Properties, in Ricardo d'Agostino et al (editor): Plasma Processes and Polymers: 16th International Symposium on Plasma Chemistry, Taormina, 2003, Willey-VCH Verlag GmbH & Co. KGaA, Weinheim, 2005, ISBN 3-527-40487-2, page 253-270.

[71] Thomas Lippert, J. Thomas Dickinson: Chemical and Spectroscopic Aspects of Polymer Ablation: Special Features and Novel Directions, Chem. Rev. 103, 2003, page 453-485.

[72] Samuel S. Mao: Experimental and Theoretical Studies of Picosecond Laser Interactions with Electronic Materials-Laser Ablation (PhD Thesis), University of California, Berkeley, 2000.

[73] N. Bityurin, B. S. Luk'yanchuk, M. H. Hong, T. C. Chong: Models for Laser Ablation of Polymers, Chem. Rev., 103, 2003, page 519-552.

[74] Thomas Lippert: Interaction of Photons with Polymers: From Surface Modification to Ablation, Plasma Processes and Polymers, 2005, 2, 525–546.

[75] Thomas Lippert: UV Laser Ablation of Polymers: From Structuring to Thin Film Deposition, in A. Miotello, P. M. Ossi (editors): Laser-Surface Interactions for New Materials Production Tailoring Structure and Properties, Springer, 2010, ISBN 978-3-642-03306-3.

[76] D. P. Subedi, R. B. Tyata, D. Rimal: Effect of UV-Treatment on the Wettability of Polycarbonate, Kathmandu University Journal Of Science, Engineering And Technology, Vol. 5, No. II, 2009, page 37-41.

[77] Claire O'Connell, Richard Sherlock, Michael D. Ball, Balazs Aszalo´s-Kiss, Una Prendergast, Thomas J. Glynn: Investigation of the hydrophobic recovery of various polymeric biomaterials after 172 nm UV treatment using contact angle, surface free energy and XPS measurements, Applied Surface Science 255, 2009,

page 4405–4413.

[78] P. Laurens, M. Ould Bouali, F. Meducin, B. Sadras: Characterization of modifications of polymer surfaces after excimer laser treatments below the ablation threshold, Applied Surface Science 154–155, 2000, page 211–216.

[79] Kiran P. Adhi, Roger L. Owings, Tarak A. Railkar, W.D. Brown, A. P. Malshe: Femtosecond ultraviolet (248 nm) excimer laser processing of Teflon (PTFE), Applied Surface Science 218, 2003, 17–23.

[80] Hong-Lae Sohn, Bong-Ju Lee: Improved Adhesive Strength of Vulcanized Rubber upon Laser Treatments, Macromolecular Research, Vol. 12, No. 5, 2004, page 540-543.

[81] Jiří Hejduk: The Impact of Physical Properties of Rubber Roller Surfaces on the Effectivity of Ink Transfer (PhD Thesis), University of Pardubice, 2010.

[82] M. Dadsetan, H. Mirzadeh, N. Sharifi-Sanjani: Surface modification of polyethylene terephthalate film by CO_2 laser-induced graft copolymerization of acrylamide, Journal of Applied Polymer Science, Vol. 76, Issue 3, 2000, page 401–407.

[83] Masayuki Okoshi, Masataka Murahara: Photochemical Modification of Polyethylene Surface With Excimer Laser Irradiation, Journal of Photopolymer Science and Technology, Vol. 7, Number 2, 1994, page 381- 388.

[84] Thomas Lippert: Laser Application of Polymers, Advanced Polymer Science, 168, 2004, page 51–246.

[85] G. Wu, M. D. Paz, S. Chiussi, J. Serra, P. González, Y. J. Wang, B. Leon: Excimer laser chemical ammonia patterning on PET film, J Mater Sci: Mater Med 20, 2009, 597–606.

[86] Ellane J. Park, Gregory T. Carroll, Nicholas J. Turro, Jeffrey T. Koberstein: Shedding light on surfaces–using photons to transform and pattern material surfaces, Soft Matter, 5, 2009, page 36–50.

[87] Vera-Maria Graubner, Rainer Jordan, and Oskar Nuyken: Photochemical Modification of Cross-Linked Poly(dimethylsiloxane) by Irradiation at 172 nm, Macromolecules, 37, 2004, page 5936-5943.

[88] Vera-Maria Graubner, Rainer Jordan, Oskar Nuyken, Rüdiger Kötz, Thomas Lippert, Bernhard Schnyder, Alexander Wokaun: Wettability and surface composition of poly(dimethylsiloxane) irradiated at 172 nm, Polymeric Materials: Science & Engineering, 88, 2003, page 488.

[89] Juergen Reif: Basic Physics of Femtosecond Laser Ablation: in Antonio Miotello, Paolo M. Ossi (editors): Laser-Surface Interactions for New Materials Productions: Tailoring Structure and Properties, Springer Verlag, Berlin, 2010, ISBN 978-3-642-03307-0.

[90] Computer to Plate in North American Newspapers: Impact and effectiveness of the Southern Lithoplate Alliance, The Chesapeake Resource Group LLC, Stevensville, 2007.

[91] Matthew A. Meitl, Zheng-Tao Zhu, Vipan Kumar, Keon Jae Lee, Xue Feng, Yonggang Y. Huang, Ilesanmi Adesida, Ralph G. Nuzzo, John A. Rogers: Transfer printing by kinetic control of adhesion to an elastomeric stamp, Nature Materials, Vol. 5, 2006.

[92] Sarah Thévenet: General approach for the application of Supramolecular NanoStamping (SuNS) to surfaces of all types (master thesis), Massachusetts Institute of Technology, 2007.

[93] Bryan Crowther (editor): The Handbook of Rubber Bonding, Rapra Technology Limited, 2003, ISBN 1-85957-394-0, page 145-146.

[94] James. E. Mark (editor): Polymer Data Handbook, Oxford University Press, 1999.

[95] Shinzo Kohjiya, Astushi Katoh, Junichi Shimanuki, Toshinori Hasegawa, Yuko Ikeda: Three-dimensional nano-structure of in situ silica in natural rubber as revealed by 3D-TEM/electron tomography, Polymer 46, 2005, page 4440–4446.

[96] André Wahmeier, Joachim Fröchlich: Advanced Filler Systems for Rubber Reinforcement (presentation), Evonik Industries, 2008.

[97] Anke Blume: Silica/silane - a winning reinforcement formula, Rubber World, 2000.

[98] Alenka Vesel, Ita Junkar, Uroš Cvelbar, Janez Kovač, Miran Mozetič: Surface modification of polyester by oxygen- and nitrogen-plasma treatment, Surface and Interface Analysis, Volume 40, Issue 11, 2008, page 1444–1453.

[99] Miran Mozetič, Uroš Cvelbar: Determination of the neutral atom density in weakly ionized plasma with catalytic probes, 19th Europhysics Conference on the Atomic and Molecular Physics of Ionized Gases, Grenada, 2008.

[100] Miran Mozetič, Uroš Cvelbar: Determination of the neutral oxygen atom density in a plasma reactor loaded with metal samples, Plasma Sources Sci. Technol. 18, 2009.

[101] Renate Förch, Holger Schönherr, A. Tobias A. Jenkins: Surface Design: Applications in Bioscience and Nanotechnology, Wiley-VCH Verlag, Weinheim, 2009, page 484.

[102] Bob Hafner: Scanning Electron Microscopy Primer, University of Minnesota - Twin Cities, 2007.

[103] W. Suëtaka, J. T. Yates, Jr.: Surface Infrared and Raman Spectroscopy: Methods and Applications, Plenum Press, New York, 1995, ISBN 0-306-44963-3.

[104] John C. Vickerman, Ian S. Gilmore (editors): Surface analysis; the Principal Techniques, John Wiley & Sons, 2009, ISBN 978-0- 470-017630-0, page 7.

[105] Gottfried W. Ehrenstein, Gabriela Riedel, Pia Trawiel: Thermal Analysis of Plastics: Theory and Practice, Hanser, 2004, ISBN-10: 3-446-22673-7.

[106] Hyun Wook Kang, et al.: Liquid Transfer Experiment for Micro-Gravure-Offset Printing Depending on the Surface Contact Angle, APCOT 2008.

8 APPENDIX

Overview of papers and presentations, published in the proceedings of international conferences:

IARIGAI, Stockholm, 2009

Gorazd Golob, Miran Mozetič, Kristina Eleršič, Ita Junkar, Dejana Đorđević, Mladen Lovreček: **Rubber blanket surface energy modification using oxygen plasma treatment.**

SGA, Pardubice, 2009

Gorazd Golob, Miran Mozetič, Mladen Lovreček: **Rubber raw material surface energy modification using oxygen plasma treatment.**

Tiskarstvo, Stubičke toplice, 2010

Gorazd Golob, Mladen Lovreček, Miran Mozetič, Alenka Vesel, Odon Planinšek, Marta Klanjšek Gunde, Diana Gregor Svetec: **Determination of surface free energy and chemical modifications of plasma treated elastomer surface.**

ISNG, Ljubljana, 2010

Gorazd Golob, Mladen Lovreček, Miran Mozetič, Odon Planinšek, Marie Kaplanová: **Surface free energy determination of EPDM and NBR rubber blankets.**

IARIGAI, Montreal, 2010

Gorazd Golob, Mladen Lovreček, Miran Mozetič, Alenka Vesel, Odon Planinšek, Marta Klanjšek Gunde, Vilibald Bukošek: **Surface and Structural Properties of EPDM and NBR Rubber Blankets.**

Rubber blanket surface energy modification using oxygen plasma treatment

Gorazd Golob[1], Miran Mozetič[2], Kristina Eleršič[2], Ita Junkar[2], Dejana Đorđević[1], Mladen Lovreček[3]

[1]University of Ljubljana, Faculty of Natural Sciences and Engineering
Snežniška 5, 1000 Ljubljana, Slovenia
gorazd.golob@ntf.uni-lj.si, dejana.djordjevic@ntf.uni-lj.si
[2]Jožef Stefan Institute - Ljubljana, Department of Surface Engineering and Optoelectronics
Jamova cesta 39, 1000 Ljubljana, Slovenia
miran.mozetic@ijs.si, kristina.elersic@ijs.si, ita.junkar@ijs.si
University of Zagreb, Faculty of Graphic Arts
Getaldićeva 2, 10000 Zagreb, Croatia
lovrecek@grf.hr

Abstract: The goal of investigation was to determine surface free energy, roughness and other properties of NBR and EPDM rubber blankets, modification of the surface properties using oxygen plasma treatment and defunctionalization of the surface. Characterization of the surface free energy by contact angle measurements using different disperse and polar liquids, SEM and roughness analysis of the investigated untreated and plasma treated elastomers gives a quantitative description of achieved surface modifications. Plasma treated rubber blankets achieved higher surface free energy and have become more hydrophilic but a superhydrophilic stage with contact angle with water near 0º was not achieved during the investigation. Contact angle with water remained almost unchanged after 24 hours. Roughness of treated surface has arisen. There were no significant differences between NBR and EPDM rubber blankets.
Keywords: EPDM rubber blanket, NBR rubber blanket, oxygen plasma, surface free energy

1 Introduction

Rubber blanket is a well-known ink transfer media in lithographic offset and other conventional or digital printing techniques. Mechanical properties, composition of surface layer, its roughness and other surface properties should give a good ink transfer factor as a necessary condition for high print quality. The surface energy of the blanket should be higher than surface energy of the ink and print areas of the printing plate and lower than the surface energy of the print substrate - usually paper. By modification of blanket surface energy we open a possibility to use a wide pallet of different printing inks, not only those based on synthetic or vegetable oil vehicle but also water-based and other types of inks.

Contact angle based measurements of surface energy are widely used in research and industry. By using different polar and non-polar liquids and proper calculation methods we should get information about polar and disperse part of surface energy of the material and indirectly we can conclude about its hydrophilic/oleophilic or hydrophobic/oleophobic properties.

By plasma (or corona) treatment of plastic film or other print substrates by the material producer or on the press we can raise its surface energy, usually over 40 mN/m. There is no other known wide use of plasma treatment in printing industry, except some experiments with treatment of printing plates for flexo printing.

During our investigation we tried to modify the surface energy of different rubber blankets to raise their surface energy and achieve nearly perfect hydrophilic surface. We also studied the stability of achieved modifications, methods for a reverse process and changes on the blanket surface at different stages during the experiments.

2 Research methods

In the experimental phase, four different blanket samples were used:

1. EPDM rubber for UV printing, non-polar, silica filler (RED)
2. EPDM rubber for UV printing, non-polar, soot/carbon conductive filler (BLACK)

3. NBR/TM (90/10) blend rubber for conventional printing, polar, silica filler (BLUE)
4. NBR blend rubber for conventional printing, polar, silica filler (LIGHT BLUE)

For oxygen plasma treatment of the samples we use lab plasma reactor with a vacuum pump and an inductively coupled RF generator at the power of approximately 200 W. Each sample was exposed to oxygen plasma with the neutral atom density of $5x10^{21}$ m^{-3}, the electron density of $8x10^{15}$ m^{-3} and the electron temperature of 35000 K for 0, 3, 9, 27, 81, 243 and 729 s. The samples were kept at floating potential that was -15V (Cvelbar, Mozetič).

For the first set of contact angle measurements we used 3 µl drops of distilled water and a CCD camera connected to a computer to get contact angle. Contact angle measurements were performed immediately after treatment and repeated after 3 and 24 hours. At the end we used the test-pen method, too.

For the second set of measurements we used the same samples, treated for 27 s by oxygen plasma under same conditions. We measured contact angles after approximately 24 hours on Krüss DSA 100 apparatus with three liquids: water (1 µl), diiodomethane (0.5 µl) and formamide (1 µl). For calculation of surface free energy we used Wu (Wu), Owens Wendt (OW) and AcidBase theory (AB) methods, supported by Krüss software (Brady, Erbil). Surface free energy data of test liquids were obtained from Krüss database. For each measurement set we performed at least 6 measurements and excluded results with extreme deviation to mean value.

SEM images at 1000 × and 8000 × magnification show the changes of the surface on untreated and samples treated for 243 s.

Measurement of roughness using Perthometer gave us information about modification of surface morphology after plasma treatment.

3 Results

Results of the first set of contact angle measurements to find out ageing resistant after plasma treatment are presented in Table 1. Because of thermal degradation at the edges of samples exposed for long time to oxygen plasma we did not use very long time of plasma treatment for LIGT BLUE samples. We repeated the measurements for RED, BLACK and BLUE samples several times and got very similar results that are not published in this report. Test-pen for surface energy testing indicated over 44 mN/m on all untreated and treated samples.

Table 1: Contact angles of RED, BLACK, BLUE and LIGHT BLUE rubber blankets.

Plasma	RED			BLACK			BLUE			LIGHT BLUE		
treatment	Contact angle (º) for water after											
time (s)	0 h	3 h	24 h	0 h	3 h	24 h	0 h	3 h	24 h	0 h	3 h	24 h
0	130.0	130.0	130.0	121.0	121.0	121.0	125.1	125.1	125.1	135.4	135.4	135.4
3	83.0	82.3	81.7	75.2	74.1	76.5	75.9	78.6	75.0	70.2	78.7	78.6
9	72.4	74.3	73.5	65.2	71.5	73.0	68.0	65.2	69.7	67.6	71.0	74.2
27	71.5	73.0	71.6	61.5	68.5	69.6	62.5	62.9	68.3	61.5	60.5	68.5
81	63.6	62.6	63.8	52.6	61.5	61.0	60.2	58.9	60.0	53.7	54.6	51.1
243	39.9	51.0	49.3	46.8	57.6	56.7	58.0	51.0	49.0	-	-	-
729	36.7	44.2	44.7	53.7	64.5	66.7	51.4	50.4	47.4	-	-	-

Results of second set of measurements of contact angles of treated and untreated samples using different liquids are presented in Table 2.

Results of calculations using Owens Wendt, Wu and AcidBase theory methods, presented in Tables 3 and 4 give us very different or even negative values of surface free energy in some cases.

Results of surface free energy (total, disperse and polar part) of untreated and treated samples using Owens Wendt method are presented in Figure 1.

Table 2: Contact angles for different liquids (water – W, diiodomethane – D, formamide – F) of untreated and plasma treated samples.

Sample	Contact angle (º) untreated			Contact angle (º) plasma 27 s		
	W	D	F	W	D	F
RED	132.4	75.3	104.2	66.7	48.3	62.9
BLACK	108.9	65.4	98.3	57.3	34	51.7
BLUE	100.2	49.9	76.9	52.8	39.5	38.7
LIGHT BLUE	111.0	65.9	99.8	50.3	41.7	44.8

Table 3: Surface free energy of untreated samples (total – T, disperse – D, polar – P, acidbase – AB, acid – A, base – B).

Surface free energy (mN/m) untreated										
	Owens-Wendt			Wu			AcidBase theory				
Sample	T	D	P	T	D	P	T	D	AB	A	B
RED	21.28	19.70	1.58	19.83	23.41	-3.58	21.48	19.96	1.51	0.48	1.19
BLACK	21.40	21.36	0.04	25.12	27.19	-2.07	20.55	25.47	-4.93	2.16	2.81
BLUE	32.73	32.59	0.14	35.01	34.75	0.27	33.66	34.33	-0.67	0.14	0.79
LIGHT BLUE	21.16	21.16	0.00	24.63	27.06	-2.44	20.62	25.19	-4.57	2.31	2.26

Table4: Surface free energy of plasma treated samples (total – T, disperse – D, polar – P, acidbase – AB, acid – A, base – B).

Surface free energy (mN/m) plasma 27 s										
	Owens-Wendt			Wu			AcidBase theory				
Sample	T	D	P	T	D	P	T	D	AB	A	B
RED	40.15	29.34	10.81	43.25	32.12	11.13	31.52	35.22	-3.70	0.14	24.46
BLACK	49.00	35.70	13.29	51.70	37.57	14.13	39.27	42.49	-0.32	0.09	28.89
BLUE	50.32	33.46	16.86	52.86	35.42	17.26	39.46	39.86	-0.40	0.01	33.22
LIGHT BLUE	51.98	33.22	18.76	54.29	34.95	19.34	42.39	38.74	3.65	0.10	32.94

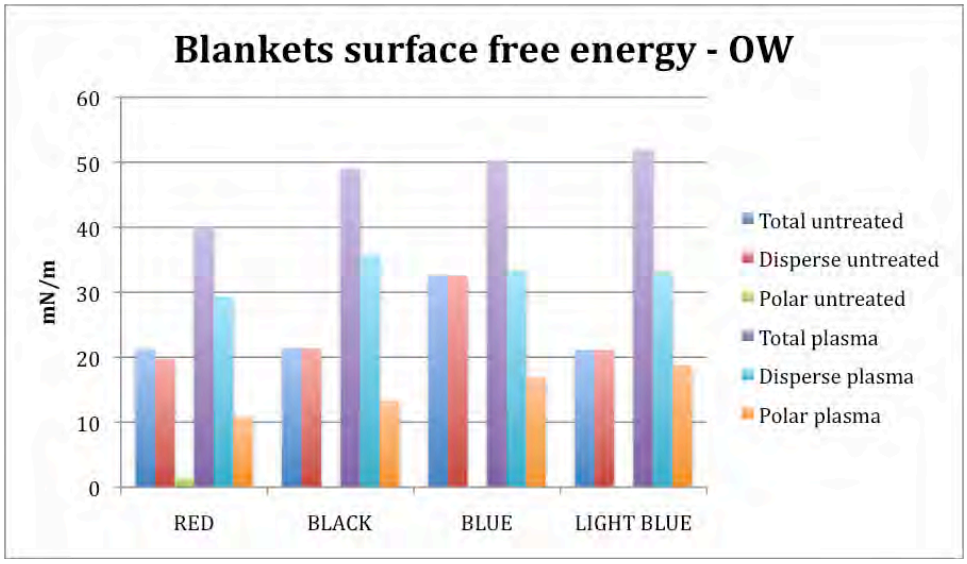

Figure 1: Surface free energy of untreated and treated samples, calculated using Owens Wendt method.

SEM images at 8000 × magnification of RED, BLACK and BLUE samples are presented in Figure 2, 3 and 4 where each image pair of untreated and plasma treated (243 s) samples gives us the basic visual information about surface changes.

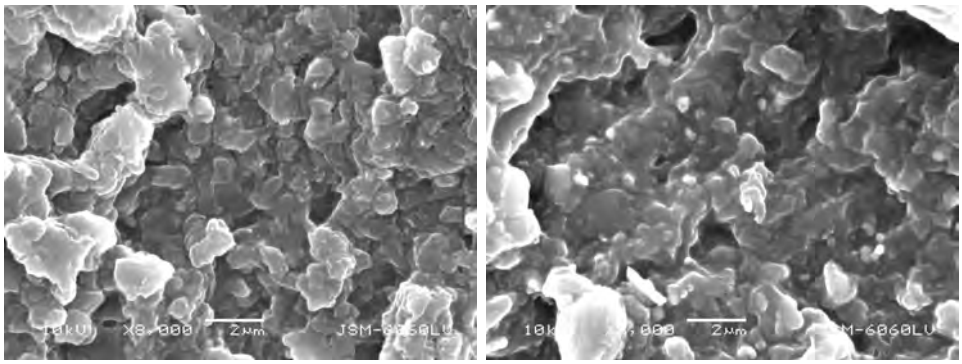

Figure 2: RED rubber blanket untreated (left) and treated (right).

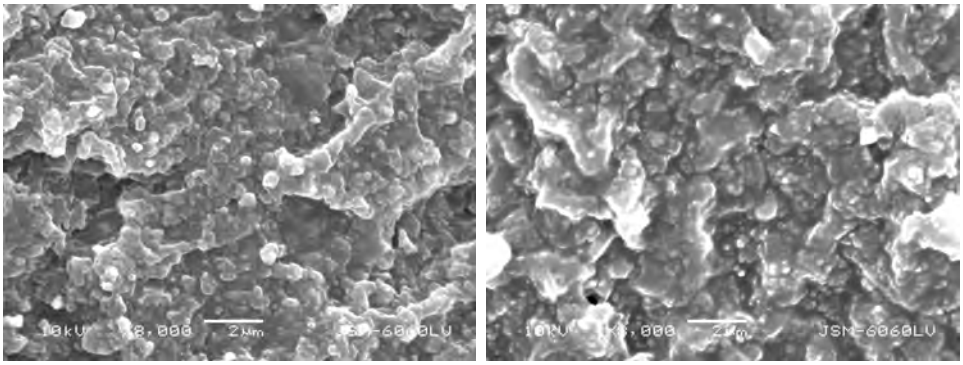

Figure 3: BLACK rubber blanket untreated (left) and treated (right).

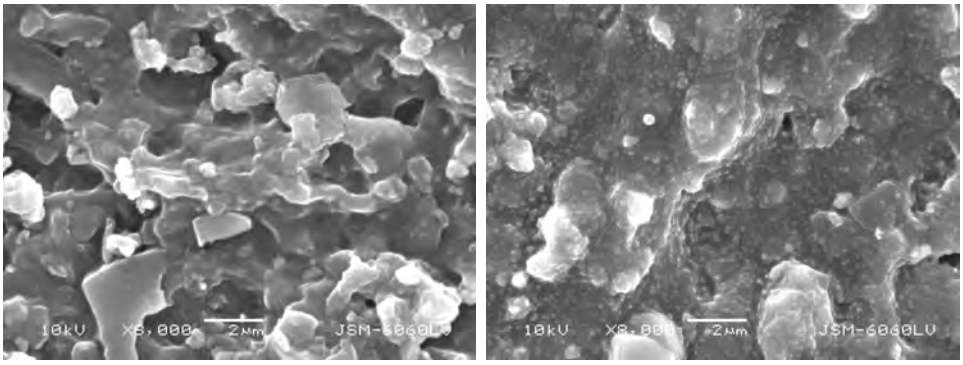

Figure 4: BLUE rubber blanket untreated (left) and treated (right).

Changes in roughness after treatment in oxygen plasma (729 s) for RED, BLACK and BLUE sample are presented in Table 5 as average roughness.

Table 5: Average roughness (Ra) of untreated and treated of RED, BLACK and BLUE samples.

	Untreated samples	Plasma treated samples
Sample	Ra (μm)	Ra (μm)
RED	1.040	1.160
BLACK	0.708	1.100
BLUE	0.736	0.797

Results of reversible process or defunctionalisation of the surface properties using hot air dryer or laser show only limited success. Results of achieved contact angles for RED, BLACK and LIGHT BLUE samples, treated after 9 days for 10 min at 100 ºC in hot air dryer are presented in Table 6.

Table 6: Contact angles for RED, BLACK and CYAN samples after hot air treatment.

	Contact angle (º)		
	Water	Diiodomethane	Formamide
RED	100.9	60.1	71.2
BLACK	96.1	58.9	78.6
LIGHT BLUE	71.6	50.8	60.4

4 Discussion

Different types of rubber blankets give us similar results after treatment with oxygen plasma. For the first 25 s of treatment the colour of the plasma was red, typical for oxygen. After that the colour changed to white. The colour of the samples remained the same at short treatment time, BLACK and BLUE changed their colour at 243 s and RED at 729 s because of thermal degradation. For LIGHT BLUE sample we observed some traces of burning at the edges and therefore we used only short time for treatment up to 81 s. With all samples we saw traces of burning at the edges after treatment for 729 s.

Untreated samples were very hydrophobic, after short treatment of 3 s they became slightly hydrophilic and by increasing the treatment time the hydrophilicity increased (Gojo, Lovreček, Mozetič). The hydrophilic condition remained very stable during 24 h. During our investigation we used equipment at different locations. Stability of the samples hydrophilicity gave us opportunity for contact angle measurements using different liquids after 24 h at another location. After oxygen plasma treatment surface free energy has arisen in all samples.

Results of contact angle measurements and surface energy calculations are not reliable and we have to repeat this part of investigation. Reasons could be in inappropriate handling with equipment, test liquids with characteristics that are not the same as in database, unhomogenity and roughness of rubber blanket surface, differences in air temperature and humidity or some other reason. It is well known from references that different methods for surface free energy give us different results and that some methods are not appropriate for all solid materials. At this stage of investigation we got enough information about influence of oxygen plasma on different types of rubber to continue with measurements of surface free energy using other types of rubber blankets and raw materials like basic polymers and fillers for rubber production.

It is interesting that so called polar NBR rubber shows us almost no polar part of surface free energy before treatment and non-polar EPDM rubber has higher amount of polar part compare to NBR rubber. After treatment with oxygen plasma we have achieved higher level of total surface free energy and polarity with NBR rubber, but defunctionalisation seems better using EPDM rubber. Reason for such deviation could be impurities at the rubber surface. The untreated samples were wiped with ethanol five minutes before measurements and plasma treatment but obviously this treatment was not efficient and for now chemical structure of untreated and plasma treated samples remains unknown.

During the investigation we did not achieve very hydrophilic stage with contact angle near 0º on our rubber blanket samples. On many other metal and organic materials we achieved super hydrophilic surface in very short time during oxygen plasma treatment. We observe some unusual phenomena like raised water drop on wet surface of the rubber and wicking of the water drop on the surface.

Surface roughness is slightly higher after treatment for RED and BLUE rubbers filled with silica, for BLACK sample it raised for 55 %. Roughness measurements are confirmed by SEM images where we see some changes in surface structure, caused by plasma etching of rubber components in the surface layer. Rubber consists of ten or more components like one or more polymers, fillers, additives for cross-linking of basic monomer, additives for hardness and elasticity control, pigments and dyes (Salamone). According to manufacturer's specifications of silica fillers we expected conglomerates of silica in dimensions up to 80 nm but at SEM images we can observe round shapes with bigger diameter. The shape of surface layer structure was typical for ground finished surface layer, it remained almost unchanged after plasma treatment and obviously there was no significant etching of polymer on surface layer.

5 Conclusions

To get more reliable results the analysis of pure basic materials before and after plasma treatment is necessary. We should continue our investigation using typical EPDM, NBR and other types of crude rubber and different fillers to get surface free energy of untreated and plasma treated basic rubber components. After that new set of rubber samples should be prepared for further investigations.

XPS analysis should give us chemical fingerprint of the sample surface. Surface free energy measurements are not sufficient to determine hydrophilic/hydrophobic or oleophilic/oleophobic character of the surface before and after treatment. Impact of impurities at the rubber surface layer is still unknown and with repeated series of plasma treatments and defunctionalisation we should get pure surface to perform measurements of surface free energy and chemical analysis. .

In this paper the first results of oxygen plasma treatment of rubber blanket surface are presented. It can be concluded that such a treatment gives us a rubber blanket with new characteristics that open new opportunities for improvements of their characteristics and new functionality of blankets in different printing processes.

Acknowledgements

We would like to thank coleagues from Savatech, Kranj; Faculty of Pharmacy, University of Ljubljana and from Department of Graphic Arts and Photophysics, University of Pardubice for technical support and cooperation.

References

Brady, Robert: *Comprehensive Desk Reference of Polymer Characterization and Analysis*, Oxford University Press, 2003, ISBN 0 8412 3665 8.

Cvelbar Uroš, Miran Mozetič: *Method for improving of electrical connection properties of a surface of a product made from a polymer matrix composite*, international patent WO 2006/029642.

Erbil, H. Yildrim: *Surface Chemistry of Solid and Liquid Interfaces*, Blackwell Publishing, 2006, ISBN 1 4051 1968 3.

Gojo, Miroslav; Lovreček, Mladen: *Characterisation of Surfaces on the Offset Printing Plate*, Proceedings of Lectures and Posters, 1st International Symposium of Novelties in Graphics, Ljubljana : Faculty of Natural Sciences and Engineering, 1998. 253-260

Lovreček, Mladen; Gojo, Miroslav; Dragčević, Krešimir: *Interfacial Characteristics of the Rubber Blanket - Dampening Solution System*, Bristow, J., Anthony (ur.). Leatherhead, Surrey, UK : Pira International, 1999. Str. 370.

Mozetič Miran, Alenka Vesel, Cvelbar Uroš: *Method and device for local functionalization of polymer materials*, international patent WO 2006/130122.

Mozetič, Miran: *Controlled oxidation of organic compounds in oxygen plasma*. Vacuum. [Print ed.], 2003, vol. 71, p. 237-240.

Salamone, J.: *Polymeric Materials Encyclopedia*, CRC Press, Taylor & Francis LLC, 1996, ISBN 9780849324703.

Rubber raw material surface energy modification using oxygen plasma treatment

Gorazd Golob[1], Miran Mozetič[2], Mladen Lovreček[3]

[1]University of Ljubljana,
Faculty of Natural Sciences and Engineering

[2]"Jožef Stefan" Institute,
Department of Surface Engineering and Optoelectronic

[3]University of Zagreb,
Faculty of Graphic Arts

Abstract

Rubber blanket is well known ink transfer media in lithographic offset and other conventional or digital printing techniques. Mechanical properties, composition of surface layer, it's roughness and other surface properties should give us good ink transfer factor as a necessary condition for high print quality. Different rubber blankets including NBR and EPDM based elastomer with different silica fillers have been investigated. Rubber blankets and raw materials for their production with different surface energy, polarity and roughness give us a good starting point for the study of the efficiency of different surface treatment methods. Increased surface energy was achieved by treatment with low-pressure gaseous plasma. Plasma was created in oxygen by an inductively coupled radiofrequency discharge. The discharge power was up to a few 100W, the gas pressure up to 100 Pa.

After plasma treatment the surface energy was determined from measured contact angles using different liquids. Surface properties and particle size of silica filler were measured using inverse gas chromatography and laser beam diffraction method.

Keywords: *rubber blanket, NBR, EPDM, plasma, contact angle, surface energy*

1 Introduction

Modern rubber blanket consist of several layers of fabric, cord or some other textile material giving stability and strength to the end product, different layers of rubber and one or more compressible layers (Figure 1). Thin surface layer of NBR, EPDM or other types and blends of rubber is most important for good ink transfer and print quality.

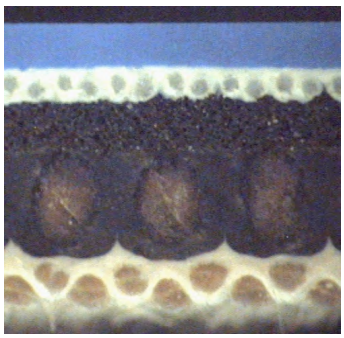

Figure 1: Typical structure of Sava offset print blanket (Advantage new, 1.95 mm).

Surface energy, roughness and other technical properties of surface layer depend on type of elastomer, filler, vulcanization agent, additives and production methods and conditions. Polar NBR rubber is mainly used for conventional non-polar oil-based printing inks and non-polar-EPDM rubber for polar UV inks. Surface layer could be finished as moulded, buffed in different grades or textured.

Our goal is to determine surface energy of raw materials for rubber used for typical surface layers of offset print blanket. We choose raw materials in cooperation with Savatech, producer of offset print blankets used for our previous investigations. In this report we give some findings on surface characteristics of different NBR and EPDM crude rubbers (basic polymer for rubber production) and silica as typical filler.

2 Research methods

Preparation of samples, plasma treatment and measurements was conducted at different locations and in most cases within 24 h. The first set of experiments was conducted on blanket samples to find out the influence of oxygen plasma on surface free energy and roughness and time dependence (ageing) of treated samples. We conclude that changes of surface characteristics are significant after few seconds and this new stage remains almost unchanged after 24 h [1].

2.1 Raw materials used

We used three NBR crude rubbers with different polarity based on different acrylonitrile groups content and one EPDM crude rubber (Table 1). The number in the name of NBR crude rubber gives us the content of acrylonitrile groups and viscosity. Crude rubber is very tough, elastic, sticky material so it is not possible to cut it in flat, smooth samples. We diluted pieces of crude rubber in toluene and got a thin polymer film (0.2 mm thick wet layer) on glass micro slides after evaporation of solvent. Even after 24 h of dilution some "undiluted" parts remained in "liquid" of Europrene 19.45 GRN that gave us uneven structured surface of final sample. Some other samples, especially Krynac 33.30 F, remained sticky after evaporation of solvent.

Table 1: Crude rubbers used.

Name	Code
NBR (Acrylonitrile-Butadien Rubber)	
Europrene 19.45 GRN	1047
Krynac 33.30 F	2215
Europrene 45.60 N	7167
EPDM (Ethylene Propylene Diene Rubber)	
Keltan 8340 A	7394

Two different silica filler were examined (Table 2), untreated and treated. First we made tablets from silica powder for measurement of surface free energy and for laser treatment. During preliminary tests we found out that because of very high surface activity and porosity measurements of contact angle are not possible. We decided to measure relative differences of two powder silica samples by inverse gas chromatography method on Agilent Technologies

6890N apparatus using acetone vapour. For particle size we used silica powder samples, dispersed in ethanol and treated for 5 minutes by ultrasound. Measurements were performed in Malvern Instruments Master Sizer apparatus, based on laser beam diffraction.

Table 2: Silica used.

Name	Code	Description
Ultrasil 7000	6577	unmodified, agglomerates up to few mm
Coupsil 6508	7112	modified, fine dust

2.2 Plasma treatment

We used lab low vacuum oxygen plasma generator with a vacuum pump at 75 Pa and inductively coupled RF generator at the power of about 200 W. Each sample was exposed to oxygen plasma with the neutral atom density of $5x10^{21}$ m^{-3}, the electron density of $8x10^{15}$ m^{-3} and the electron temperature of 35000 K for 27 s. The samples were kept at floating potential of -15V.

2.3 Contact angle measurements and surface free energy calculation

We measured contact angle using circle fitting sessile drop technique at Krüss DSA apparatus with three liquids: water (1 μl), diiodomethane (0.5 μl) and formamide (1 μl). For calculation of surface free energy we use Wu (Wu), Owens Wendt (OW) and AcidBase theory (AB). All measurements of oxygen plasma treated samples were conducted approximately 24 h after treatment. For each measurement set we performed at least 6 measurements and excluded results with extreme deviation to mean value.

3 Results

Results of contact angle measurements are presented in Table 3 and surface free energy calculations using Owens Wendt method in Figure 2. Calculations using Wu and AB theory method give us very low, negative or unexpected values of surface free energy. All values of AB part of surface free energy of untreated samples were negative. We repeated some measurements but results remained very similar. We have decided not to publish results that are obviously problematic.

Table 3: Results of contact angle measurements of untreated and plasma treated polymers.

	Contact angle – untreated (°)			Contact angle – plasma treated (°)		
Elastomer	Water	Diiodo-methane	Formamid	Water	Diiodo-methane	Formamid
Europrene 19.45 GRN	101.0	55.2	92.5	68.0	30.8	55.1
Krynac 33.30 F	85.7	47.8	80.2	62.5	46.4	52.9
Europrene 45.60 N	83.9	33.1	60.8	68.6	40.9	52.6
Keltan 8340 A	98.6	58.6	88.4	85.4	54.0	60.0

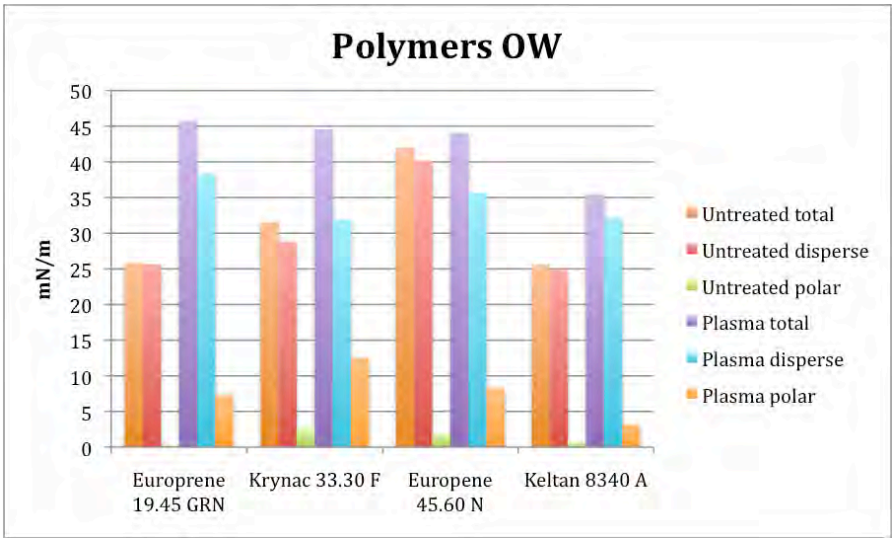

Figure 2: Results of surface free energy calculated by Owens Wendt method.

Results of inverse gas chromatography are given as retention time under solvent vapour treatment of sample (Table 4).

Table 4: Retention time for two silica samples treated by chloroform solvent.

Sample	Position	Quantity (mg)	Time (min)
Ultrasil 7000	front	11	1.395
Coupsil 6508	front	10	1.070
Ultrasil 7000	back	16	2.470
Coupsil 6508	back	14	1.263

Measurements of particle size for Ultrasil 7000 show us wide distribution from approx. 2 μm up to 800 μm with peek at 90 μm. For Coupsil 6508 we get much narrower distribution in the range of 2 μm up to 40 μm with peek at 15 μm.

4 Discussion and conclusion

Surface free energy of untreated polymers is typicaly very low. In our case it is about 25 mN/m for NBR crude rubber with small amount of acrylonitrile groups and non-polar EPDM crude rubber. With higher amount of acrylonitrile groups surface free energy rises up to 42 mN/m. The disperse part of surface free energy is close to total and polar part is very low, even at NBR crude rubber, declared in literature as polar rubber [2].

After oxygen plasma treatment we get samples with higher surface free energy near 45 mN/m for NBR crude rubber and about 35 mN/m for EPDM crude rubber. Polar part of surface free energy is higher at all samples.

Krynac 30.33 F has highest polar part of surface free energy before and after plasma treatment so it is possible that besides the amount of acrylonitrile groups something else may also have

strong impact on polarity. This polymer is from other producer than others and has some specific visual and tactile noticeable characteristics.

According to literature inverse gas chromatography is proven and useful method for surface free energy measurement [3]. During our investigation we intended to measure and modify surface free energy of silica using plasma treatment. Plasma treatment of silica is hard and expensive to realize because we have to build new plasma reactor with moving vital parts. There are chemical modified silica on the market, Coupsil 6508 is only one representative, with higher surface free energy, that bond well to polymer and other raw materials in rubber. We will continue our investigation using different modified silica filler and other suitable materials.

In technical documentation of producers [4] and in other literature [5] the particle sizes of silica in rubber is typical described as particles in sizes from 5 to 30 nm, aggregates consists of several particles and agglomerates consist of many particles with sizes up to 600 nm. Our measurements of untreated and treated silica show us much higher values so we have to investigate the dimensions and distribution of silica particles in final product using plasma etching of surface and SEM observations.

During our investigation we found out that oxygen plasma modification gave us noticeable higher surface free energy of NBR and EPDM crude rubber. We assume that surface free energy of final product – surface layer of offset blanket could be modified using plasma treatment and we will continue our investigation using some other types of raw material, improved method of plasma surface treatment and improved methods of measurements and calculations of surface free energy.

5 References

1 Golob G., et al: *Rubber blanket surface energy modification using oxygen plasma treatment*, IARIGAI, 36th International Research Conference, Stockholm, 2009.

2 Salamone, J.: *Polymeric Materials Encyclopedia*, CRC Press, Taylor & Francis LLC, 1996, ISBN: 9780849324703.

3 *Determination of surface properties of solid and semisolid materials by solid and semisolid materials with inverse phase gas chromatography (research project, head Srčič, S.)*, University of Ljubljana, Faculty of Pharmacy, 2003-2005, http://www.ist-world.org.

4 www.degussa.com/degussa/en/products

5 Biron, M.: Silicas as polymer additives, SpecialChem, 2003, http://www.specialchem4polymers.com.

Acknowledgment

We would like to thank coleagues from Savatech, Kranj, Faculty of Pharmacy, University of Ljubljana and from Department of Graphic Arts and Photophysics, University of Pardubice for technical support and cooperation.

Determination of surface free energy and chemical modifications of plasma treated elastomer surface

Gorazd Golob, University of Ljubljana, Faculty of Natural Sciences and Engineering
Mladen Lovreček, University of Zagreb, Faculty of Graphic Arts
Miran Mozetič, "Jožef Stefan" Institute, Ljubljana
Alenka Vesel, "Jožef Stefan" Institute, Ljubljana
Odon Planinšek, University of Ljubljana, Faculty of Pharmacy
Marta Klanjšek Gunde, National Institute of Chemistry Slovenia, Ljubljana
Diana Gregor Svetec, University of Ljubljana, Faculty of Natural Sciences and Engineering

Abstract

The aim of presented work is investigation of surface free energy and chemical properties of unmodified and plasma treated NBR and EPDM based elastomer. Rubber blanket, covered with thin elastomer surface layer, is a well known ink transfer media in lithographic offset and other conventional or digital printing techniques where it is used as secondary printing forme. Characterization of the surface energy by contact angle measurements using different polar and disperse liquids combined with proper calculation methods based on Owens-Wendt, Wu or Oss&Good AcidBase theory, give us information about polar and disperse part of surface energy of the material so indirectly we can conclude about its adsorption potential and its hydrophilic/oleophilic or hydrophobic/oleophobic properties.

For oxygen plasma treatment of the samples we used a lab plasma reactor with a vacuum pump and an inductively coupled RF generator at the power of approximately 200 W. Each sample was exposed to oxygen plasma with the neutral atom density of $5x10^{21}$ m^{-3}, the electron density of $8x10^{15}$ m^{-3} and the electron temperature of 35 000 K for 27 s. The samples were kept at floating potential of -15V.

For surface free energy measurements we used Krüss DSA100 apparatus to obtain contact angle and DSA software with database of water, diiodomethane and formamide test liquids properties for calculations.

We used Perkin Elmer FTIR-ATR spectrometer in mid IR area (wavenumber 500 – 4000 cm^{-1}, 2.5 – 20 μm) to get IR spectra of untreated and plasma treated elastomer samples. Analysis of spectra was performed using KnowItAll software with spectral database to get reliable results. Typical peaks of absorption spectra give us information of elements, chemical groups or bonds on surface that are in correlation with the surface energy, polarity and other surface characteristics of the mentioned materials.

Keywords: elastomer, rubber blanket, plasma, surface energy, IR spectrum

1 Introduction

Rubber blanket is used in lithographic offset and other conventional or digital printing techniques as secondary printing forme. The surface energy of the blanket should be higher than surface energy of the ink and print areas of the printing plate and lower than the surface energy of the print substrate - usually paper. By modification of blanket surface energy we open a possibility to use a wide pallet of different printing inks, not only those based on synthetic or vegetable oil vehicle but also water-based and other types of inks.

By using different polar and non-polar liquids for contact angle measurements and proper calculation methods we should get information about polar and disperse part of surface energy of the material and indirectly we can conclude about its hydrophilic/oleophilic or hydrophobic/oleophobic properties.

During our investigation we tried to modify the surface energy of different rubber blankets to raise their surface energy and achieve nearly perfect hydrophilic surface. We also studied the stability of achieved modifications, methods for a reverse process and changes on the blanket surface at different stages during the experiments. In this paper some most important results are presented for typical NBR rubber blanket (BLUE) for conventional and EPDM rubber blanket (RED) for UV offset lithographic printing.

2 Research methods

For oxygen plasma treatment of the samples we use lab plasma reactor with a vacuum pump and inductively coupled RF generator at the power of approximately 200 W. Each sample was exposed to oxygen plasma with the neutral atom density of 5x1021 m-3, the electron density of 8x1015 m-3 and the electron temperature of 35000 K for 0, 3, 9, 27, 81, 243 and 729 s. The samples were kept at floating potential that was -15V (Cvelbar, Mozetič).

For the first set of contact angle measurements we used 3 µl drops of distilled water and a CCD camera connected to a computer to get contact angle. Contact angle measurements were performed immediately after treatment and repeated after 3 and 24 hours. At the end we used the test-pen method, too. Test-pen method results were almost the same on all samples, not in correlation with contact angle measurement results and are not presented. We obtain maximal surface free energy change after 27 s and it remains unchanged for 24 h (Golob et al).

For the second set of measurements we used the same samples, treated for 27 s by oxygen plasma under same conditions. We measured contact angles after approximately 24 hours on Krüss DSA 100 apparatus with three liquids polar and non-polar liquids with different characteristics:

•water – (total 72.8 mN/m; disp. 21.8 mN/m; polar 51.0 mN/m), 1μl drop

•diiodomethane – (total 50.8 mN/m; disp. 0 mN/m; polar 0 mN/m), 0.5 μl drop

•formamide – (total 58.0 mN/m; disp. 39.0 mN/m; polar 19.0 mN/m), 1 μl drop.

For calculation of surface free energy we used Wu (Wu), Owens Wendt (OW) and AcidBase theory (AB) methods, supported by Krüss software (Brady, Erbil). Surface free energy data of test liquids were obtained from Krüss database. For each measurement set we performed at least 6 measurements and excluded results with extreme deviation to mean value.

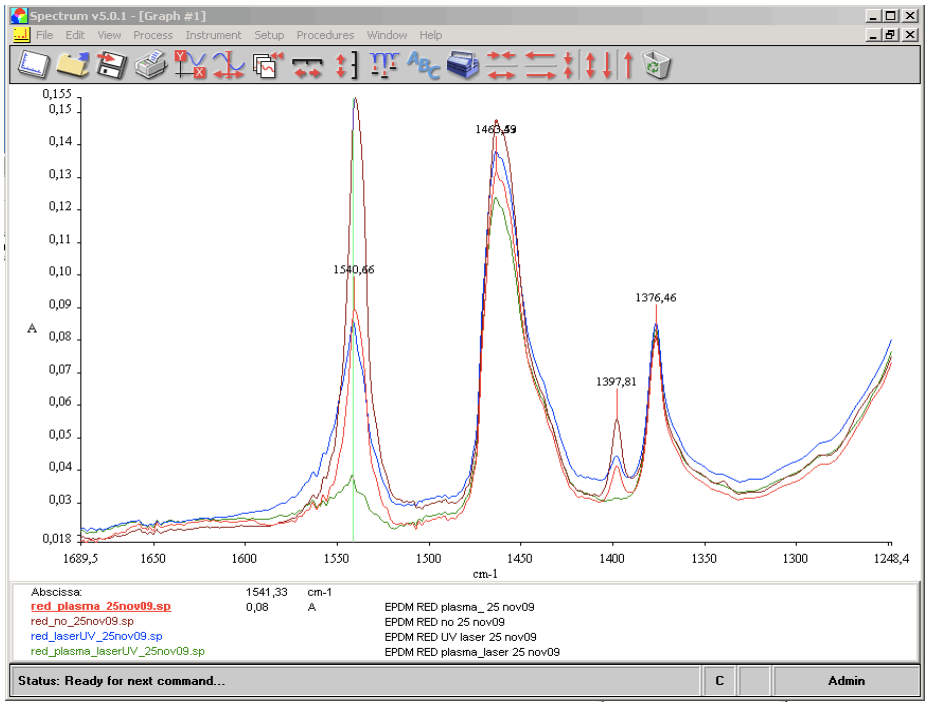

Figure 1: Typical FTIR-ATR spectra of RED rubber blanket sample.

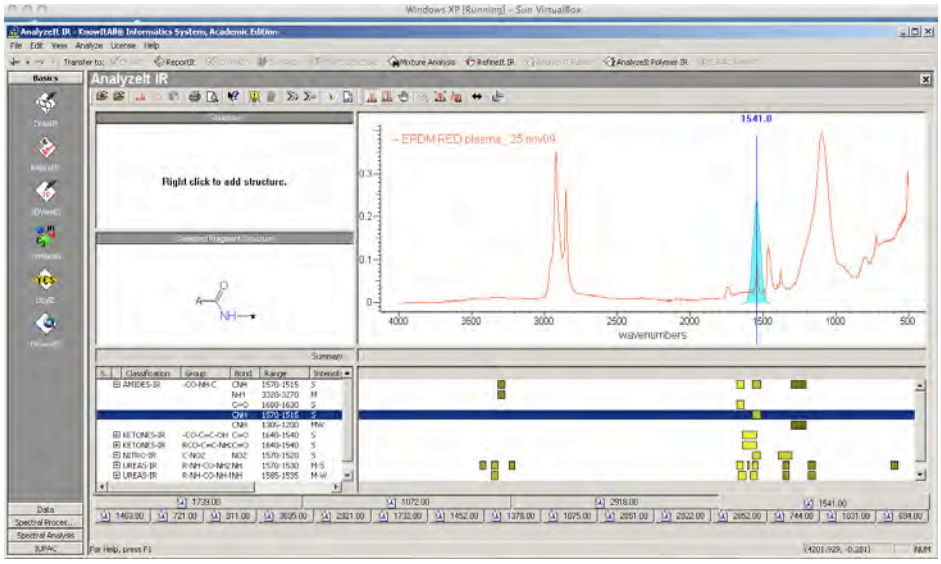

Figure 2: Image of open window in spectra analyzing software KnowItAll.

We used Perkin Elmer FTIR-ATR spectrometer type Spectrum GX1 in mid IR area (wavenumber 500 – 4000 cm^{-1}, 2.5 – 20 μm) to get IR spectra of untreated and plasma treated rubber blanket samples. For each sample we performed 64 scans. Analysis of spectra was performed using KnowItAll software with spectral database to get reliable results.

Typical IR spectra obtained using FTIR-ATR method for RED sample (untreated, oxygen plasma treated, UV laser treated and plasma and UV laser treated) are presented in Figure 1. In Figure 2 a part of spectral analyzing procedure is presented.

3 Results

Contact angle measurements and calculated surface free energy using Owens Wendt, Wu and AcidBase theory method are presented in Table 1 and 2. Calculated surface free energy according to Wu and AcidBase theory, presented in Table 2 are not reliable because of some negative values.

Table 1: Contact angles for different liquids (water – W, diiodomethane – D, formamide – F) of untreated and oxygen plasma treated samples.

	Contact angle (°) untreated			Contact angle (°) plasma 27 s		
Sample	W	D	F	W	D	F
BLUE	100.2	49.9	76.9	52.8	39.5	38.7
RED	132.4	75.3	104.2	66.7	48.3	62.9

Table 2: Surface free energy of untreated and oxygen plasma treated samples (total – T, disperse – D, polar – P, acidbase – AB, acid – A, base – B).

Surface free energy (mN/m)											
	Owens-Wendt			Wu			AcidBase theory				
Sample	T	D	P	T	D	P	T	D	AB	A	B
BLUE untreated	32.73	32.59	0.14	35.01	34.75	0.27	33.66	34.33	-0.67	0.14	0.79
BLUE plasma	50.32	33.46	16.86	52.86	35.42	17.26	39.46	39.86	-0.40	0.01	33.22
RED untreated	21.28	19.70	1.58	19.83	23.41	-3.58	21.48	19.96	1.51	0.48	1.19
RED plasma	40.15	29.34	10.81	43.25	32.12	11.13	31.52	35.22	-3.70	0.14	24.46

Results of BLUE and RED samples are presented in Figures 3 to 6 as a general overview of spectra and zoomed part where noticeable changes during plasma treatment occurred. Characteristic peaks are marked by wavenumber (frequency).

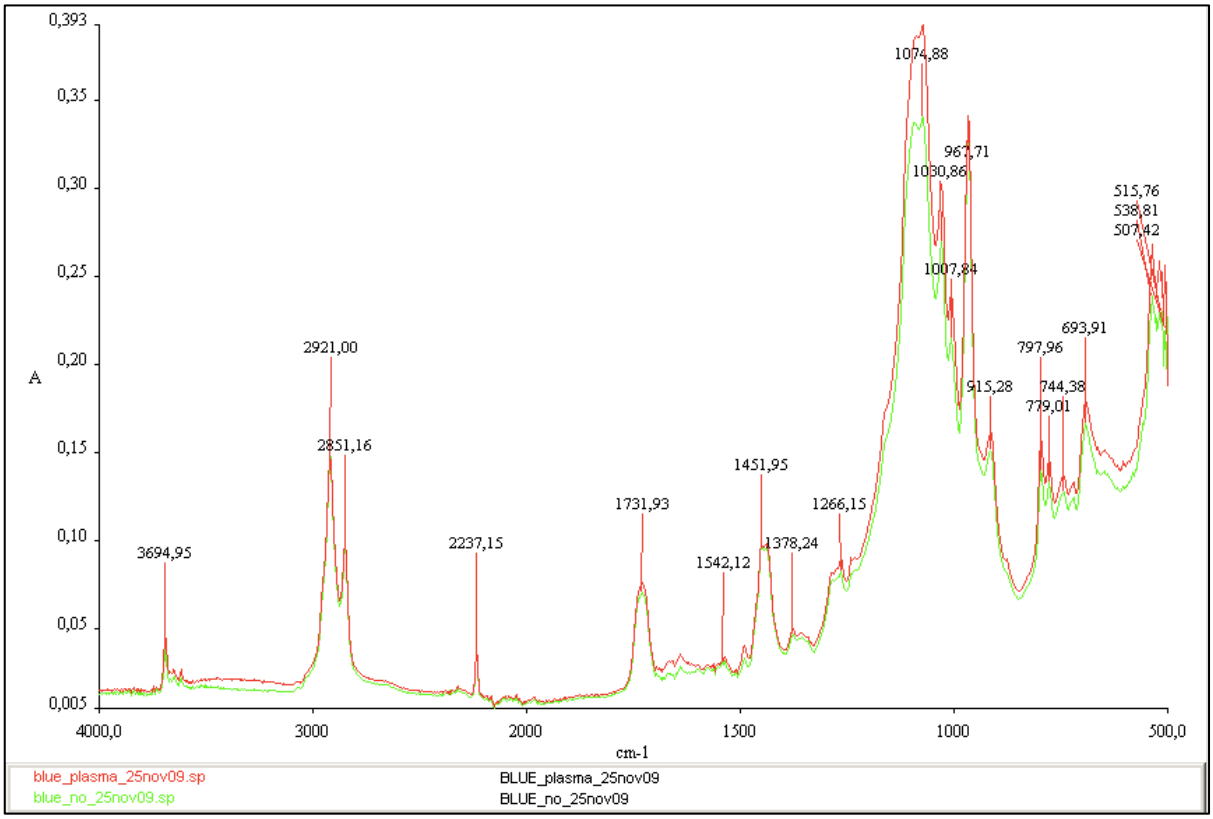

Figure 3: Absorption spectra of untreated and treated BLUE samples.

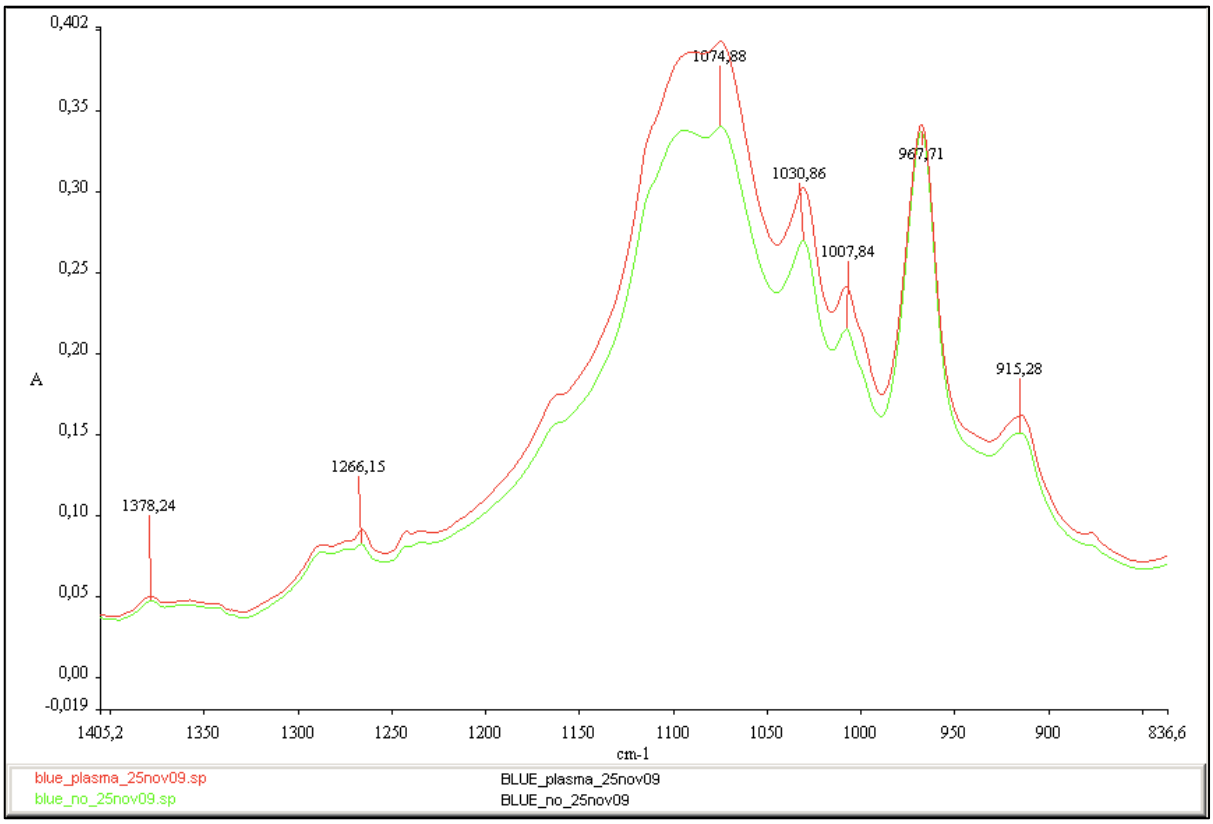

Figure 4: Zoomed part of spectra from Figure 4 for untreated and oxygen plasma treated BLUE sample.

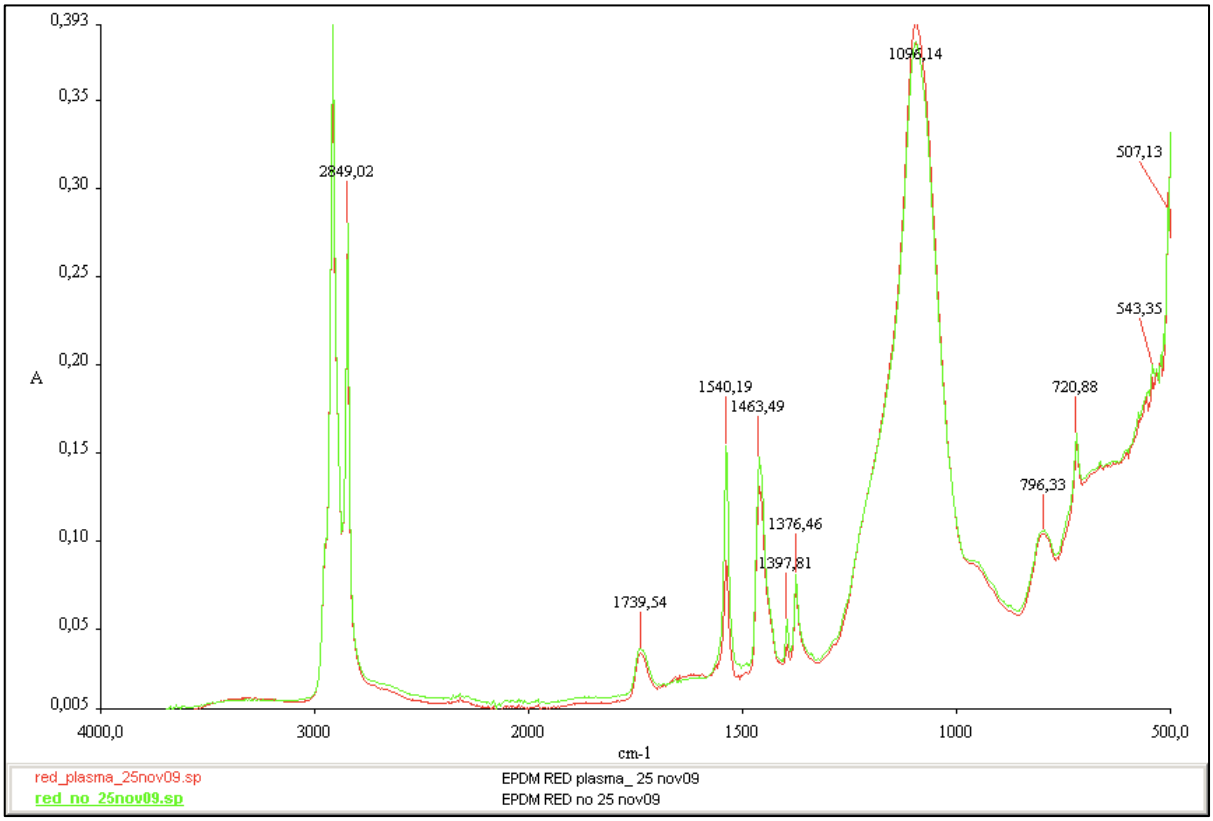

Figure 3: Absorption spectra of untreated and treated RED samples.

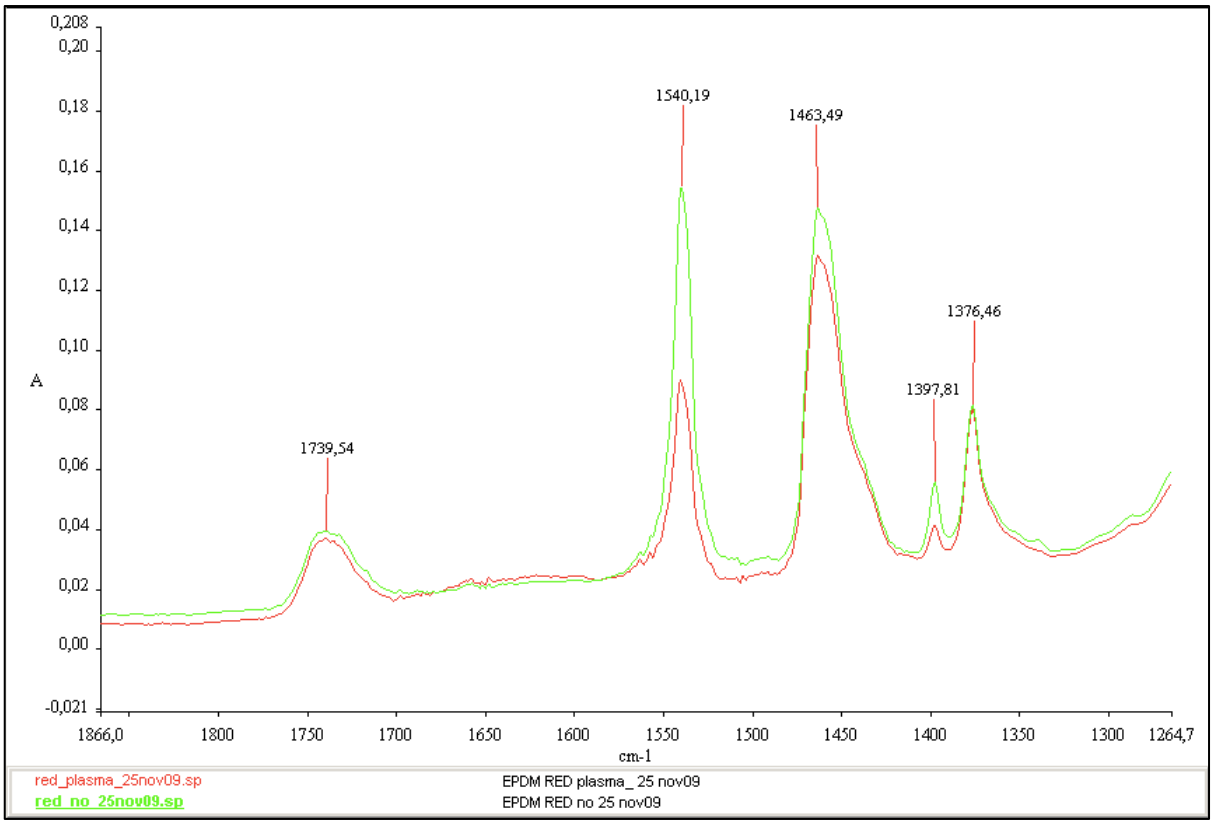

Figure 4: Zoomed part of spectra from Figure 4 for untreated and oxygen plasma treated RED sample.

Significant changes between untreated and plasma treated BLUE samples were achieved at 1074.94 cm^{-1} peak wavenumber. This is characteristic peak for anhydrides (C-O-C), ethers at 1103 cm^{-1} (C-O-C), 5 ring ethers (C-O-C), silicons (Si-O-Si), sulfur (S=O) with strong peaks and some other chemical groups with weak peaks.

Significant changes between untreated and plasma treated RED samples were achieved at 1397.81, 1463.49 and 1540.19 cm^{-1} wavenumber. 1397.81 cm^{-1} is characteristic strong peak for sulfur (SO_2). 1463.49 cm^{-1} is characteristic medium strong peak for many alkanes (CH), amides (N-H) and aromatic (ring) chemical groups and some impurities – water vapor (OH). 1540.19 cm^{-1} is characteristic for amides (CNH), nitro (NO_2) with strong and ureas (NH) with medium peak.

4 Discussion

Rubber consists of ten or more components like one or more polymers, fillers, additives for crosslinking of basic monomer, additives for hardness and elasticity control, pigments and dyes (Salamone). Surface structure was typical for ground finished surface layer, it remained almost unchanged after plasma treatment and obviously there was no significant etching of polymer on surface layer. Stability of the samples hydrophilicity gave us opportunity for contact angle measurements using different liquids after 24 h at another location. After oxygen plasma treatment surface free energy has arisen in all samples.

During the investigation we did not achieve very hydrophilic stage with contact angle near 0^o on our rubber blanket samples. On many other metal and organic materials we achieved super hydrophilic surface in very short time during oxygen plasma treatment.

Results of contact angle measurements and surface energy calculations are not reliable and we have to repeat this part of investigation. Reasons could be in inappropriate handling with equipment, test liquids with characteristics that are not the same as in database, unhomogenity and roughness of rubber blanket surface, differences in air temperature and humidity or some other reason. It is well known from references that different methods for surface free energy give us different results and that some methods are not appropriate for all solid materials. At this stage of investigation we got enough information about influence of oxygen plasma on different types of rubber to continue with measurements of surface free energy using other types of rubber blankets and raw materials like basic polymers and fillers for rubber production.

It is interesting that so called polar BLUE rubber shows us almost no polar part of surface free energy before treatment and non-polar RED rubber has higher amount of polar part compare to BLUE NBR type of rubber blanket sample.

After treatment with oxygen plasma we have achieved higher level of total surface free energy and polarity with BLUE compared to RED rubber. The ratio of surface cleaning effect compared to chemical modification during oxidation process is still unknown. The untreated samples were wiped with ethanol five minutes before measurements and plasma treatment but obviously this treatment was not efficient and therefore we try to determine chemical structure of untreated and plasma treated samples by IR spectra analysis using FTIR-ATR method.

Comparing spectra analysis of BLUE and RED we see that significant changes of spectra peaks are at different wavenumber. At BLUE sample after oxygen plasma treatment amount of chemical groups with bonded oxygen and sulfur were higher (higher peak). At RED sample spectra peaks after plasma treatment were lower, changes occurred on NO_2, SO_2 and other groups without bonded oxygen. There were no additional peaks formed by new chemical groups. In general spectral curve of BLUE sample was positioned slightly higher compared to untreated sample due to higher roughness. At RED sample both spectral curves remain almost at the same level with exception of some peaks.

5 Conclusions

To get more reliable results the analysis of pure basic materials before and after plasma treatment is necessary. We should continue our investigation using typical EPDM, NBR and other types of crude rubber and different fillers to get surface free energy of untreated and plasma treated basic rubber components. After that new set of rubber samples should be prepared for further investigations.

XPS analysis should give us chemical fingerprint of the sample surface. Surface free energy measurements and FTIR-ATR spectra analysis method are not sufficient to determine hydrophilic/hydrophobic or oleophilic/oleophobic character of the surface before and after treatment.

Impact of impurities at the rubber surface layer is still unknown and with repeated series of plasma treatments and defunctionalisation we should get pure surface to perform measurements of surface free energy and chemical analysis.

It can be concluded that oxygen plasma treatment gives us a rubber blanket with new characteristics that open new opportunities for improvements of their characteristics and new functionality of blankets in different printing processes.

Acknowledgements

We would like to thank colleagues from Savatech, Kranj for technical support.

References

Brady, Robert: *Comprehensive Desk Reference of Polymer Characterization and Analysis*, Oxford University Press, 2003, ISBN 0 8412 3665 8.

Cvelbar Uroš, Miran Mozetič: *Method for improving of electrical connection properties of a surface of a product made from a polymer matrix composite*, international patent WO 2006/029642.

Erbil, H. Yildrim: *Surface Chemistry of Solid and Liquid Interfaces*, Blackwell Publishing, 2006, ISBN 1 4051 1968 3.

Gojo, Miroslav; Lovreček, Mladen: *Characterisation of Surfaces on the Offset Printing Plate*, Proceedings of Lectures and Posters, 1st International Symposium of Novelties in Graphics, Ljubljana : Faculty of Natural Sciences and Engineering, 1998. 253-260.

Golob, Gorazd; Mozetič, Miran; Eleršič, Kristina; Junkar, Ita; Đorđević, Dejana; Lovreček, Mladen. *Rubber blanket surface energy modification using oxygen plasma treatment*. 36th International Research Conference iarigai, 13-16 September 2009, Stockholm, Sweden. *Advances in printing and media technology : [book of extended abstracts]*. Stockholm: INNVENTIA AB: International Association of Research Organizations for the Information, Media and Graphic Arts Industries, 2009.

Lovreček, Mladen; Gojo, Miroslav; Dragčević, Krešimir: *Interfacial Characteristics of the Rubber Blanket - Dampening Solution System*, Bristow, J., Anthony (ur.). Leatherhead, Surrey, UK : Pira International, 1999. Str. 370.

Mozetič Miran, Alenka Vesel, Cvelbar Uroš: *Method and device for local functionalization of polymer materials*, international patent WO 2006/130122.

Mozetič, Miran: *Controlled oxidation of organic compounds in oxygen plasma*. Vacuum. [Print ed.], 2003, vol. 71, p. 237-240.

Salamone, J.: *Polymeric Materials Encyclopedia*, CRC Press, Taylor & Francis LLC, 1996, ISBN 9780849324703.

Surface free energy determination of EPDM and NBR rubber blankets

Gorazd Golob[1], Mladen Lovreček[2], Miran Mozetič[3],
Odon Planinšek[4], Marie Kaplanová[5]
[1]University of Ljubljana, Faculty of Natural Sciences and Engineering
[2]University of Zagreb, Faculty of Graphic Arts
[3]"Jožef Stefan" Institute, Ljubljana
[4]University of Ljubljana, Faculty of Pharmacy
[5]University of Pardubice, Faculty of Chemical technology

Abstract:

Surface free energy may be defined as the excess energy at the surface of the material compared to the bulk. For liquids the surface tension (N/m) and surface energy density (J/m^2) are identical. For solids, especially polymers with low surface free energy, direct measurements are not possible. The most convenient method is calculations based on contact angle measurements of sessile drop using different liquids. During our research work we use polar and non-polar liquids: water, diiodomethane, formamide and ethyleneglycol.

For surface free energy measurements we use Krüss DSA100 apparatus with original software and database of test liquids for calculations. Additional measurements have been done using other simple devices and improved calculation methods.

For calculations of surface free energy we use Owens-Wendt method (geometric mean equation), Wu method (harmonic mean equation) and so-called "acid-base theory of surfaces", developed by Van Oss, Chaudury and Good with the help of the acid-base model according to Lewis. Using those equations we get values for total, disperse and polar (acid and base) part of total surface free energy of rubber blankets. First experience with contact angle measurements on rough and heterogeneous surface using different calculation methods show us significant differences in obtained results. Comparing and improving wide applied methods we are able to achieve best possible results in surface free energy determination of rubber blankets, according to our knowledge.

Keywords*: surface free energy, Owens-Wendt, Wu, Van Oss acid-base, rubber blanket*

1 INTRODUCTION

The aim of our investigation is study of surface free energy of rubber blankets used in offset planographic printing as ink transfer media during printing process. Optimal printing conditions are achieved, under other conditions, when surface free energy of rubber blanket is higher comparing to ink and print areas of printing plate and lower of print substrate. Modification of blanket surface free energy using low pressure gaseous plasma and laser beam for discrete defunctionalization should give us a blanket with improved properties and as a final goal we intend to merge functionality of printing forme with rubber blanket.

Surface free energy may be defined as the excess energy at the surface of the material compared to the bulk. For liquids the surface tension (N/m) and surface energy density (J/m^2) are identical. For solids, especially polymers with low surface free energy, direct measurements are not possible, therefore calculations using Young's and other equations based on contact angle measurements of sessile drop should give us appropriate results.

During our investigation we used two sets of four rubber blanket samples and we have repeated our measurements for several times. Obtained results have relatively small variance within a set of measurements but significant deviance between them, depending on measurement device, time, sample preparation, implementation of the method or some other reasons.

We try to exclude some factors with strong influence at the contact angle of sessile drop measurements, like surface electric charge, using air ionizator but without great success. Additional method using measurements of residue ink at the blanket surface after splitting gives us confirmation of other measurements.

2 EXPERIMENTAL

In the experimental phase, four different blanket samples were used:
- EPDM rubber for UV printing, non-polar, silica filler (RED),
- EPDM rubber for UV printing, non-polar, soot/carbon conductive filler (BLACK),
- NBR/TM (90/10) blend rubber for conventional printing, polar, silica filler, stronger cured (BLUE),
- NBR/TM (90/10) blend rubber for conventional printing, polar, silica filler (LIGHT BLUE).

All rubber blankets are commercially available products from Savatech, Kranj. We perform a lot of different measurements of untreated and treated samples, therefore we spend them during eight months and obtain a new set of samples (marked old and new). At the surface of grinded blankets some traces of rubber dust remain, so we clean samples with ethanol and wipe the surface with paper tissue at least 15 minutes before measurement.

We use high-end Krüss DSA100 apparatus (Ljubljana) with software and test liquids database for calculations and as alternative simple apparatus with manual syringe (Pardubice) and proprietary software for contact angle measurement and calculations. Polar and non-polar liquids were used:
- water (total 72.8 mN/m; disp. 21.8 mN/m; polar 51.0 mN/m, acid 25.5 mN/m, base 25.5 mN/m),
- diiodomethane (total 50.8 mN/m; disp. 50.8 mN/m; polar 0 mN/m, acid 0.0 mN/m, base 0.0 mN/m),
- formamide (total 58.0 mN/m; disp. 39.0 mN/m; polar 19.0 mN/m, acid 2.30 mN/m, base 39.6 mN/m),
- ethylene glycol (total 48.0 mN/m; disp. 29.0 mN/m; polar 19.0 mN/m, acid 1.92 mN/m, base 47.0 mN/m).

All of the theories and methods start with the Young (1) and Young-Dupre (2) equation, relating contact angle to work of adhesion:

$$\gamma_{SV} - \gamma_{SL} = \gamma_{LV} \cos\theta, \quad (1)$$

$$W_a = \gamma_{LV} (1 + \cos\theta), \quad (2)$$

where γ_{SV} is surface energy of solid-vapour, γ_{SL} is surface energy of solid-liquid, γ_{LV} is surface energy of liquid-vapour and W_a (or W_{SL}) is the work of the adhesion.

Methods for calculations of surface free energy, used at our investigation:
- Owens-Wendt method (geometric mean equation),
- Wu method (harmonic mean equation),
- Acid-Base calculations by Van Oss, Chaudury and Good with the help of the acid-base model according to Lewis (geometric mean equation).

Measurements for BLUE new and RED new has been performed using additional treatment of the samples with ionizator Conrad model 02/05 (power 3W, ion emission > $1\times 10^3/cm^3$) for 60 s at the distance of 10 mm.

As a confirmation of the method based on sessile drop contact angle measurements and calculations of surface free energy we used the original method based on measurements of the amount of remaining ink on the rubber samples after splitting a drop of ink between flat rubber and paper surfaces (Figure 1).

Figure 1: Process of weighing, splitting of flexo printing ink droplet and projection of splited droplet at the screen to control the experiment (method of M. Kaplanová).

3 RESULTS

Mean values from 3 to 10 measurements of contact angle are presented in Table 1. The differences are presented in Figure 2 and Figure 3.

Table 1: Contact angles for different test liquids, measured in Ljubljana (L) and in Pardubice (P).

Sample	Contact angle (°)							
	Water		Diiodomethane		Formamide		Ethylene glycol	
	L	P	L	P	L	P	L	P
BLUE new	122.4	120.1	72.3	67.0	109.0	113.7	91.3	92.8
BLUE old	115.5	112.5	42.0	55.7	90.7	99.6	85.9	86.7
LIGHT BLUE new	122.5	124.9	61.2	77.8	84.5	113.6	87.1	94.2
LIGHT BLUE old	121.5	127.3	83.8	81.6	107.9	117.2	92.2	109.4
RED new	127.3	130.2	78.3	72.5	114.3	109.8	102.2	108.9
RED old	134.5	148.4	74.8	77.2	117.9	118.3	98.7	105.5
BLACK new	128.7	132.4	85.9	80.3	117.8	109.9	103.4	108.6
BLACK old	125.7	132.0	71.0	71.0	106.0	108.9	87.8	99.3

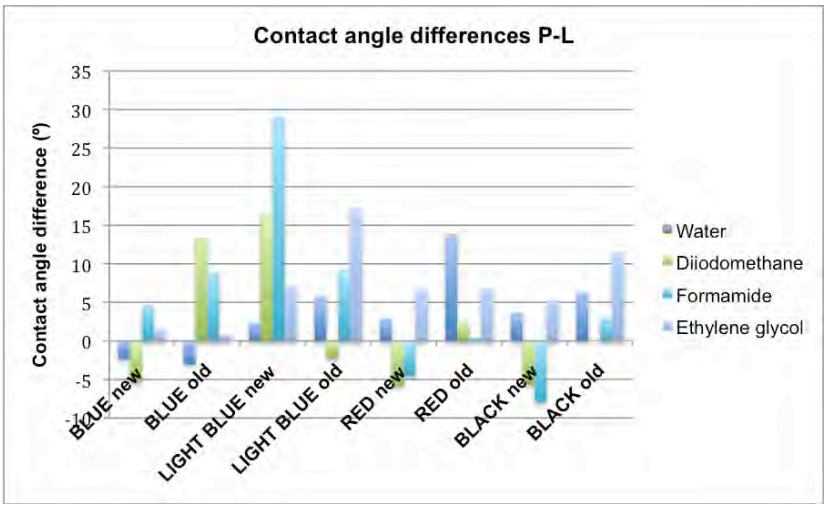

Figure 2: Contact angle differences for different test liquids performed in Pardubice and Ljubljana.

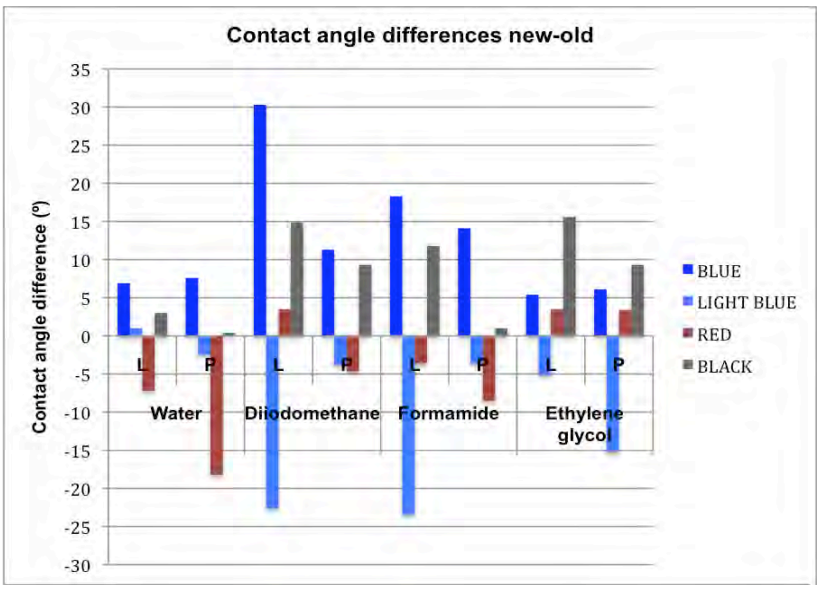

Figure 3: Contact angle differences between new and old samples for different test liquids.

Results of surface free energy calculations, performed on both locations, based on same database of test liquids, using Owens-Wendt, Wu and Van Oss Acid-Base methods are presented in Table 2 and in Figure 4.

Table 2: Surface free energy of rubber blanket samples, calculated from data in Table 1.

Sample		Surface free energy (mN/m)								
		Owens-Wendt			Wu			Acid-Base		
		Total	Disp.	Polar	Total	Disp.	Polar	Total	Disp.	Polar
BLUE new	L	19.72	19.35	0.37	21.4	23.94	-2.55	20.94	20.61	0.33
BLUE old		35.72	34.42	1.29	35.31	38.79	-3.49	39.07	38.10	0.98
LIGHT BLUE new		31.58	30.34	1.24	28.45	30.52	-2.07	28.3	28.19	0.11
LIGHT BLUE old		14.95	14.94	0.01	17.98	19.11	-1.13	14.95	14.93	0.01
RED new		16.31	15.75	0.56	18.23	21.46	-3.24	18.02	17.70	0.32
RED old		20.22	18.41	1.81	19.11	22.81	-3.69	21.05	19.17	1.88
BLACK new		13.00	12.72	0.29	15.54	18.24	-2.69	14.10	13.93	0.17
BLACK old		22.66	21.85	0.81	22.3	24.68	-2.38	21.99	21.33	0.66
BLUE new	P	20.04	19.66	0.38	22.75	26.09	-3.34	22.52	23.22	-0.70
BLUE old		26.00	25.81	0.20	28.82	31.68	-2.86	28.93	30.07	-1.14
LIGHT BLUE new		16.93	16.61	0.33	18.96	21.47	-2.51	17.95	17.65	0.31
LIGHT BLUE old		13.65	13.26	0.40	16.58	20.15	-3.57	15.57	16.20	-0.64
RED new		19.89	18.42	1.47	20.26	24.44	-4.18	22.40	21.28	1.12
RED old		23.12	18.96	4.17	35.00	30.00	5.00	21.58	18.25	3.33
BLACK new		17.13	16.01	1.11	17.53	21.00	-3.47	18.32	17.21	1.11
BLACK old		22.84	20.98	1.86	21.26	24.90	-3.64	23.58	21.71	1.86

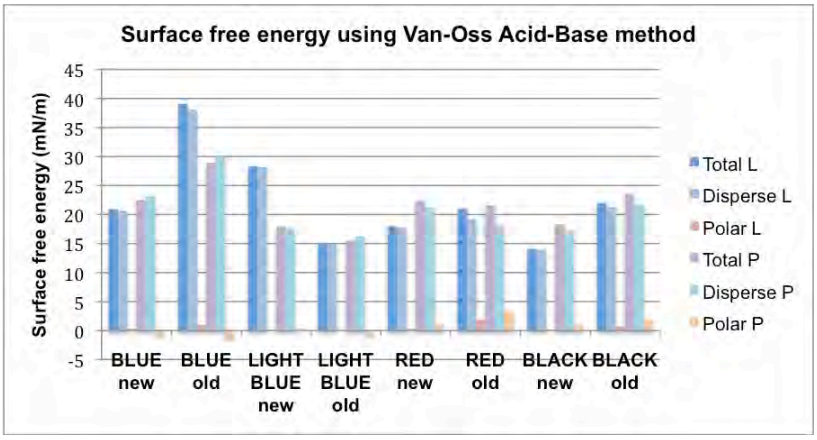

Figure 4: Presentation of surface free energy calculation results from Table2.

Contact angles of measurements without and with ionizator are presented in Table 3 for BLUE new and RED new samples only.

Table 3: Results of contact angle measurements without and with ionizator (15 s).

Sample	Contact angle (°)							
	Water		Diiodomethane		Formamide		Ethylene glycol	
	no ioniz.	ionizator	no ioniz.	ionizator	no ioniz.	ionizator	no ioniz.	ionizator
BLUE new	124.2	123.6	54.2	56.9	100.2	99.5	86.4	89.2
RED new	131.9	132.3	84.9	83.9	117.7	116.8	103.2	105.3

Ink transfer factor was calculated according to amount of flexo printing ink at the rubber blanket sample after splitting from paper substrate. Results are given in Table 4.

Table 4: Ink transfer factor.

Sample	Ink transfer (%)
BLUE new	29.8
BLUE old	28.9
LIGHT BLUE new	30.1
LIGHT BLUE old	27.6
RED new	24.5
RED old	29.3
BLACK new	33.6
BLACK old	21.6

4 DISCUSSION

Results of contact angle measurements are not reliable, especially for BLUE old and for LIGHT BLUE new samples, where significant differences of measurements between two labs occurred. It seems that BLUE new sample was somehow contaminated so we have to repeat a part of measurements in Ljubljana, because with first sample at the beginning of this part of investigation in Ljubljana (not published) we got contact angle near 0º for diiodomethane. Other measurements before mentioned set of measurements (old) and after it (new), including measurements in Table 3, gave us different results in most cases closer to results from Pardubice. We assume that reasons for significant deviations of the results are mostly due to characteristics and preparation of the samples.

Calculated surface free energy therefore shows us significant differences for BLUE old and LIGHT BLUE new samples comparing results from Ljubljana and Pardubice. With exception of LIGHT BLUE we got lower values of surface free energy for new samples, probably because of ageing of material, chemical changes at the surface, adsorption of impurities or blooming residues of some rubber components.

Different calculation methods for determination of surface free energy give us different results and in some cases the values are even negative. All known and used methods are useful under ideal lab conditions (air temperature, humidity), test liquids with characteristics according to used database and with perfect, smooth, flat, homogeneous surface. Our samples are rough, non-homogeneous, they bend and swell in contact with some liquids, lab conditions were not close to ideal in all cases ... According to other authors each method has advantages or disadvantages for determination of surface free energy for a set of materials like polymers, minerals or metals. There is no unique opinion and prove for the use of some known methods for elastomers, so according to our knowledge and experience we decide to use Van-Oss Acid-Base method as most appropriate for presentation of our results. [1, 2, 3, 4, 5]

Treatment of the samples with ionizator gave us no significant advantage for contact angle measurements.

Measurements of ink transfer factor with higher percentage for new samples (with exception for RED new) gave us a confirmation of lower surface free energy for BLUE new, LIGHT BLUE new and BLACK new samples. [6]

5 CONCLUSIONS

During our investigation we recognized many difficulties of rubber blanket samples. Convenient methods for contact angle measurements and surface free energy calculations, suitable for perfect samples are not the best for porous, non-homogeneous, rough rubber samples and should be improved.

Preparation of rubber blanket samples is very important and should be controlled to get more reliable results. Measurements of roughness should be included into investigation to determine suitable model (Wenzel for droplet in contact with rough surface or Cassie–Baxter model for droplet on underlay of air bubbles in pores) for improved calculation method of surface free energy. Chemical analysis (FTIR-ATR and XPS) of the surface should give us information about impurities and chemical composition of the surface.

Statistical analysis of variance (ANOVA) and other statistical tools to compare experimental data from all measurements for several conditions simultaneously should give us more useful results with high statistical probability.

6 REFERENCES

1 Brady, Robert: *Comprehensive Desk Reference of Polymer Characterization and Analysis*, Oxford University Press, 2003, ISBN 0 8412 3665 8.

2 Erbil, H. Yildrim: *Surface Chemistry of Solid and Liquid Interfaces*, Blackwell Publishing, 2006, ISBN 1 4051 1968 3.

3 Oxsher, Allison; Robertshaw, Virginia; Rulison, Christopher: *Surface Energy Characterization and Adhesion Properties of High Viscosity Ink Pastes*, Application Note #239e, Krüss.

4 Verplanck, Nicolas, et al.: *Wettability Switching Techniques on Superhydrophobic Surfaces*, Nanoscale Res. Lett. (2007).

5 Lovreček, Mladen; Gojo, Miroslav; Dragčević, Krešimir: *Interfacial Characteristics of the Rubber Blanket - Dampening Solution System*, Bristow, J., Anthony (ur.). Leatherhead, Surrey, UK : Pira International, 1999.

6 Hyun Wook Kang, et al.: *LIQUID TRANSFER EXPERIMENT FOR MICRO-GRAVURE-OFFSET PRINTING DEPENDING ON THE SURFACE CONTACT ANGLE*, APCOT 2008.

ACKNOWLEDGEMENT

We would like to thank coleagues from Savatech, Kranj for technical support and cooperation.

CORRESPONDING AUTHOR

Gorazd Golob MSc
University of Ljubljana
Faculty of Natural Sciences and Engineering
Snežniška 5
1000 Ljubljana

gorazd.golob@ntf.uni-lj.si

Surface and Structural Properties of EPDM and NBR Rubber Blankets

Gorazd Golob
University of Ljubljana, Faculty of Natural Sciences and Engineering
gorazd.golob@ntf.uni-lj.si

Mladen Lovreček
University of Zagreb, Faculty of Graphic Arts
mlovrece@grf.hr

Miran Mozetič
"Jožef Stefan" Institute, Ljubljana
miran.mozetic@guest.arnes.si

Alenka Vesel
"Jožef Stefan" Institute, Ljubljana
alenka.vesel@guest.arnes.si

Odon Planinšek
University of Ljubljana, Faculty of Pharmacy
Odon.Planinsek@ffa.uni-lj.si

Marta Klanjšek Gunde
National Institute of Chemistry Slovenia, Ljubljana
marta.k.gunde@KI.si

Vilibald Bukošek
University of Ljubljana, Faculty of Natural Sciences and Engineering
vilibald.bukosek@a.ntf.uni-lj.si

1 Introduction

During our research work we studied surface properties of lithographic offset rubber blankets based on polar NBR/TM and non-polar EPDM elastomer blends, modification of surface free energy using oxygen plasma treatment and defunctionalization of surface properties using IR and UV high power laser devices.

We studied surface properties of untreated and plasma or laser treated elastomer material as a basis for the improvements and understanding of new functionality of rubber blankets with discrete hydrophilic/oleophobic and hydrophobic/oleophilic areas. First results of plasma treatment were already presented at IARIGAI and other international research conferences (Golob et al, IARIGAI 2009, SGA 2009, Tiskarstvo 2010). Results of defunctionalization or modification of blanket surface properties using proper IR or UV laser are presented in this paper.

2 Research methods

Our investigation included surface free energy determination using contact angle measurements with different liquids, chemical analysis of the surface using FTIR-ATR spectroscopy and dynamic mechanical (structural) analysis of elastomer samples to find correlations between surface and bulk properties of rubber samples. According to our experience during investigation we performed sample treatment and measurements within 24 hours to avoid degradation of achieved surface changes. Presented results are mean value of 10 or more measurements of contact angles, IR spectra were measured at least twice for each sample. Dynamic mechanical analysis (DMA) were performed only once per sample.

2.1 Materials

Four different blankets, commercial products of Savatech, Kranj, were used:

- Advantage UV Red - EPDM rubber for UV printing, non-polar, silica filler (RED)
- Advantage UV Black - EPDM rubber for UV printing, non-polar, soot/carbon conductive filler (BLACK)
- Advantage DUAL - NBR/TM (90/10) blend rubber for conventional printing, polar, silica filler, stronger cured (BLUE)
- Advantage Expression - NBR/TM (90/10) blend rubber for conventional printing, polar, silica filler (LIGHT BLUE)

In this abstract only results of two typical rubber blankets, RED and BLUE, are presented in detail. For DMA, special rubber plates consisting of blanket surface layer only, were prepared.

2.2 Oxygen plasma treatment

For oxygen plasma treatment (Mozetič, 2003, 2006) of the samples we used a lab plasma reactor with a vacuum pump and an inductively coupled RF generator at the power of approximately 200 W. Each sample was exposed to oxygen plasma with the neutral atom density of $5x10^{21}$ m^{-3}, the electron density of $8x10^{15}$ m^{-3} and the electron temperature of 35 000 K for 27 s. The samples were kept at floating potential of -15V.

2.3 Defunctionalization by laser treatment

Defunctionalization of oxydized hydrophilic rubber surface, described in literature, is achieved with warming at high temperature for long time. In our case our intention was to get hydrophobic stage on different types of plasma treated rubbers using proper laser source for heating.

Professional IR laser (1050 nm) device, built by LPKF for marking, ablation and cutting systems with power from 1 W to 12 W in pulsed or CW mode gave us good results on all samples with exception of BLACK sample, where strong ablation occurred. High power UV laser (355 nm) in range from 0.17 W to 3.80 W gave us acceptable results, but different comparing to IR laser.

2.4 Surface free energy

During most of our research work we used Young and other equations based on contact angle measurements of sessile drop with polar and non-polar liquids: water, diiodomethane and formamide. For calculations of surface free energy we used Owens-Wendt method (geometric mean equation), Wu method (harmonic mean equation) and acid-base calculation by Lewis (Erbil, 2006).

For surface free energy measurements we used Krüss DSA100 apparatus with software and test liquids database for calculations.

2.5 FTIR-ATR Spectrometry

FTIR-ATR (Fourier Transform Infrared – Attenuated Total Reflectance) spectroscopy is an established method for analysis of solids and other samples. In ATR, the sample is placed in contact with a high refractive index crystal. The IR beam enters the crystal and rays at or beyond a critical angle to the sample interface are reflected. The beam penetrates into the sample up to a few μm, most of reflection is from the surface layer of the sample. Typical peaks of absorption spectra give us information of chemical elements, chemical groups or bonds at the surface.

We used Perkin Elmer FTIR-ATR spectrometer type Spectrum GX1 in mid IR area (wavenumber 500 – 4000 cm^{-1}) to get IR spectra of untreated and treated samples. Analysis of spectra was performed using KnowItAll software with spectral database.

2.6 Dynamic mechanical analysis

T_g (glass transition temperature) is a property of only the amorphous portion of a semi-crystalline solid depends on the cooling rate, molecular weight distribution and could be influenced by additives. At a low temperature the amorphous regions of a polymer are in the glassy state. If the polymer is heated the molecules can start to wiggle around and polymer reach its rubbery state. Tan δ is a measure of elastomer dampening and ratio of loss to storage modulus (Brady, 2003).

We used TA Instruments Q800 DMA (Dynamic Mechanical Analyzer) with GCA (Gas Cooling Accessory) for cooling up to -80 ºC for measurements of T_g, tan δ and other bulk material properties.

3 Results

Results of surface free energy (total, disperse and polar part) calculated using Owen Wendt method, are presented in Figure 1.

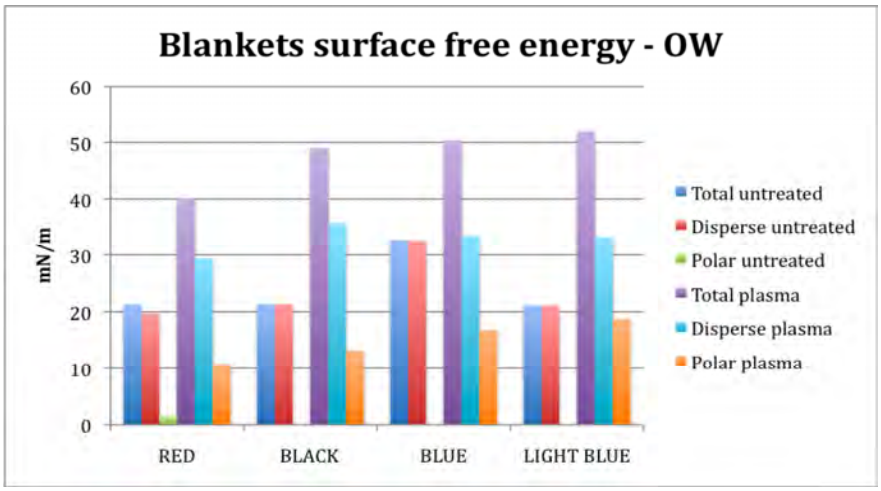

Figure 1: Surface free energy of rubber blankets with their polar and disperse parts.

Figure 2 shows us contact angles for water of untreated, oxygen plasma treated and laser treated rubber blanket for all four samples.

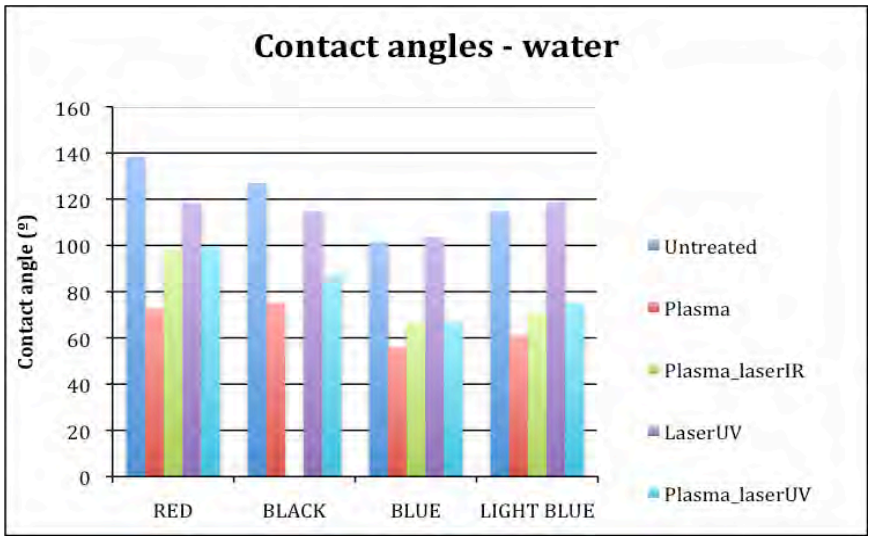

Figure 2: Contact angles of untreated, plasma and laser treated rubber blanket samples.

Figures 3, 4 and 5 show us FTIR ATR absorption spectra of untreated, plasma and laser treated RED samples.

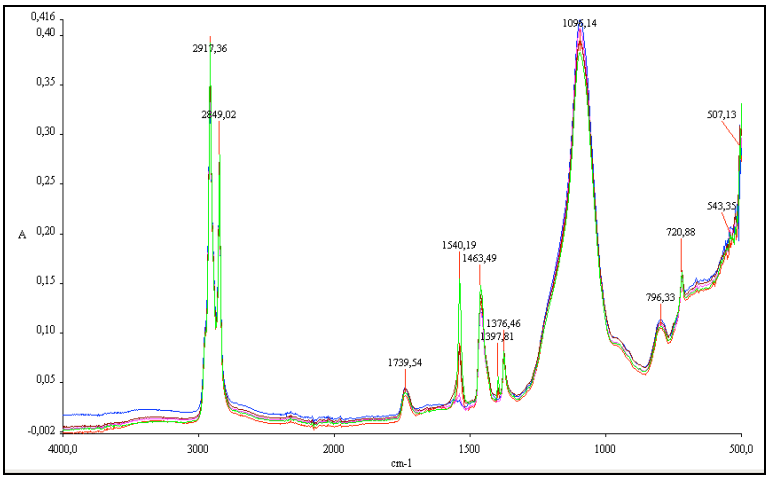

Figure 3: Absorption spectra of RED rubber blanket spectra (green – no treatment, red – oxygen plasma treatment, blue – oxygen plasma and IR laser treatment, violet – oxygen plasma and UV laser treatment, brown – UV laser treatment).

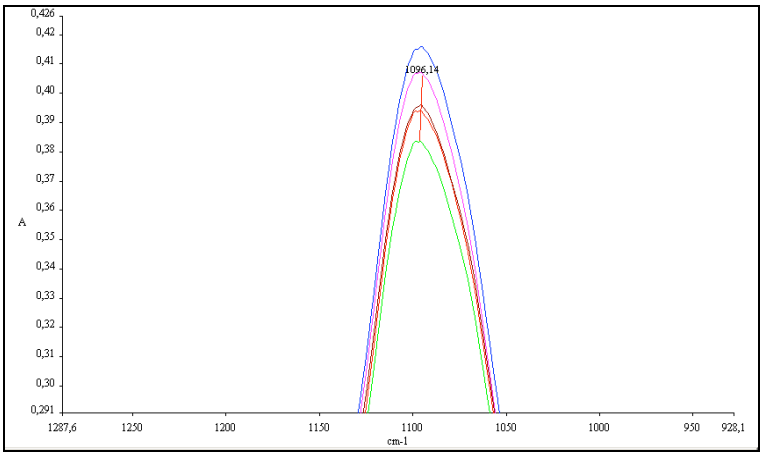

Figure 4: Zoomed part of absorption spectra of RED rubber blanket spectra with significant peak at 1096.14 cm^{-1}.

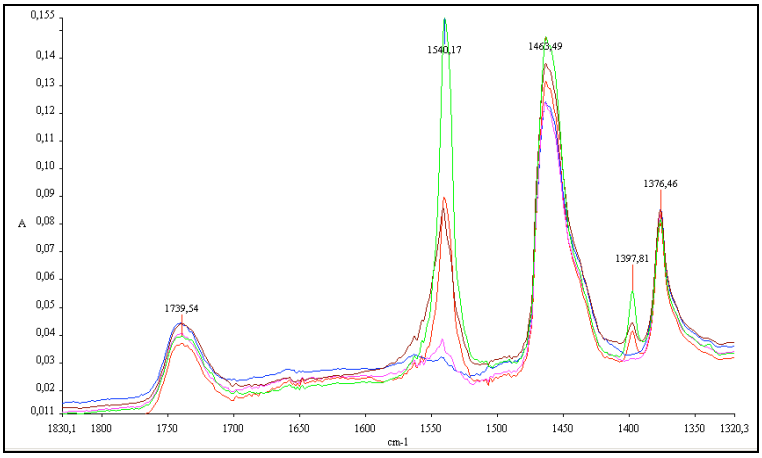

Figure 5: Zoomed part of absorption spectra of RED rubber blanket spectra with significant peaks at 1397.81 cm^{-1}, 1463.49 cm^{-1} and 1540.17 cm^{-1}.

Significant changes between untreated and plasma treated RED samples were achieved at 1096.14, 1397.81, 1463.49 and 1540.19 cm^{-1}.

1096.14 cm^{-1} is characteristic strong peak for alcohols (C-O), anhydrides (C-O-C), ethers (C-O-C), silicons (Si-Ph) and medium strong peak for sulfur (C=S). At this peak lowest absorption is achieved for untreated sample and highest for oxygen plasma combined with IR laser treated sample.

1397.81 cm^{-1} is characteristic strong peak for sulfur (SO_2). 1463.49 cm^{-1} is characteristic medium strong peak for many alkanes (CH), amides (N-H), aromatic (ring) chemical groups and some impurities – water vapor (OH). 1540.19 cm^{-1} is characteristic for amides (CNH), nitro (NO_2) groups with strong and ureas (NH) with medium peak. At this peaks the highest absorption was achieved at untreated samples and lowest at plasma combined with IR or UV laser treated samples.

Figures 6 and 7 show us spectra of BLUE samples after same treatment with oxygen plasma, IR and UV lasers.

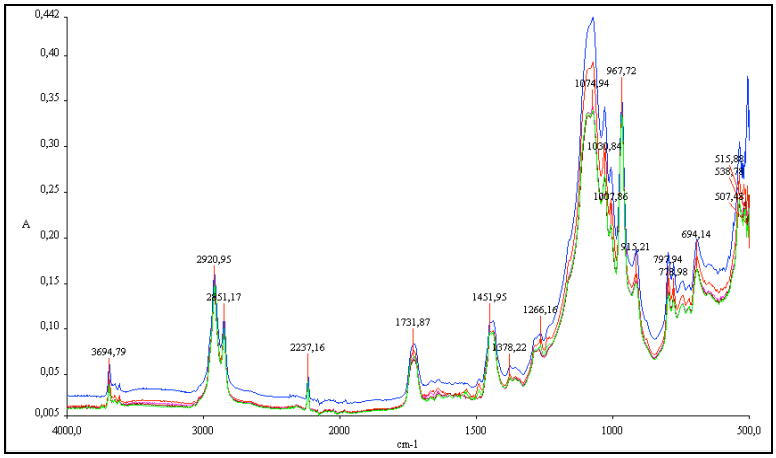

Figure 6: Absorption spectra of BLUE rubber blanket spectra (green – no treatment, red – oxygen plasma treatment, blue – oxygen plasma and IR laser treatment, violet – oxygen plasma and UV laser treatment, brown – UV laser treatment).

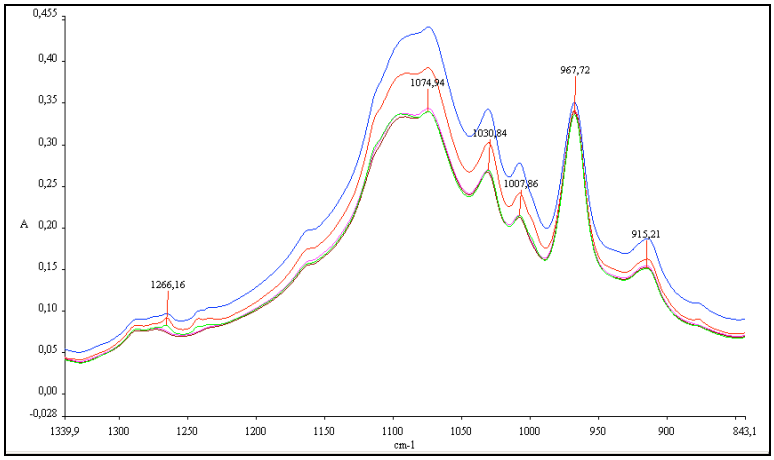

Figure 7: Zoomed part of absorption spectra of BLUE rubber blanket spectra with significant peak at 1074.94 cm^{-1}.

Significant changes between untreated and plasma treated BLUE samples were achieved at 1074.94 cm^{-1}. This is characteristic peak for anhydrides (C-O-C), ethers at 1103 cm^{-1} (C-O-C), 5 ring ethers (C-O-C), silicons (Si-O-Si), sulfur (S=O) with strong peaks and some other chemical groups with weak peaks. Highest absorption is achieved at oxygen plasma treated and oxygen plasma treated combined with IR laser treated samples.

Figures 8 and 9 show us results of dynamic mechanical analysis.

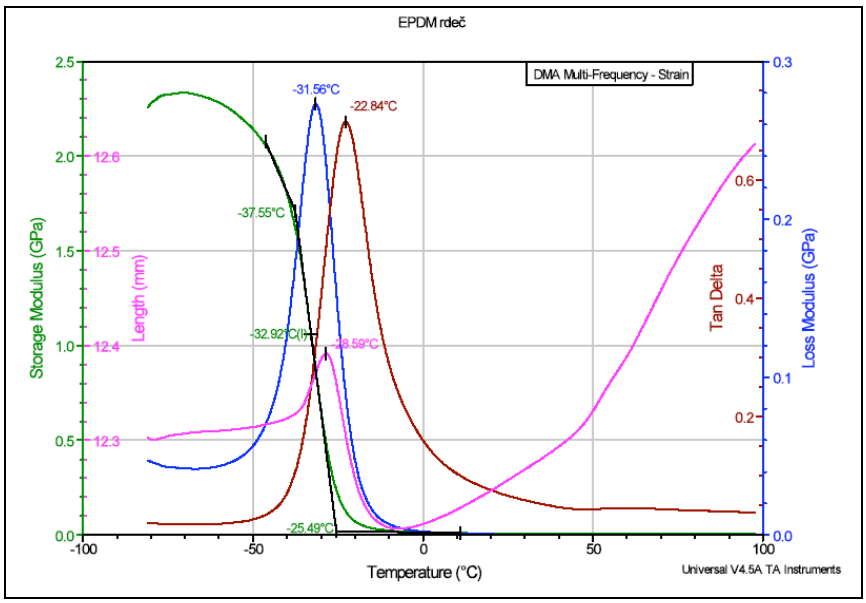

Figure 8: DMA analysis of RED sample, indicating T_g = -32.92 ºC and tan δ with one peak at -22.84 ºC.

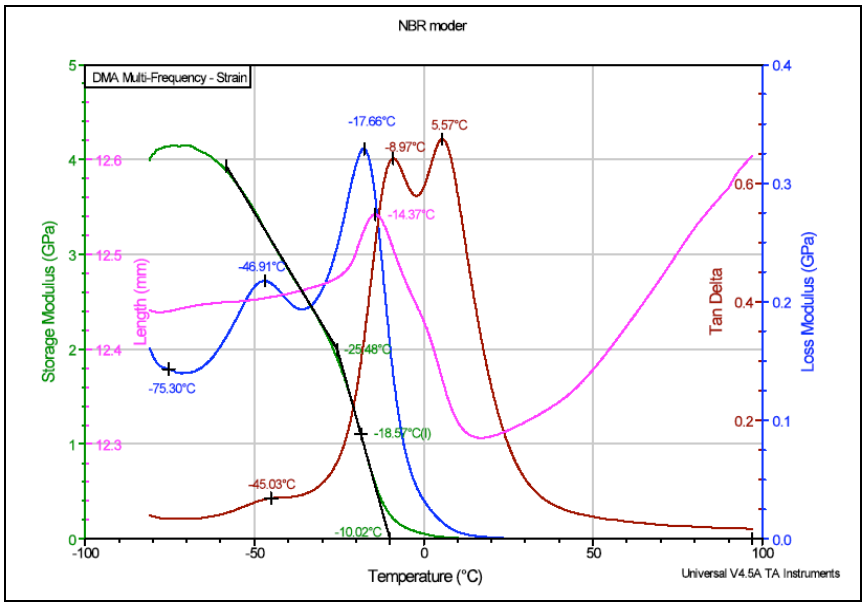

Figure 8: DMA analysis of BLUE sample, indicating T_g = -18.75 ºC and tan δ with two peaks at -8.97 ºC and 5.57 ºC.

4 Conclusions

After treatment with oxygen plasma we achieved higher level of total surface free energy and polarity with BLUE compared to RED rubber. The ratio of surface cleaning effect compared to chemical modification during oxidation process is still unknown but it seems that surface cleaning or ablation effect using oxygen plasma has stronger impact on surface free energy compared to oxidation. To avoid influence of impurities at the surface of untreated samples they were wiped with ethanol five minutes

before measurements and/or plasma treatment but obviously this treatment was not enough efficient comparing to plasma treatment. Contact angle measurement and surface free energy calculation of untreated samples compared to oxygen plasma treated samples show us significant differences between samples. After additional IR and UV laser treatment of the same the values of surface free energy did not return to the former state of untreated samples, as we expected. We are able to reach about half of water contact angle value differences only at RED sample. Treatment using only UV laser gives us lower contact angle for water at RED and BLACK samples, but slightly higher for BLUE and LIGHT BLUE samples. Obviously UV laser treatment gives us different results for EPDM and NBR types of rubber. We intend to continue our research of plasma and laser treatment of rubber blanket surface in the future to find out their highest possible differences of surface free energy and polarity.

Surface free energy measurements and FTIR-ATR spectra measurement and analysis of chemical structure are not sufficient to determine hydrophilic/hydrophobic or oleophilic/oleophobic character of the surface before and after oxygen plasma and/or IR or UV laser treatment. Comparing spectra analysis of BLUE and RED we see that significant changes of spectra peaks are at different wavenumber. At BLUE sample after oxygen plasma treatment, amount of chemical groups with bonded oxygen and sulfur were higher (higher peak). At RED sample spectra peaks after plasma treatment were lower, changes occurred on NO2, SO2 with bonded oxygen and other chemical groups without oxygen. There were no additional peaks formed by new chemical groups. In general spectral curve of BLUE and RED samples treated with oxygen plasma and IR laser was positioned slightly higher compared to untreated sample perhaps due to higher roughness of treated samples. Apparently chemical changes during plasma and laser treatment were not significant but they are different for EPDM and NBR type of rubber. During our further investigation we will try to find out other possible reasons for significant changes of surface free energy and polarity after plasma treatment like roughness, porosity and heterogeneous composition of the surface.

DMA analysis is a method for material bulk analysis. It gives us opportunity to compare surface properties with internal structure of rubber blankets, determined by glass transition temperature and dampening. Glass transition temperature difference between RED and BLUE samples gives us basic information about macromolecular structure of both elastomers. Tan δ with double peak at BLUE sample confirmed that a blend of two crude rubbers is a basic raw material in this case.

5 Acknowledgements

We would like to thank colleagues from Savatech, Kranj for technical support.

6 References

Brady, Robert: *Comprehensive Desk Reference of Polymer Characterization and Analysis*, Oxford University Press, 2003, ISBN 0 8412 3665 8.

Erbil, H. Yildrim: *Surface Chemistry of Solid and Liquid Interfaces*, Blackwell Publishing, 2006, ISBN 1 4051 1968 3.

Gorazd Golob, Miran Mozetič, Kristina Eleršič, Ita Junkar, Dejana Đorđević, Mladen Lovreček: *Rubber blanket surface energy modification using oxygen plasma treatment*, 36th International Resarch Conference IARIGAI, Stockholm, 2009.

Gorazd Golob, Miran Mozetič, Mladen Lovreček: *Rubber raw material surface energy modification using oxygen plasma treatment,* SGA Pardubice, 2009.

Gorazd Golob, Mladen Lovreček, Miran Mozetič, Alenka Vesel, Odon Planinšek, Marta Klanjšek Gunde, Diana Gregor Svetec: *Determination of surface free energy and chemical modifications of plasma treated elastomer surface*, Tiskarstvo 2010, Stubičke Toplice.

Mozetič Miran, Alenka Vesel, Cvelbar Uroš: *Method and device for local functionalization of polymer materials, international patent WO 2006/130122*.

Mozetič, Miran: *Controlled oxidation of organic compounds in oxygen plasma*. Vacuum. [Print ed.], 2003, vol. 71, p. 237-240.

Gorazd Golob – CV

Gorazd Golob, born in Celje, Slovenia in 1955, started his working experience as a lithographic printer at the printing house Delo in Ljubljana in 1973. After two years, he went as a full-time student to the College of Graphic Arts in Zagreb. With his first diploma in 1978, he became a technologist at the printing house Delo and was responsible for the development of technology, new products, investments, organization of the production process and other tasks. In 1983, he took up a part-time study at the newly established Joint Study of Graphic Arts Technology at the University of Zagreb, which later evolved into a regular study programme at the Faculty of Graphic Arts. After the graduation in 1986, he became a manager responsible for the job and production planning, and estimating at the printing house Delo. From 1990 to 1993, he worked at the printing house Tiskarna Ljubljana as a technical manager and afterwards spent one year as a lecturer at the Technical School of Graphic Arts and Paper in Ljubljana and another three years as a technical manager at the printing house KRO. Since 1997, he has been employed as a lecturer (senior lecturer since 2005) at the University of Ljubljana, Faculty of Natural Sciences and Engineering. In 2005, he finished his postgraduate study at the University of Ljubljana, Faculty of Arts and attained the title Master of Library Science.

In 2007, he became a postgraduate student at the Doctoral study programme at the University of Zagreb, Faculty of Graphic Arts.

He is a member of the Slovenian Colorists Association, Lightning Engineering Society of Slovenia (national coordinator for Slovenia in Div.8, CIE) and an active member of the Technical Committee for Graphic Arts and Photography at SIST, national body member of ISO.